Abrupt changes in sea ice and dynamics of Dansgaard-Oeschger events

Mari Fjalstad Jensen

Avhandling for graden philosophiae doctor (ph.d.)

ved Universitetet i Bergen

2017

Dato for disputas: 01.12.2017

Abstract

Changes in sea ice are proposed as an important component in Dansgaard-Oeschger events; the abrupt climate change events that occurred repeatedly during the last ice age. Paleoclimatic reconstructions suggest an expansion of sea ice in the Nordic Seas during the cold stadial periods of the Dansgaard-Oeschger cycles. However, as the present configuration of the Nordic Seas does not allow for an extensive sea-ice cover in this region, the hydrography must have been different during glacial times. In fact, reconstructions show that the Nordic Seas hydrography during cold stadial periods was similar to the stratification of the Arctic Ocean today. However, the dynamic impacts of changing freshwater input and Atlantic water temperature on the Arctic stratification and sea ice are unclear.

This study aims to assess the potential for Arctic-like stratification in the Nordic Seas during the last glacial period and the dynamics behind Dansgaard-Oeschger events, using models and theory. The results are presented in three papers. In the first paper, we develop a simple conceptual two-layer ocean model including sea ice representing the Nordic Seas during stadial times. Here, we find that a sea-ice cover is sensitive to changes in freshwater input, subsurface temperature, and the representation of vertical mixing. Abrupt changes in sea ice can occur with small changes to surface freshwater supply or Atlantic water temperatures. In the second paper we apply a three-dimensional eddy resolving numerical model to the same problem and find further support for the conclusions from Paper I; the stability of a sea-ice cover in the Nordic Seas is dependent on the background climate and large changes in stratification and sea ice occur with small changes in forcing. In addition, additional results presented in this dissertation (Sec. 6.2.1) show self-sustained oscillations in sea-ice cover without a change in forcing. From Paper II we learn that an extensive sea-ice cover and an Arctic-like stratification with a fresh surface layer and a halocline can exist in the Nordic Seas without an external freshwater supply. Under sufficient cold conditions, a halocline capped by sea ice emerges spontaneously due to redistribution of freshwater through sea-ice formation and melt. We find that an extensive sea-ice cover slows down the local overturning in the Nordic Seas; decreases the heat import to the basin; warms intermediate waters, and cools deep waters. In Paper III, the importance of background climate is further stressed. In this study, we move away from studying an Arctic-like stratification, and focus on sea-surface temperature variability in the region of the Nordic Seas and North Atlantic. We compile all available planktic foraminifera records from the North Atlantic with a sea-surface temperature reconstruction from the Dansgaard-Oeschger events. These are then combined with fully coupled climate model simulations using a proxy surrogate reconstruction method. The resulting spatial sea-surface temperature patterns agree over a number of different general circulation models and simulations. However, forced runs from glacial times are needed to

capture the amplitude of the temperature variability as seen in the proxy records. We suggest that sea-ice changes are important in extending the oceanic temperature signals to land.

Combined, the three papers argue for an important role of the Nordic Seas during Dansgaard-Oeschger events, consistent with paleoclimatic reconstructions. Our results are also relevant for understanding potential future changes in Arctic sea-ice cover, and we argue that changes in Atlantic water temperature are of large importance.

List of papers

1. Jensen, M. F., J. Nilsson, and K. H. Nisancioglu, *The interaction between sea ice and salinity-dominated ocean circulation: implications for halocline stability and rapid changes of sea ice cover*, Clim. Dyn. **47**, 3301–3317, 2016, doi:10.1007/s00382-016-3027-5.

2. Jensen, M. F., K. H. Nisancioglu, and M. A. Spall, *Sea-ice cover in the Nordic Seas and the sensitivity to Atlantic water temperature*, prepared for submission to J. Climate.

3. Jensen M. F., A. Nummelin, S. B. Nielsen, H. Sadatzki, E. Sessford, B. Risebrobakken, C. Andersson, A. Voelker, W. H. G. Roberts, and A. Born, *A spatio-temporal reconstruction of sea-surface temperatures in the North Atlantic during Dansgaard-Oeschger events 5-8*, Clim. Past Discuss., doi:10.5194/cp-2017-103. Under review for Clim. Past.

Contents

Chapter 1

Introduction

The history of the climate system is characterized by large variability on different time scales. Apart from the orbital-scale glacial-interglacial cycles, some of the more prominent variability is the large and re-occurring millennial-scale climate fluctuations during the last glacial period: the Dansgaard-Oeschger (DO) events. The focus of this dissertation is the dynamics behind the DO-events in particular related to changes in sea ice.

The DO-events were first discovered in ice-cores on Greenland where temperature reconstructions show a climate on Greenland that flickered between warm and cold conditions. This climate instability has later been found in marine and terrestrial records all over the world, suggesting that the climate system is capable of large and abrupt changes on a global scale.

Interestingly, the mechanism behind the abrupt climate change events of the last glacial period is still debated. One hypothesis explaining these events involves rapid changes in the sea-ice cover of the Nordic Seas. With the Nordic Seas being located in the proximity to Greenland and sea ice affecting the energy exchange between the ocean and the atmosphere, rapid change in sea ice is a likely agent causing or contributing to the large temperature fluctuations on Greenland. As new evidence from paleoclimatic reconstructions shows an intermittent sea-ice cover in the Nordic Seas during glacial times, it is becoming clear that sea-ice changes play a role during DO-events.

However, the present day climate and circulation of the Nordic Seas do not allow for extensive sea-ice cover in the area and hence the configuration must have been different during glacial times. As marine reconstructions are limited, we aim to better understand the changes in the hydrography of the Nordic Seas that would allow for a sea-ice cover in the region using models and theory. In doing so, we also aim to validate the information from the paleoclimatic reconstructions.

If the hypothesis that sea-ice changes in the Nordic Seas affected temperatures on Greenland to such a large degree, the ongoing sea-ice changes in the Arctic Ocean could have profound impact on Greenland temperatures and ice-sheet mass balance. The latter is not addressed directly in this dissertation, however, it motivates further for the understanding of the role of sea ice in the abrupt climate change events of the last glacial period.

Details of the DO-events are given in Sec. 1.1. The two main hypothesis for the DO-events, changes in ocean circulation and sea ice, is presented in Sec. 1.2, and the modern configuration of the Nordic Seas and Arctic Ocean in Sec. 1.3.

1.1 Dansgaard-Oeschger events

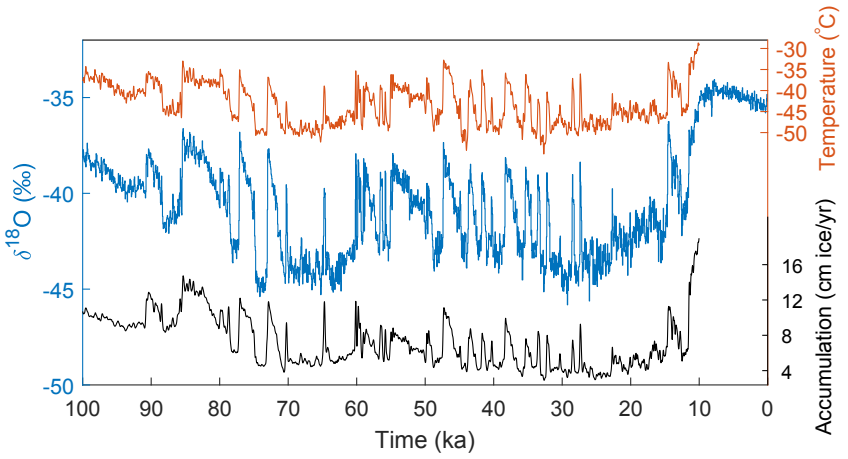

Figure 1.1: Ice-core reconstructions from NGRIP. Oxygen isotope measurements from North Greenland Ice Core Project members (2004, blue) and accumulation rate (black) and temperature reconstructions from Kindler et al. (2014, red).

1.1.1 Paleoclimatic reconstructions

Ice-cores

The Dansgaard-Oeschger (DO) events were first identified in ice cores on Greenland where oxygen isotope (δ^{18}O)[1] measurements of the ice showed alternating high and low values throughout the last glacial period (∼20-100 ka[2], Johnsen et al., 1972; Dansgaard et al., 1982). The high δ^{18}O-values were surprisingly close to those of interglacial times and these time periods were thus named "interstadials". The time periods with lower δ^{18}O-values more typical of glacial periods were named "stadials". The irregularity was first assumed to be disturbances in the ice or a local signal only, but as more ice cores showed the same signal, and at locations with limited disturbances in the ice, the signals were thought to be due to a large-scale shift in the climate system (Johnsen et al., 1992; Dansgaard et al., 1993). Since then an increasing number of paleoclimatic reconstructions have shown a similar type of variability and the dynamics behind the DO-events, or the Greenland stadial/interstadial cycles, have become one of the large mysteries of the climate system.

The DO-events on Greenland are characterized by abrupt changes in temperature. The δ^{18}O-value of the ice is a proxy for temperature (Johnsen et al., 1992); the ice cores were therefore thought to reflect a climate on Greenland which alternated between cold stadial and warm interstadial conditions. The amplitudes of the temperature fluctuations were surprisingly high ($\sim \pm 10$°C), and as other factors in addition to

[1] δ^{18}O is the ratio between the stable oxygen isotopes ^{18}O and ^{16}O

[2] 1 ka=1000 years ago

the local temperature change affect the δ^{18}O-values, the large amplitudes were questioned. However, in recent years, the original numbers have been backed up by several independent measurements showing equally high amplitudes. For example δ^{15}N measurements of the trapped air in the ice show temperature rises of 3-16.5$\pm$3°C (Landais et al., 2004; Kindler et al., 2014, Fig. 1.1). As of now, the DO-events on Greenland are characterized by an abrupt warming of 10$\pm$5°C in only a few decades (Landais et al., 2004; Huber et al., 2006; Kindler et al., 2014). During the warm interstadial conditions on Greenland the climate cools gradually before a more abrupt transition back to cold stadial conditions. A full cycle is usually referred to as a Greenland stadial/interstadial-cycle, but we will keep the notion of a "DO-cycle" here and a "DO-event" for the abrupt stadial-interstadial transitions.

There are about 25 main DO-events during the last glacial period (North Greenland Ice Core Project members, 2004), but also several smaller sub-events are identified and named (Rasmussen et al., 2014a). A very rough period of the DO-cycle is 1500 years, but this varies from event to event as an interstadial lasts for 300-2500 years and a stadial from hundreds to thousands of years (Wolff et al., 2010). The ice cores do not only show large temperature changes but also changes in e.g., dust content (Mayewski et al., 1994; Ruth et al., 2003), greenhouse gas concentration (Stauffer et al., 1998; Huber et al., 2006), and accumulation rate of snow (Fig. 1.1) suggesting large-scale atmospheric changes.

The Antarctic ice cores also show millennial scale climate variability, although with a much smaller amplitude (Blunier and Brook, 2001, EPICA Community Members, 2006). The Antarctic ice cores show a cooling during the warm Greenland interstadials and a warming during the cold Greenland stadials. Due to the globally well mixed distribution of methane, ice cores from the two different hemispheres can be synchronized. This was recently done with a new high-resolution ice-core from the West-Antarctic Ice Sheet where an approximate 200 year lead in the Greenland records is found (WAIS Divide Project Members, 2015) together with an anti-phase relationship between the warming of the two hemispheres. WAIS Divide Project Members (2015) identify one Antarctic warming event for each DO-event giving evidence to the whole globe being affected by the abrupt climate change events of the last glacial period.

Marine records

The millennial-scale climate variability has also been found all over the world in other climate archives in addition to the ice-cores (Voelker, 2002, and references therein). Examples include speleothem records from caves (e.g., Dorale et al., 1998) and lake-records (e.g., Stockhecke et al., 2016). Due to difficulties in precise dating of many of these records, there are uncertainties in the synchronization to ice-cores, but the characteristic shape, time scale, and number of events leave little doubt to whether the reconstructed variability is linked to the changes on Greenland. Greenland interstadials are typically associated with warmer and wetter conditions in the Northern Hemisphere, a northward migration of the Atlantic inter-tropical convergence zone (ITCZ), forest expansion, and enhanced Asian summer monsoon (Voelker, 2002, and references therein).

Marine sediment cores dominate the abundance of information from the DO-events (Voelker, 2002). The millennial scale climate variability was first discovered in the

ocean by Bond et al. (1993) who show that properties from marine sediment cores correlate with the δ^{18}O-signals on Greenland. Marine sediment cores are limited to locations with high sediment accumulation allowing for high-resolution records, and the information from Marine Isotope 3 (MIS3, $\sim$ 29-60 ka, the ocean nomenclature for parts the last glacial period when most of the DO-events occur) is thus restricted to specific regions. The largest abundance of paleoclimatic proxy records from the ocean is found in the North Atlantic (Voelker, 2002) where the presence of continental slopes suitable for drilling cores, and the vicinity to Greenland, the DO-event's "hotspot", have led to numerous research cruises. The largest oceanic variability is found in the North Atlantic with systematic different water mass properties over the DO-cycles (e.g., Curry and Oppo, 1997). Bond et al. (1993) were perhaps the first to show that the North Atlantic sea-surface temperatures are typically cold during stadials and warm during interstadials, but this information has been supported by numerous new records with both higher sedimentation rates allowing for better resolution, and different proxies for temperature reconstructions. Examples include planktic (surface or close to surface dwellers) foraminifera assemblages which show a dominant abundance of Atlantic species during interstadials and increased abundance of cold polar species during stadials, alkenone unsaturation ratios (e.g., Sachs and Lehman, 1999), Mg/Ca-concentrations, and planktic foraminifera isotope records. Other records show a warming of the sea-surface temperatures during stadials (Labeyrie et al., 1999; Waelbroeck et al., 2001), and studies suggest movements in the fronts between Atlantic and polar waters (Eynaud et al., 2009; Voelker and de Abreu, 2013; Rasmussen et al., 2016). However, the sea-surface temperature increase during stadials has in some records been interpreted as a subsurface signal (e.g., Wary et al., 2015) as the planktic foraminiferas move away from the fresh surface layers. This is especially true for the Nordic Seas which we will come back to in Sec. 1.1.2.

Marine paloeclimatic reconstructions also suggest changes in ocean circulation over the DO-cycles, although the proxies are still elusive. The intermittent presence or absence of North Atlantic Deep Water (NADW) at core locations is often interpreted as a change in the large-scale ocean circulation with a reduction of NADW during stadials proposing less NADW formation and a less vigorous ocean circulation (e.g., Marchitto et al., 1998; Curry et al., 2013; Henry et al., 2016). Magnetic properties in cores from the North Atlantic also indicate reduced bottom current strength during stadials, suggested to be linked to changes in NADW (Kissel et al., 1999, 2008). However, Yu et al. (1996) show an active NADW formation also during stadials and Elliot et al. (2002) argue that there is little evidence for systematic large-scale changes in ocean circulation during DO-events and that the significant changes in the global overturning circulation only occur during Heinrich events[3]. Recently, new records suggesting reduced ocean circulation during stadials have been presented: Henry et al. (2016) show protactinium thorium reconstructions suggesting a less vigorous ocean circulation during stadials but increased Antarctic Bottom Water formation. Gottschalk et al. (2015) show an increased presence of NADW in the South Atlantic during almost every interstadial compared to stadials.

Other oceanic features are sea level fluctuations of 20-30 m over the DO-events

[3]The Heinrich events occurred at the end of some, but not all, of the stadials. They are associated with iceberg release from the Laurentide Ice Sheet as layers of ice rafted debris are found throughout the North Atlantic (Heinrich, 1988; Hemming, 2004). We view these events as "independent" from the DO-events

(Siddall et al., 2008); the sea-level during MIS3 was in general 60-90 m below the present level (Chappell and Shackleton, 2002; Waelbroeck et al., 2002; Siddall et al., 2008), and a cooling of southern ocean sea-surface temperatures during interstadials (Ninnemann et al., 2013).

1.1.2 The Nordic Seas during MIS3

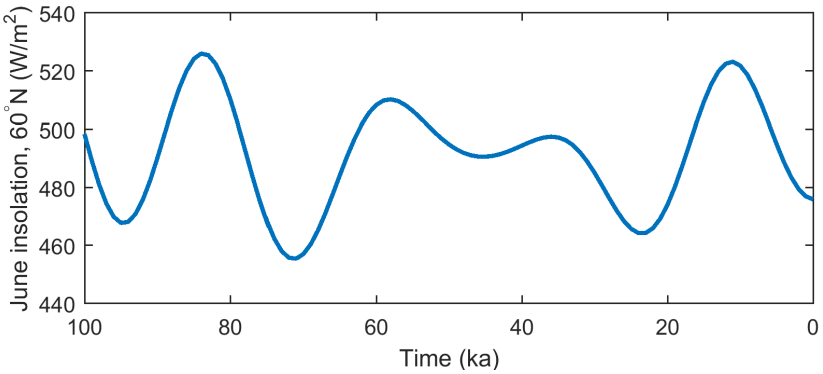

Figure 1.2: Summer insolation in the southern Nordic Seas. Values from Berger and Loutre (1991)

Paleoclimatic reconstructions suggest large changes in the Nordic Seas during MIS3. The main difference between the Nordic Seas during modern times (see Sec. 1.3.1) and the last glacial period is probably the presence of large continental ice sheets during glacial times. The Nordic Seas region was surrounded by the Laurentide and Fennoscandian Ice Sheets (Fig. 1.3). The Barents Sea was probably covered with an ice sheet (Svendsen et al., 1999) during most of the glacial period, while it is hypothesized that also the Arctic Ocean was covered in km-thick sea ice (Jakobsson et al., 2016). Note that the solar insolation at the latitudes of the Nordic Seas was slightly higher than present during MIS3 (Fig. 1.2). However, with the large ice sheets surrounding the area and the consequent higher albedo and cold winds, the Nordic Seas region was most likely much colder than present. Still, there is evidence for warm water (above freezing) entering the Nordic Seas throughout MIS3 (Rasmussen and Thomsen, 2004; Ezat et al., 2014).

Proxy reconstructions suggest systematic hydrographic changes in the Nordic Seas between the warm and cold periods on Greenland (Rasmussen et al., 1996; Dokken and Jansen, 1999; Rasmussen and Thomsen, 2004; Dokken et al., 2013; Rasmussen et al., 2014b; Ezat et al., 2014). During Greenland interstadials, proxy reconstructions using foraminifera assemblages suggest a Nordic Seas hydrography similar to modern conditions with a warm surface and weak stratification (Rasmussen et al., 1996; Rasmussen and Thomsen, 2004; Dokken et al., 2013, Fig. 1.4b). Cold periods on the other hand, differ from today's stratification and resemble more the conditions in the Arctic Ocean with warm water at subsurface-depths and a cold fresh surface layer (Rasmussen and Thomsen, 2004; Dokken et al., 2013; Ezat et al., 2014, Fig. 1.4a). A halocline is thought to be present below the upper surface layer, protecting the surface from the warm Atlantic water below. The subsurface is therefore warmer during cold stadi-

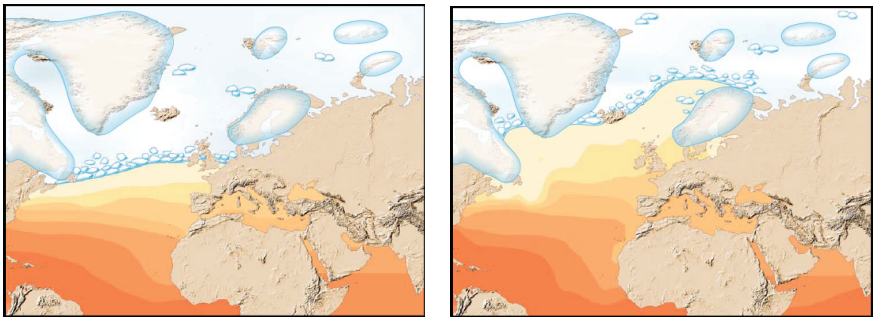

(a) (b)

Figure 1.3: The hypothesized configuration of the Nordic Seas during a) Stadial and b) Interstadial conditions on Greenland. Figure adapted from Dokken et al. (2013).

als than warm interstadials. Enhanced ice rafted debris and low seawater oxygen isotope values suggest a fresher surface layer during the stadial periods (e.g., Dokken and Jansen, 1999), but also toward the end of the interstadials (Dokken et al., 2013). Using planktic foraminifera assemblages, Dokken et al. (2013) show a gradual warming of the subsurface during stadials and a warm overshoots at the start of each interstadials. This is further described in Sec. 1.2.2.

Circulation changes during DO-events are also thought to occur in the Nordic Seas. The evidence for deep-water convection in the Nordic Seas is generally elusive and indirect. Open ocean convection probably occurred during interstadials (Rasmussen et al., 1996; Kissel et al., 1999; Dokken and Jansen, 1999; Rasmussen et al., 2014b). Deep-water formation through open ocean convection is suggested to stop during stadials due to an insulating sea-ice cover and/or fresh surface layer as indicated by lowered δ^{13}C (stable carbon isotope) signals of planktic foraminifera (Dokken et al., 2013). Ezat et al. (2014) reconstructed bottom water temperatures (here: at 1179 m) from Mg/Ca measurements, showing an increase of 2-5°C during stadials as opposed to the colder values during interstadials. This is interpreted as a pause in deep-water production as the marine sediment core is located in an overflow area. Lower δ^{18}O-values on benthic (deep-dwelling) foraminiferas are also interpreted as showing a warming of the deep ocean during stadials. In contrast, Dokken and Jansen (1999) and Dokken et al. (2013) interpret the values as a brine signal from enhanced sea-ice production during stadials. Brine is released when sea ice freezes and the salty water may penetrate to depths depending on its density. Dokken and Jansen (1999) suggest that brine production from surface waters with low δ^{18}O-values sinks to the deep ocean and contributes to the low benthic δ^{18}O-signal.

Sea ice has been hypothesized to be present in the eastern Nordic Seas during stadials based on the Arctic-like stratification (Dokken et al., 2013) and fore-mentioned benthic δ^{18}O-signal. More direct evidence is emerging as new records of IP25 (a biomarker for sea ice) are presented (Hoff et al., 2016, H. Sadatzki et al. 2017; under review for Nat. Geosc.). On the other hand, studies based on dinoflagellate cyst assemblages (Eynaud et al., 2002; Wary et al., 2016) suggest a warmer surface in the Nordic Seas during stadials and more sea ice during interstadials. However, the more extensive sea ice during interstadials is not consistent with the majority of other proxy

records.

The presence of an intermittent perennial sea-ice cover in the eastern Nordic Seas is a remarkable difference from modern conditions with sea-surface temperatures exceeding 8°C throughout the year (see Sec. 1.3.1).

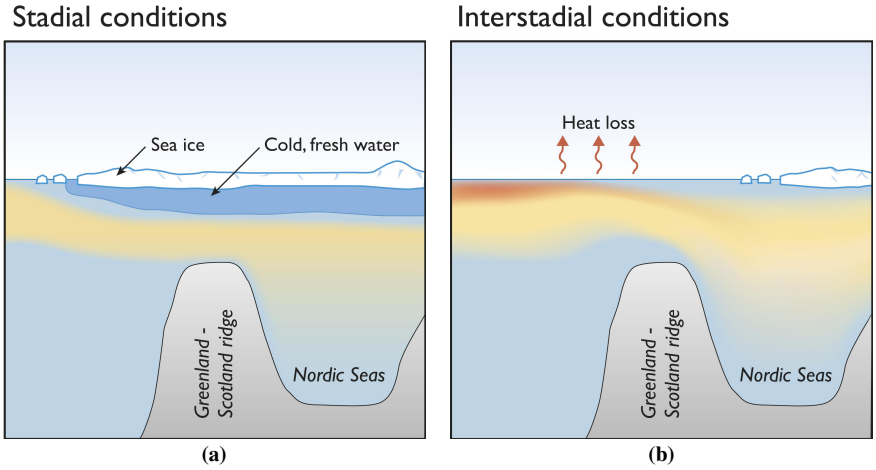

Figure 1.4: The hypothesized stratification of the Nordic Seas during a) Stadial and b) Interstadial conditions on Greenland. Figure adapted from Dokken et al. (2013)

1.2 Hypothesized mechanisms explaining DO-events

Several mechanisms have been proposed as the driver of the DO-events. Examples include changes in the location of NADW formation (Labeyrie et al., 1995; Ganopolski and Rahmstorf, 2001; Arzel et al., 2010; Colin de Verdiere and Raa, 2010; Curry et al., 2013; Sevellec and Fedorov, 2015); switches in the heat transport to the North Atlantic due to either internal instabilities in the Atlantic Meridional Overturning circulation (AMOC, Broecker et al., 1990; Tziperman, 1997; Marotzke, 2000; Ganopolski and Rahmstorf, 2001), or a salt oscillator (Peltier and Vettoretti, 2014; Vettoretti and Peltier, 2016); superposition of the orbital cycles (Braun et al., 2005), or orbitally driven changes in the tropical Pacific (Clement et al., 2001); stochastic resonance with meltwater from ice sheets (Alley et al., 2001); changes in the sea-ice cover of the Nordic Seas (Broecker, 2000; Gildor and Tziperman, 2003; Masson-Delmotte et al., 2005; Li et al., 2005; Dokken et al., 2013; Petersen et al., 2013). Many of these hypothesized mechanisms are linked to each other and the driver might potentially be a combination of them all.

1.2.1 Changes in AMOC

The leading mechanism has for many years been changes in the Atlantic Meridional Overturning Circulation (AMOC) typically associated with a reduction in the formation of NADW. The AMOC is associated with cold deep-water formation in the polar

regions of both hemispheres, southward flow at depth, and a northward transport of heat at the surface. Switches in the strength of the heat transport could therefore explain a warming of the North Atlantic and a cooling of the South Atlantic as more heat is transported northwards. The centennial lag between the two hemispheres supports large-scale ocean features as a contributor to the DO-variability. In addition, both simple analytical (Stommel, 1961) and early low resolution coupled general circulation models (GCM, Manabe and Stouffer, 1988) suggest a bi-stability in the AMOC. Thus for many years, switches between two different modes of the AMOC have been thought to drive the temperature variability on Greenland. Broecker et al. (1985) first suggested that the AMOC and the NADW formation switched between an "off" and an "on" mode, forced by changes in the freshwater supply to the North Atlantic from the continental ice sheets surrounding the region (Broecker et al., 1990; Birchfield and Broecker, 1990). However, as paleoclimatic reconstructions show an active NADW formation also during stadials (e.g., Yu et al., 1996) and further improvements of GCMs led to an active AMOC at all times, the hypothesis was moderated to an AMOC that strengthens and weakens. To simulate a reduced AMOC, many GCM simulations with large freshwater supplies to the North Atlantic, so-called "hosing" experiments, have been performed. The hosing is motivated by the release of icebergs from the continental ice sheets and intermittent glacial lake releases. The hosing experiments show a weakening of the AMOC with a capping of the convection sites in the North Atlantic where NADW forms. The simulated weakened AMOC leads to a colder North Atlantic, warmer Southern Ocean (Crowley, 1992; Stocker and Johnsen, 2003), a southward shift of the Atlantic ITCZ, and weakened summer monsoon (e.g., Zhang and Delworth, 2005), all consistent with what the proxy records suggest occurs during stadials.

However, the proxy records do not completely support the AMOC hypothesis. A typical hosing experiment shows an abrupt weakening of the AMOC coinciding with the freshwater forcing, and thereafter a gradual recovery back to full strength lasting for decades to centuries after the freshwater input stops (e.g., Manabe and Stouffer, 1995; Stouffer et al., 2006). Contrary, the ice cores show that it is the warming events (associated with an AMOC recovery), and not the cooling events, which are the more abrupt (Fig. 1.1). The duration of the stadial periods is dependent on the freshwater forcing and often last only as long as the hosing occurs (e.g., Ganopolski and Rahmstorf, 2001). In addition, the amount of freshwater needed for a significant change is large (in order of several Sverdrups (Sv)[4]) and the impact depends on the region where it is added. Thus, a large and persistent freshwater source is needed for each stadial; time periods when the climate system is cold and less supportive of freshwater input. However, other studies show that only a small periodic change in the freshwater flux is needed; e.g., Ganopolski and Rahmstorf (2002) show that an ocean-atmosphere climate model run with stochastic freshwater forcing, together with a weak periodic forcing, produces interstadial conditions with similar time and spatial patterns as the paleoclimatic record. The recovery time of the AMOC after a freshwater perturbation is also shown to depend on the background climate as the recovery rate is different in a last glacial maximum (LGM) climate than in a modern climate (Ganopolski and Rahmstorf, 2001; Bitz et al., 2007). Modelling the AMOC and deep-water formation is difficult as high resolution and good parametrizations of processes like convection, ad-

[4] 1 Sv=$10^6 m^3 s^{-1}$

vection, and diffusion are needed. Recent improvements of GCMs have led to a more stable AMOC than previously thought (Vellinga et al., 2002; Gildor and Tziperman, 2003).

Another problem with the AMOC-hypothesis is the debate on how much effect the AMOC actually has on North Atlantic climate (e.g., Wunsch, 2005). Changes in the heat transport alone cannot account for the full temperature increase on Greenland that ice cores suggest happened; hosing simulations only show a temperature change on Greenland of a couple of degrees (e.g., Vellinga et al., 2002). Note also that sensitivity studies with model simulations without the northward oceanic heat transport show that the oceanic heat transport may not be so important for the North Atlantic climate as previously thought (Seager, 2006). Also the horizontal circulation is important for the heat transport as the subtropical and subpolar gyres contribute to the poleward heat transport by the ocean. Proxy data suggest a change in the NADW formation over the DO-cycles, but it is not clear whether changes in NADW only impact the circulation and water mass properties of the deep or the transport of heat at the surface in addition (Lozier, 2012; Buckley and Marshall, 2016).

As the debate continues on how stable the AMOC is and how much impact it actually has on the atmospheric temperature of the northern North Atlantic, it is still likely that the AMOC played a role in the abrupt warming events. However, whether AMOC changes were the driver or mainly a response to the climate change is not obvious. It is however quite clear that AMOC changes alone cannot account for the full temperature variability as seen on Greenland. In recent years, the role of sea ice in the DO-cycles is becoming more convincing and change in sea ice has the potential to enhance the temperature response on Greenland associated with AMOC changes.

1.2.2 Sea-ice changes

Sea-ice changes are hypothesized as a big component in the large temperature fluctuations on Greenland (Broecker, 2000; Gildor and Tziperman, 2003; Masson-Delmotte et al., 2005; Li et al., 2005; Dokken et al., 2013; Petersen et al., 2013). Paleoclimatic reconstructions suggest a fluctuating sea-ice cover co-varying with the temperature variability on Greenland (Hoff et al., 2016) and changes in sea ice have the potential to influence the atmospheric temperature due to changes in albedo and heat release from the ocean. Sea ice acts as an insulating layer, protecting the ocean from the cold atmosphere above. In addition, the high albedo of sea ice leads to a larger reflection of incoming solar radiation when sea ice is present than when absent. A reduction in sea-ice cover would therefore lead to a warming of the atmosphere above, both by release of oceanic heat and increased absorption of solar radiation. The positive feedback associated with the changing albedo with changing ice-cover; i.e., the ice-albedo feedback (Curry et al., 1995), leads to large changes in sea-ice cover with a small first perturbation or weak change in forcing (Maykut and Untersteiner, 1971). Changes in sea-ice cover is therefore a likely mechanism for the abrupt warming associated with the DO-events.

Changes in sea ice and the sea-ice edge can explain more than just the rapid temperature increases on Greenland. Deuterium excess measurements from ice cores suggest that the source region for the precipitation that falls on the ice core region changes over the cycles (Jouzel et al., 2005). A sea-ice cover would prevent evaporation, thereby

shifting the evaporation site farther south. The observed dust changes over the DO-events can also be explained by a sea-ice shift as sea-ice changes can divert the storm tracks (Mayewski et al., 1997). Changes in sea ice also explain the observed accumulation changes on Greenland during DO-events and show a larger temperature response on Greenland during winter than summer, consistent with ice-core reconstructions (Li et al., 2005).

In addition to paleoclimatic reconstructions, model studies support sea-ice changes as a player in the DO-events. Li et al. (2005) use an atmospheric GCM and show that the removal of a typical LGM sea-ice cover in the North Atlantic can explain an annual 7°C temperature increase on Greenland, comparable to the magnitude of the ice-core reconstructions and larger than the warming associated with changes in AMOC only. Li et al. (2010) show that Greenland is more sensitive to changes in the sea-ice cover of the Nordic Seas than to sea-ice changes of the western North Atlantic. Similar to the hosing experiments, model studies with changes in sea-ice extent can explain changes in the sea-surface temperatures in the North Atlantic, shifts in the position of the ITCZ (Chiang and Bitz, 2005) and the summer monsoon (Pausata et al., 2011), all consistent with the proxy records. Changes outside the northern North Atlantic can be explained by the sea ice's effect on the meridional temperature gradient and atmospheric circulation or by the effect on deep-water formation (Gildor and Tziperman, 2001a).

Rapid changes in sea ice have also been shown to shift the AMOC (Gildor and Tziperman, 2001b). The effect of sea ice on the stability of the AMOC has been studied with conceptual models, however not necessarily over millennial time scales (e.g., Yang and Neelin, 1993, 1997; Jayne and Marotzke, 1999). Jayne and Marotzke (1999) showed that the effect of sea ice on the meridional temperature gradient and atmospheric moisture transport destabilize the thermally dominated circulation. Yang and Neelin (1993) highlighted the role of brine release through sea-ice formation and show self-sustained oscillations in the thermal circulation. Yang and Neelin (1997) tried to differentiate the sea-ice feedbacks on heat and freshwater fluxes and show that a decay in circulation due to changes in forcing is prolonged when sea ice is included. Gildor and Tziperman (2001b) also find self-sustained oscillations with sea ice as the switch causing AMOC instabilities. The latter study has been related to millennial time scale variability showing sea ice as a negative feedback on the AMOC strengthening (Timmermann et al., 2003).

Although the evidence for a role of a changing sea-ice cover in the DO-events is becoming more and more convincing, the reasons behind the sea-ice switches are not clear. Sea-ice changes could be the mechanism behind the DO-events due to intrinsic changes, or be forced by an external forcing and thereby driving the DO-events. However, the sea-ice changes could also just be a response to the "real" mechanism, most likely enhancing the local responses or being more active in modulating the original mechanism. The sea-ice changes could be forced from above or below, from the south or the north, or be intrinsic to the Nordic Seas. Hypothesized mechanisms for the sea-ice changes include shifts in wind near the sea-ice edge, small changes in the AMOC (Gildor and Tziperman, 2003), or a subsurface warming below the sea-ice cover destabilizing the water column (Dokken et al., 2013). Dokken et al. (2013) show a gradual warming of the subsurface in the Nordic Seas during stadials and an overshoot in surface warming at the start of each interstadial. The authors proposed that the gradual warming of the subsurface gradually breaks down the protective halocline and even-

tually makes the water column unstable. When this happens, convective overturning starts, bringing up the subsurface heat which melts the sea ice and releases heat to the atmosphere. However, it is not clear how much the subsurface needs to warm to start convective overturning, or whether a subsurface warming without an external forcing is possible. In addition, it is not clear how a sea-ice cover can exist in the Nordic Seas as the present day configuration does not allow for an extensive sea-ice cover.

1.3 Modern oceanography of the Nordic Seas and Arctic Ocean

The Nordic Seas: the Greenland, Iceland and Norwegian Seas, is a collection of deep basins and shallow shelf areas (Fig. 1.5) and the main gateway between the North Atlantic and the Arctic Ocean. Although small in extent, the Nordic Seas region is a large player in today's climate system and hypothesized to be important in the abrupt changes of the last glacial period. Here, the modern oceanographic conditions of the Nordic Seas and the potential importance of the Nordic Seas on the climate system are discussed (Sec. 1.3.1). As the Nordic Seas stratification is hypothesized to resemble the Arctic Ocean during stadial times, also some features of the Arctic Ocean are presented (Sec. 1.3.2).

1.3.1 The Nordic Seas

The Nordic Seas are located in the northern North Atlantic, situated between Greenland and Norway (Fig. 1.5). The southern boundary to the Atlantic Ocean is the Greenland Scotland Ridge (GSR), the ridge from the eastern coast of Norway to the Shetland Islands and Greenland, with the Faroe Islands and Iceland on top of the ridge. The GSR has a mean depth of roughly 500 m, but depths exceeding 800 m are also found. The ridge is important in constraining the exchanges between the Nordic Seas and the North Atlantic. The northern boundary to the Arctic Ocean is the Fram Strait at about 79°N, and the north-eastern boundary is at about 20°E from Svalbard to northern Norway. The eastern boundary is the Norwegian coast, while Greenland constitutes the western boundary. The area of the Nordic Seas is approximately 2.5×10^6 km^2 (Segtnan et al., 2011) and thus constitutes only 0.75% of the world's oceans.

The bathymetry of the Nordic Seas is diverse with depths exceeding 3500 m in the Greenland Sea and Norwegian Basin and shallow shelves along the margins. Steep continental slopes off the shelves are thought to be important for the flow patterns in the area (Orvik and Niiler, 2002; Nøst and Isachsen, 2003). The Nordic Seas region experiences strong interaction with the atmosphere, in momentum, heat, freshwater and gases. The Nordic Seas is one of the key regions where CO_2 is taken up by the ocean (Skjelvan et al., 2013). The dynamical length scales are typically small, so modelling of the Nordic Seas is difficult and high resolution and good parametrizations of processes are needed to capture the different mechanisms in the area (Drange et al., 2013a; Nurser and Bacon, 2014). The northern and western parts of the Nordic Seas are partially covered in sea ice during winter (Kvingedal, 2013). Most of the sea ice is due to transport out of the Arctic Ocean, which has increased in recent decades (Smedsrud et al., 2017).

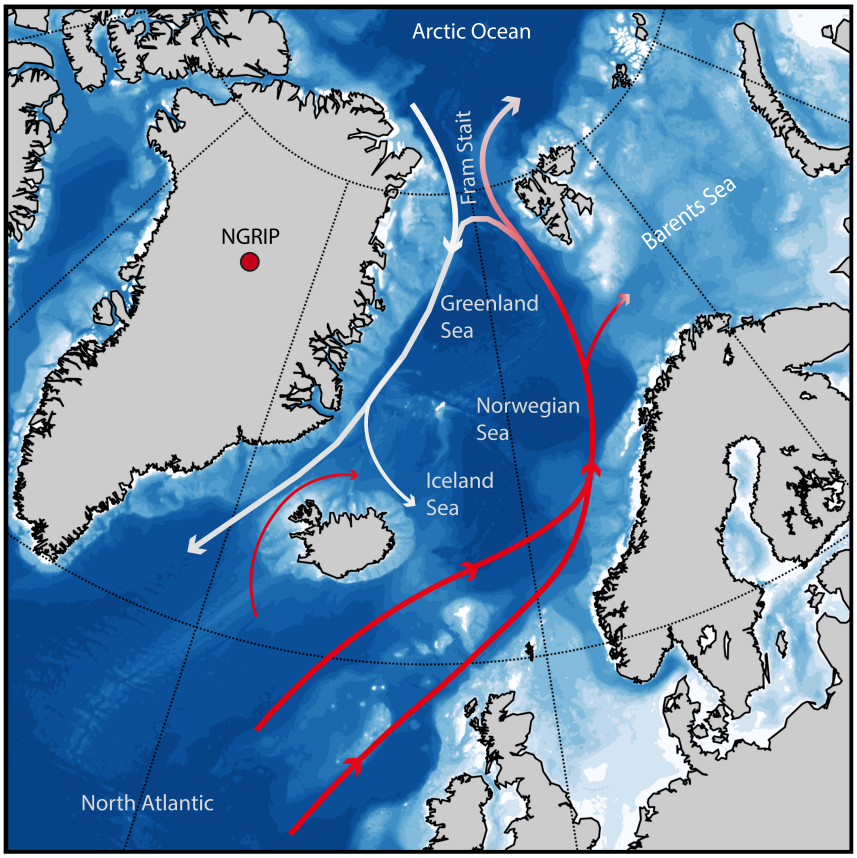

Figure 1.5: The modern bathymetry of the Nordic Seas and northern North Atlantic. Lines with arrows indicate the general surface circulation of the area. The colors of the lines indicate the temperature of the current where red is warmer than white. The location of the ice core NGRIP is shown with a red circle.

The warm Atlantic water

Probably the most distinct characteristic of this region is the anomalous heat; the central and eastern Nordic Seas are 10-20°C warmer than the corresponding zonal mean (Drange et al., 2013b). The anomalous heat input is mainly due to the prevailing southwesterly winds and poleward transport of heat by the ocean (Seager, 2006). The main inflow of warm water from the Atlantic to the Nordic Seas, the Atlantic water inflow, occurs across the GSR, both west and east of the Faroe Islands (e.g., Hansen and Østerhus, 2000, Fig. 1.5). According to Hansen and Østerhus (2000), 110 and 140 TW of heat (relative to 0°) enter the Nordic Seas west and east of the Faroe Islands, respectively. Blindheim and Østerhus (2013) estimated an Atlantic volume influx of 7.7 Sv into the Nordic Seas with the largest contribution from the Faroe Current. The majority of the Atlantic water inflow forms the Norwegian Atlantic Current which carries heat and salt toward the Arctic Ocean (Orvik and Niiler, 2002). Heat is lost to the atmosphere in the Nordic Seas and the Atlantic water which enters the Nordic Seas with a temperature of roughly 8°C (Hansen and Østerhus, 2000; Seidov et al., 2013, 2015) has cooled to around 5°C at the entrance to the Barents Sea and 4°C close to Svalbard (Skagseth et al., 2008). Using oceanic observations and atmospheric reanalysis from the 1990s, Segtnan et al. (2011) estimated the total heat loss in the Norwegian Sea to be 119 TW.

Warm water from the Nordic Seas enters the Arctic Ocean either through the Fram Strait or through the Barents Sea (Fig. 1.5). In the Arctic, the warm water meets cold and fresh polar water and continues as a subsurface flow, typically at 200-900 m (Coachman and Barnes, 1963). The warm Atlantic water flows cyclonically along the basin (Rudels et al., 1994) and is found below a fresh surface layer and a seasonal or annual sea-ice cover. The Atlantic water cools and freshens, and most of the water that enters the Arctic Ocean circulates back to the Nordic Seas (Mauritzen, 1996; Rudels et al., 2000; Cisewski and Krause, 2003). As a consequence, the western Nordic Seas consists of Atlantic water that has either circulated the Arctic Ocean or been deflected from the West Spitsbergen Current at the entrance to the Arctic Ocean (Bourke et al., 1988; Rudels et al., 2000, Fig. 1.5). The transformed Atlantic water flows along the coast of Greenland together with cold polar waters (Hansen and Østerhus, 2000). The waters either leave the Nordic Seas or are transported eastward again (Mauritzen, 1996; Hansen and Østerhus, 2000, Fig. 1.5). As most of the waters that enter the Arctic Ocean from the Nordic Seas return, the circulation regime of the Nordic Seas and the Arctic Ocean can be viewed as one: the Arctic Mediterranean.

The main driver of the heat inflow to the Nordic Seas is not clear. The AMOC contributes to the heat transport to the area, but its role and forcing is debated (e.g., Seager, 2006; Lozier, 2012). The horizontal circulation further south, in particular the gyres, also contribute in transporting heat to the Nordic Seas (Hátún et al., 2005). A strong subpolar gyre with a large horizontal extent is associated with a smaller heat transport to the Nordic Seas as the North Atlantic Current is restricted (Hátún et al., 2005). Winds impact the strength of the subpolar gyre and also contribute to the heat import to the Nordic Seas (Böning et al., 2006). Buoyancy forcing through heat loss within the Nordic Seas helps to drive the warm inflow as the density difference with the south increases. The Arctic Mediterranean is also viewed as an estuarine. Freshwater input in the Arctic drives a stronger Atlantic inflow as the southward fresh surface flow in-

creases and mixes up denser waters from below (Stigebrandt, 1981), or as a stronger circulation is needed to balance the increase in lateral eddy fluxes with increasing freshwater (Spall, 2013).

Freshwater

Heat loss is not the only contributor to water transformation within the Nordic Seas as also freshwater impacts the buoyancy. Segtnan et al. (2011) estimated the total freshwater gain in the Nordic Seas to be 48 mSv (referenced to a psu of 34.9) as a result of precipitation and evaporation and run-off from Norway and Greenland. The largest freshwater flux to the Nordic Seas is in the form of sea ice transported out from the Arctic through the Fram Strait (Aagaard and Carmack, 1989). As most of this freshwater is exported through the Denmark Strait, the freshwater content of the Nordic Seas is estimated to be only about 200 km^3, mainly concentrated in the Greenland and Iceland gyre (Aagaard and Carmack, 1989). Hence, unlike the Arctic Ocean where freshwater is important for the circulation, stratification, and sea ice, freshwater does not play such a large role in today's Nordic Seas. This was probably different during the last glacial period when the Nordic Seas are hypothesized to resemble the Arctic Ocean.

Potential influence on global climate

Changes in deep-water formation in the Nordic Seas have been hypothesized as a mechanism explaining the DO-events. Today, the southward transport of water out of the Nordic Seas is in the form of a surface current east of Greenland, and mainly as an overflow at depths across the GSR. About 6 Sv of cold water is estimated to spill over the GSR (Hansen and Østerhus, 2000; Blindheim and Østerhus, 2013) and the overflow is thus a source for the NADW that contributes to the global overturning circulation (Dickson and Brown, 1994). How and where this deep water is formed is, however, debated (Eldevik et al., 2009), and especially whether any of the densest waters are formed in the Nordic Seas itself or whether they have been formed in and transported out from the Arctic Ocean. The hypothesized deep-water formation mechanisms in the area are open ocean convection (mainly in the Greenland Sea), dense water production on the Arctic Ocean shelves (Aagaard et al., 1985), and transformation of Atlantic water as it cools downstream both in the Nordic Seas and the Arctic Ocean (Mauritzen, 1996). Convection does intermittently take place in the Greenland Sea during winter, but varies on interannual and decadal time scales (Dickson et al., 1996). As renewal of bottom waters corresponds to times when the atmosphere over the Greenland Sea is especially cold, it is thought that convection contributed to the deep-water production up to the 1970s, after which the convection reduced both in depth and frequency (Gerdes et al., 2013).

In addition to the debate on the formation of the overflows, it is debated whether a change in the overflows from the Nordic Seas would influence the global circulation. For example, the intermediate depths of the Nordic Seas have freshened during the recent years (Dickson et al., 2002; Blindheim and Østerhus, 2013), but a coupled climate model (HadCM3) with the same freshening has a strengthened AMOC instead of an assumed weakened circulation (Wu et al., 2004). From the observational side, it is

suggested that convection in the Labrador Sea compensates for the sometimes reduced Greenland Sea convection as the large-scale atmospheric circulation patterns impact the two convection sites differently (Dickson et al., 1996). Less formation of dense deep water in the Nordic Seas has also been shown to increase the downwelling south of the ridge (Spall, 2004; Deshayes et al., 2009). Independent of the global effect of the overflows, the Nordic Seas are still important for the global climate as they influence the Atlantic inflow to the Arctic. The Atlantic water might have a profound effect on the Arctic sea-ice cover as discussed in the following section and in the results from this dissertation.

1.3.2 Arctic stratification

Proxy reconstructions suggest that the Nordic Seas during stadial times resembled that of the Arctic Ocean today (Sec. 1.1.2). Today, warm Atlantic water enters the Arctic Ocean where it flows cyclonically around the basin at depth. The warm water is overlayed by a cold fresh surface layer, and the two water masses are separated by a halocline (e.g., Aagaard et al., 1981; Aagaard and Carmack, 1989). In parts of the Arctic Ocean, this halocline has a signature feature as the salinity increases with depth while the temperature stays constant; "the cold halocline". The formation of the cold halocline is debated: Aagaard et al. (1981) argue that advection of cold and salty water from shallow shelves creates the cold halocline, while Rudels et al. (1996) argue for a process which includes sea-ice driven convection in the deep ocean during winter and the addition of fresh water from river runoff and sea-ice melt on top.

The cold fresh surface layer and the cold halocline are thought to be responsible for the co-existence of warm waters and sea ice in the Arctic Ocean as the halocline suppresses vertical mixing of heat (Aagaard et al., 1981). In addition, the Arctic Ocean is thought to be a low-energy ocean with little vertical mixing. Therefore, it is disputed how much influence the warm Atlantic water actually has on the sea-ice cover (e.g., Polyakov et al., 2012b). However, the Arctic Ocean is changing with a thinner and less extensive sea-ice cover (e.g., Kwok and Rothrock, 2009; Serreze and Stroeve, 2015). A retreat of the cold halocline has been temporally observed (Steele and Boyd, 1998). Observations furthermore show a warming and shoaling of the Atlantic water during the recent decades (Polyakov et al., 2012a) and the Atlantic water is hypothesized to become more important to the sea-ice retreat in the future (Polyakov et al., 2017). In addition, observations are showing positive heat fluxes from the ocean in the mids of the Arctic Ocean even in winter (Peterson et al., 2017) and a larger energy-transfer to the changed Arctic Ocean is suggested. It thus seems crucial to better understand the role of the ocean and Atlantic water in sea-ice dynamics.

The stability of the stratification

The stability of the Arctic stratification is relevant both for future changes in the Arctic Ocean and the understanding of the dynamics behind DO-events. The density of the cold fresh surface layer must be lower than that of the warm water below for this stratification to exist, but there might be feedback processes complicating this understanding. The stratification could break down with e.g., changes in the freshwater supply to the surface, a warming at subsurface, or with enhanced vertical mixing. The role of sea ice

for the stratification is not straight forward as the presence of sea ice could act as a positive or negative feedback on circulation changes. One example includes an increase in oceanic heat to the sea ice which would melt the ice. The sea-ice melt would enhance the stratification which again could change the oceanic heat. The heat flux from the ocean to the ice depends on the relation between flow strength and density differences. In models that include vertical mixing, the flow strength is sensitive to how the vertical velocity is represented (Lyle, 1997; Huang, 1999; Nilsson and Walin, 2001) and this will thus impact the sea-ice growth and feedback.

Freshwater is needed for a stable stratification with a fresh surface layer above a warmer subsurface, and Nilsson and Walin (2010) show with a conceptual model that there is a minimum freshwater input below which the halocline no longer exists. However, this again depends on the representation of diapycnal mixing as in models where the flow strength increases with density differences, the salinity-dominated stratification exists for all freshwater forcing values (Zhang et al., 1999; Longworth et al., 2005). If this is the case, the Arctic stratification might be very stable and other factors besides freshwater changes, such as increasing subsurface temperatures, would be needed to destabilize the water column.

The stability between sea ice and a salinity-dominated circulation related to the Arctic stratification, has not been studied as extensively as the thermally dominated circulation. Stigebrandt (1981) studied a sea-ice covered Arctic Ocean and found abrupt changes in sea-ice cover with reductions in the freshwater input, but the stability is not studied in detail. Several studies have looked at a one-dimensional column model to better understand the Arctic stratification, but feedbacks with the circulation are thus missing. For example, Nummelin et al. (2015) investigate the response of a one-dimensional atmosphere-ocean-ice column to increases in freshwater input. The result is a fresher and more shallow surface layer, and increasing subsurface temperatures. The authors show little change in the heat flux from the ocean to the ice as the increase in the temperature of the subsurface balances the increasing stratification due to freshwater. Pemberton and Nilsson (2015) also find a shoaling of the halocline with increased freshwater input both in a conceptual model and in GCM experiments which show an increase in Atlantic water temperature with increasing freshwater. Pemberton and Nilsson (2015) argue that advection changes and less transformation processes contribute to the increase in temperature, while Nummelin et al. (2015) argue for a change in vertical mixing processes. Another column study by Singh et al. (2014) has oscillations in sea ice broadly consistent with the DO-events. A polynya is found to be crucial to sustain oscillations between an ice free and an ice covered Nordic Seas. However, the authors assume that only 10% of today's heat enters the Nordic Seas and this might not be consistent with the proxy records.

1.3.3 Summary

Detailed studies of the stability of the Arctic stratification are needed both to understand future and past changes in sea ice. Both the role of Atlantic water temperatures and changing freshwater inputs need to be better understood. The two are suggested to change during the DO-cycles, but also in the future. The physics described in this introduction are dominated by small-scale processes that are difficult to resolve and analyze. Simplified and conceptual models are thus important for our understanding of

the Arctic stratification.

Chapter 2

Objectives and Methods

Changes in the sea-ice cover of the Nordic Seas are hypothesized to drive the large warming on Greenland associated with the Dansgaard-Oeschger events of the last glacial period. Paleoclimatic reconstructions suggest that the hydrography of the Nordic Seas during stadial periods resembled the Arctic Ocean today, and that a subsurface warming led to the destruction of this stratification. However, it is not clear whether an Arctic-like stratification can exist in the Nordic Seas or which processes led to fresh and cold waters dominating the surface of the Nordic Seas. In addition, the impact of a sea-ice cover in the Nordic Seas on the ocean circulation is unresolved.

In this dissertation, we study the sensitivity of a potential sea-ice cover in the Nordic Seas to changes in ocean temperatures and freshwater input, which both affect the vertical stratification. We also study the impact of a sea-ice cover on ocean circulation and combine proxy and fully coupled climate model simulations to learn more about the ocean-state during DO-events.

Our main research questions are:

- How can a sea-ice cover and a halocline exist in the Nordic Seas in the presence of warm Atlantic water?
- How stable is the halocline and sea-ice cover in the Nordic Seas to changes in freshwater input and Atlantic water temperatures and how can the sea-ice cover abruptly disappear?
- What are the implications of a sea-ice cover on the ocean circulation?

We take a modelling and theoretical approach to learn about the Nordic Seas during DO-events outside of the proxy locations. Due to the long millennial time scale in question here, and model restrictions, transient simulations of the MIS3 are still limited. We view the cold stadial periods as quasi-steady states and use three different idealized modelling approaches to learn about the Nordic Seas during stadial times. Both Paper I and II are theoretical studies without a real time component and parts of the results can also be used to understand the changing Arctic Ocean, or other basins with similar characteristics. However, in Paper III we focus on the mid of MIS3: 30-40 ka and DO-cycles 5-8.

In Paper I we develop a simple conceptual model of a sea-ice covered area supposed to represent the Nordic Seas during stadial times. We couple an analytical sea-ice model to a two-layer ocean with a cold fresh surface layer and a warmer layer below,

and study the sensitivity to freshwater input and changing subsurface temperatures. The conceptual model is one-dimensional and does not include spatial differences in the Nordic Seas. In Paper II we move to a three-dimensional system, although still idealized. We use an eddy-resolving configuration of the Massachusetts Institute of Technology general circulation model (MITgcm) with an idealized topography to further study the impact of the inflowing warm Atlantic water on the sea-ice cover. We couple the ocean component to a thermodynamic and dynamic sea-ice model, but keep the atmosphere simple. Ocean surface temperatures are restored toward constant atmospheric temperatures, and no precipitation nor wind is included. Contrary to Paper I, external freshwater supplies are not included in Paper II. However, extra results with freshwater inputs are presented in Sec. 6.2.1. In Paper 3 we move on to fully coupled GCMs to learn about the northern North Atlantic during the DO-events. We compile all available planktic foraminifera records from the North Atlantic and 30-40 ka with a robust sea-surface temperature reconstruction. These are then combined with already run GCM simulations, both freshwater forced and control simulations, using the proxy surrogate reconstruction method. This is the first time this method has been used so far back in time and on ocean data only.

Chapter 3

Summary of Papers

Paper I: *The interaction between sea ice and salinity-dominated ocean circulation: implications for halocline stability and rapid changes of sea ice cover*

In this paper we couple a two-layer ocean model to an analytical sea-ice model to study the interaction between sea ice and oceanic heat and freshwater transports. The sensitivity of the hypothesized stratification of the Nordic Seas during stadial times is investigated with respect to freshwater, sea ice and vertical mixing of heat. The salinity-dominated circulation is known to be sensitive to changes in the freshwater supply and a halocline solution might not exist at low freshwater inputs. We show that by adding sea ice this sensitivity is reduced by the stabilizing effect of sea ice. In this paper, the stabilizing effect is through a thickness dependent ice export, but it could also be interpreted as sea-ice melt as a decreased ice export leads to a fresher surface just as increased sea-ice melt would. However, the stabilizing effect of sea ice is not enough to introduce stable solutions in all cases, and as a consequence, abrupt changes in stratification and sea ice can be expected at low freshwater supplies. In addition, increasing subsurface temperatures destabilize the system and remove sea ice at high temperatures. We show that the subsurface does not need to warm as much as previously thought for an instability in the vertical water column to occur. However, the stabilizing effect depends on the representation of the vertical mixing, and sea ice acts as a positive feedback when the vertical mixing is parametrized with a constant diffusivity. Independent of the representation, non-linear changes in sea ice can occur with small changes in freshwater input or subsurface temperatures.

Paper II: *Sea-ice cover in the Nordic Seas and the sensitivity to Atlantic water temperature*

In Paper II we use an eddy resolving idealized set-up with the ocean and sea-ice component of the Massachusetts Institute of Technology general circulation model to study the sensitivity of a sea-ice cover in the Nordic Seas to Atlantic water temperatures. We find that an extensive sea-ice cover and Arctic-like stratification can exist in the Nordic Seas-like domain without external freshwater inputs. A halocline forms due to the stratifying effect of sea-ice formation and melt, and a fresh surface layer appears. Atlantic water still enters the Nordic Seas but now at depths below the cold fresh surface layer. However, for the halocline to emerge spontaneously the heat import into

the Nordic Seas needs to reduce sufficiently. For high Atlantic water temperatures, sea ice only exists in the interior of the Nordic Seas. There is a non-linear shift in sea-ice extent with decreasing Atlantic water temperatures. We also find that the experiment that is closest to the non-linear shift has self-sustained oscillations in the sea-ice cover, probably linked to subsurface heat build-up. The sea ice has implications for the ocean circulation as the sea-ice cover reduces downwelling, overturning circulation, deep-water temperature, and heat import into the Nordic Seas.

Preliminary results from additional experiments suggest that external freshwater supplies move the limit for an extensive sea-ice cover to higher Atlantic water temperatures, and allow for larger oscillations in sea-ice volume. The addition of freshwater does not have a large impact on sea-ice volume in the already fully sea-ice covered experiments.

Paper III: *A spatio-temporal reconstruction of sea-surface temperatures in the North Atlantic during Dansgaard-Oeschger events 5-8*

In Paper III we combine proxy records and fully coupled general circulation models to learn more about the spatial picture of Dansgaard-Oeschger events 5-8. We apply the proxy surrogate reconstruction, or the analog-method, to 14 planktic foraminifera sea-surface temperature reconstructions from years 30-40 ka. The best match between a pool of possible ocean states (the output from the GCMs) and each time step in the proxy records is found, and we thus provide a spatial picture of sea-surface changes over DO-events 5-8. This is the first time this method has been applied to marine data only and to the time period of MIS3. With the limited set of general circulation models we have available, we find that forced runs are needed to capture the amplitude of the sea-surface temperature variability and to extend the sea-surface temperature signal to the atmosphere over land. Specifically, the new time series of atmospheric temperature variability that appears from constraining the model simulations with ocean data agree with temperature reconstructions from ice-core records when forced runs are included in the model pool. We have only included forced simulations in the sense of freshwater-forced simulations, which have a large impact on both the Atlantic Meridional Overturning circulation and the sea-ice cover. Using pre-industrial control simulations consistent temperature patterns are found. This suggests that the pattern of temperature variability during DO-events resembles modern internal variability, and indicates that the climate system is capable of DO-events if the boundary conditions are right. We suggest that sea-ice changes are important in extending the temperature signals to land, but that also the different boundary conditions including ice sheet and orbital forcing could be of importance.

Chapter 4

Discussion and Main Conclusions

We study the sensitivity of the Arctic stratification and sea ice to changes in freshwater and Atlantic water temperature in both Paper I and II. A comparison of these two studies is shown in Fig. 4.1. We note that the two models include different feedbacks and complexities, and a direct comparison is therefore limited. Three main differences, or caveats, are presented before the comparison is discussed.

First, the large-scale circulation is different in the two models. In Paper I, we consider a salinity-dominated stratification. The circulation of the MITgcm experiments is mainly thermally dominated with downwelling in the north and freshwater input in north acting to reduce the meridional density gradient. However, the stratification is controlled by salinity in the boundary current region when a full sea-ice cover is present in the Nordic Seas. Second, the shown results from Paper I are from the energy-constrained case where vertical mixing decreases with increasing stratification. The diffusion of heat increases with increasing vertical temperature gradients in the numerical model. There are no feedbacks between stratification and the large-scale circulation in the numerical experiments as the lower latitudes are restored to constant temperatures and salinities. However, this could also be the case for the conceptual model where the hydrography of the subsurface is representative for the open ocean farther south. Third, and final, we note that the contribution from sea-ice melt in Paper II is calculated as a freshwater flux. However, in steady-state sea-ice melt is balanced by sea-ice growth. Only external freshwater inputs are shown for the results from Paper I, although the change in sea-ice export acts as a freshwater supply. Including the latter would mainly extend the sea-ice thickness results to lower freshwater inputs. The Atlantic water temperature is the restoring temperature in the south for Paper II and the prescribed temperature of the deep in Paper I.

Despite the differences, sea-ice thickness increases with decreasing temperatures and/or increasing freshwater input for both the conceptual model and the numerical model (Fig. 4.1). The results from Paper I show high sensitivity in sea-ice thickness to increasing freshwater input when the freshwater input is small, and lower sensitivity at higher freshwater inputs. The number of experiments limits the knowledge of the sensitivity to freshwater input in the numerical model, but results suggest a threshold value in freshwater input that causes a large sensitivity in sea-ice thickness. The results from the numerical model suggest smaller sensitivities to high Atlantic water temperatures than in the conceptual model when the freshwater input is large.

The salinity-dominated circulation becomes unstable for weak freshwater supplies

and high temperatures (Paper I). The analog from the MITgcm is the WARM experiments (white cross in Fig. 4.1) which do not have a sea-ice cover in the boundary current while instead having a stable thermally dominated stratification in this region. The conceptual model was found to be stable for large freshwater supplies. We note that transient changes occur for large freshwater supplies in the MITgcm when an extensive sea-ice cover exists together with relative warm temperatures at depth. The conceptual model has prescribed deep-ocean temperatures that do not change with alterations in the stratification. Thus, a feedback between the stratification and subsurface temperatures is missing in the conceptual model, a feedback that might potentially alter the stability of sea ice to changes in stratification.

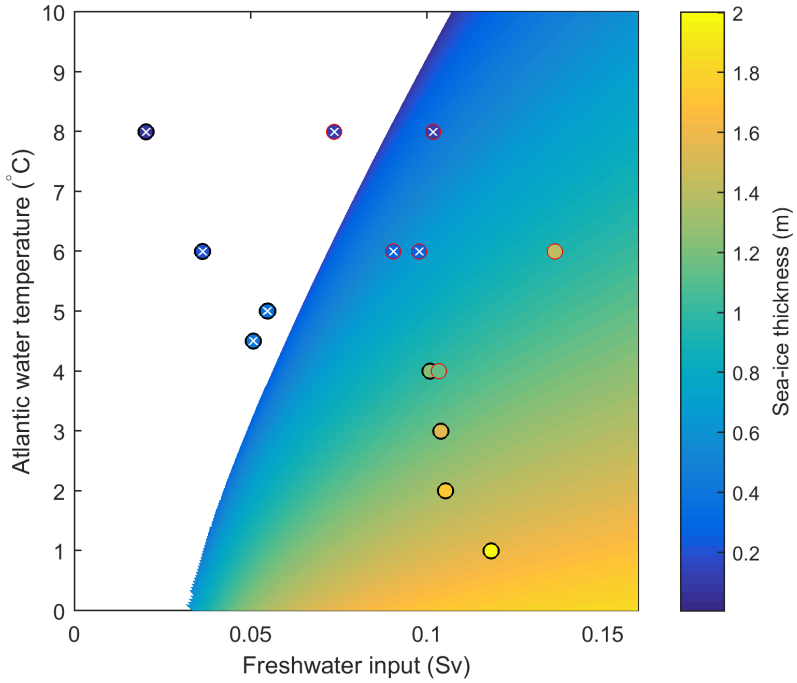

Figure 4.1: Sea-ice thickness with freshwater input and Atlantic water temperature. Background values are from Paper I and the energy-constrained case where the freshwater input is the external freshwater supply. The system turns unstable where the color disappears. Circles show the mean sea-ice thickness in the different MITgcm experiments (Paper II + extra). The freshwater input is the external supply + sea-ice melting. Experiments with external freshwater input are indicated with a red circle. White crosses indicate experiments without an extensive sea-ice cover.

Main conclusions

From the three papers we learn that

- The sea-ice cover in the Nordic Seas can abruptly disappear for small changes in surface freshwater input or Atlantic water temperature (Paper I), or occur spontaneously as a result of internal oscillations without a change in forcing (Paper II).
- Background climate is important for the sensitivity of sea ice to temperature and freshwater changes (Paper I and II). The sea-ice thickness is insensitive to small changes in forcing at large freshwater supplies and thick sea ice (Paper I), or at cold temperatures when an extensive sea-ice cover exists in the Nordic Seas (Paper II).
- For intermediate climate states, such as during the period with DO-events, only small changes in forcing are needed for large sea-ice changes, and unforced oscillations occur. In Paper III, DO-type variability is captured irrespective of background climate. However, the background climate is found to be important for the amplitude of the variability.
- Sea ice is important for the freshwater budget (Paper I and II). Sea ice dominates the freshwater budget at small external freshwater inputs in Paper I. In Paper II a halocline and fresh surface layer are present even in the absence of external freshwater supplies due to the redistribution of freshwater through sea-ice formation and melt.
- An extensive sea-ice cover can be present in the Nordic Seas even with an active overturning circulation and heat import to the Nordic Seas (Paper II and Paper III). However, an extensive sea-ice cover reduces the local circulation (Paper II).
- The presence of an extensive sea-ice cover reduces the heat release from the ocean to the atmosphere, and the oceanic heat recirculates in the ocean (Paper II). The reduction in heat transport to the atmosphere is important in extending DO-like oceanic temperature variability to Greenland (Paper III).

Chapter 5

Future Perspectives

5.1 Dynamics of the DO-events

This dissertation provides clues to how a sea-ice cover can exist in the Nordic Seas. It also provides support for the hypothesis of intrinsic sea-ice variability in the Nordic Seas as a mechanism for DO-events.

We have shown that a potential Nordic Seas ice cover is unstable to small changes in Atlantic water temperature and freshwater inputs (Paper I) and that internal unforced oscillations in the sea-ice cover can occur without a change in forcing (Paper II and Sec. 6.2.1). This argues for a similar mechanism to that of Dokken et al. (2013) who propose that a changing sea-ice cover is intrinsic to the Nordic Seas. Given sufficient cold conditions in the Nordic Seas, a sea-ice cover could develop, either aided by freshwater input from the Fennoscandian Ice Sheet as suggested by proxy reconstructions, or by the cold conditions alone. Depending on the background climate state, the sea-ice cover is unstable due to heat building up at depths leading to self-sustained oscillations in sea-ice cover. A second scenario involves small changes in forcing. We have shown that depending on the background climate small changes in freshwater or Atlantic water temperature could rapidly destroy the sea-ice covered state. Thus, only small stochastic changes in ocean circulation, freshwater input or e.g., the wind field could move the Nordic Seas into and out of a fully sea-ice covered state.

As DO-events affected areas outside the location of the Nordic Seas, intrinsic oscillations in the sea-ice cover of the Nordic Seas can only be a mechanism for DO-events if the sea-ice changes influenced regions farther south. Two likely mechanisms are through the AMOC or the atmospheric wind field.

It is not yet clear how the Nordic Seas would impact ocean circulation further south. We show in Paper II that sea-ice changes lead to changes in the downwelling and overturning of the Nordic Seas. However, whether the potential decrease in deep-water formation can change the global circulation farther south needs to be investigated more thoroughly. Two points come to mind. First, whether a change in deep-water production actually takes place should be analyzed further. A more correct representation of brine release in the MITgcm than currently included could lead to a compensating production of deep waters through brine release instead of convection. Today, deep water forms through this process on Arctic shelves (Aagaard et al., 1985), and the same could occur in the Nordic Seas during MIS3. At the same time, katabatic winds from the Fennoscandian Ice Sheet could lead to efficient deep-water production as in Antarctica

today (Gill, 1973). Paleoclimatic reconstructions indicate enhanced deep-water formation by brine release when a sea-ice cover is present in the Nordic Seas (Dokken and Jansen, 1999; Dokken et al., 2013, Sec. 1.1.2). However, this is interpreted from low δ^{18}O-values at depths, a signature which could also indicate increased deep-water temperatures (e.g., Rasmussen and Thomsen, 2004; Ezat et al., 2014). We find a warming of the subsurface when an extensive sea-ice cover is present, but our results indicate a cooling of the deep water and overflow (Paper II). Hence, our results do not support the notion of warmer deep waters during stadials. If the deep-water formation in the Nordic Seas decreased during stadials, the deep-water formation sites south of the GSR could compensate as discussed in Sec. 1.3.1. On the other hand, these convection sites could also be affected by the sea-ice cover as enhanced ice and freshwater-export from the Nordic Seas (Paper I and II) could hinder convection.

Second, whether changes in the deep-water formation in the Nordic Seas alone can affect the global climate needs to be better understood. Gildor and Tziperman (2001a) show that a North Atlantic sea-ice cover cools the temperature of the NADW. The temperature signal is transported to the Southern Ocean where it affects the stratification and increases sea ice. It would be interesting to expand the southern domain of the numerical model to see whether the same change in temperature affects the Southern Ocean. Using the conceptual model of Paper I, one could investigate whether the link between the two hemispheres is robust to different representations of vertical mixing. At present, there are no feedbacks between water mass transformation in the Nordic Seas and the stratification at low latitudes in the numerical model of Paper II. Including this would increase the spin-up time of the model but allow for a better understanding of the global effect of a Nordic Seas ice cover.

How much the northern heat transport is affected by the NADW modification is a recurring question. If the northward heat transport by the AMOC is reduced as a consequence of increased sea-ice extent, the reduction in AMOC could act as a negative feedback on the sea-ice cover with less heat import into the region. This could enhance the stability of the sea-ice cover in the Nordic Seas. In paper III, a sea-ice cover is present in the North Atlantic together with a large reduction in the AMOC. These changes are needed to enhance the DO-variability and to extend ocean temperature variability to the atmosphere over land. We have not separated the effect of the AMOC from that of the sea-ice cover, and including model simulations with changes in sea ice independent from AMOC changes could aid in this understanding. As a small change in the heat transport to the Nordic Seas could shift the sea-ice cover, and paleoclimatic reconstructions indicate ocean circulation changes over the DO-events (Sec. 1.1.1), changes in the AMOC could still be important for the DO-dynamics.

The millennial-time scale of the DO-cycles is not addressed in this dissertation. The results support a reduction in sea-ice cover as a mechanism for the abrupt warming associated with the stadial-interstadial cycles. The abrupt warming occurred in only a few decades consistent with the time scale of the removal of sea ice (Paper II and Sec. 6.2.1). However, the period of the self-sustained oscillations in sea-ice cover as shown in Sec. 6.2.1 does not agree with the millennial time scale; the oscillations occur in decades. This could be related to the idealized set-up of the simulations; the shallower than realistic basin, the missing feedbacks with wind and freshwater export, or the missing seasonal variability. How the enhancement of the stratification by summer sea-ice melt would increase the stability and time scale of the sea-ice cover is a relevant

question. The missing feedbacks could also affect the stability of the sea-ice cover.

Enhanced freshwater export from the Nordic Seas has the potential to impact the subpolar gyre which regulates heat import into the Nordic Seas (Born and Levermann, 2010; Born et al., 2015). A freshening would slow down the subpolar gyre which could allow for more heat to enter the Nordic Seas. The increased heat transport could then destroy the Nordic Seas sea-ice cover. The MITgcm experiments show a slower subpolar gyre for the experiments that have a full sea-ice cover. However, the extension of the area south of the Nordic Seas is limited, and it is not clear whether the reduced gyre is a dynamical response or an artifact. One straightforward test would be to perform the same experiments with a larger domain south of the GSR.

We have not addressed the relation between atmospheric circulation and the sea-ice cover in this dissertation. The relation could both act as a new feedback to the stability of the sea ice and lead to the DO-signatures observed in regions outside the North Atlantic. Winds influence the heat transport to the Nordic Seas and could thus affect the sea-ice cover. We did not include winds in the numerical model as similar studies did not show a large wind-impact on the heat transport in the idealized domain (Spall, 2011). However, winds could still be of importance in a different climate and especially close to the sea-ice edge where large atmospheric temperature gradients exist. In today's Arctic Ocean wind is the main energy source for vertical mixing (Fer et al., 2017). Wind changes would have the largest effect on thin sea ice and could thus be an important enhancer on a shrinking sea-ice cover. The effects of wind on a changing sea-ice cover could be investigated using Paper I where the energy supply to the vertical mixing could decrease with an increasing sea-ice cover. Winds or changing diffusion with sea-ice cover could also be included in the numerical model of Paper II. However, we note that sensitivity experiments with increased diffusion in the MITgcm suggest little relevance of the mixing and better representation of vertical mixing might be needed.

Results from paper III suggest that the pattern of sea-surface temperature variability during DO-events resemble sea-surface temperature patterns of modern internal variability, and perhaps the only thing missing in the present climate for DO-events to occur is the right boundary conditions. One interesting question is why DO-events occurred during the last glacial period but not during interglacials. All three papers from this dissertation suggest that the boundary conditions are of importance for the DO-variability and that cold enough conditions might have to occur.

5.2 Arctic Ocean

The results presented here are not only relevant for DO-events and a glacial climate, but also for the Arctic Ocean and future changes. The sea-ice cover in the Arctic is undergoing large changes with a sea-ice decline in both extent and thickness (e.g., Kwok and Rothrock, 2009; Serreze and Stroeve, 2015). At the same time, freshwater input to the Arctic Ocean is increasing through an enhancement of the hydrological cycle due to global warming (Haine et al., 2015). The temperature of the Atlantic water entering the Arctic Ocean has also been found to increase, and the ocean is hypothesized to become more important in driving the sea-ice melt than what has been assumed before (Polyakov et al., 2012a, 2017). It is debated whether the temperature of the subsurface

can affect the sea ice as the cold halocline suppresses vertical heat fluxes. However, as recent observations have shown large heat fluxes even in winter (Peterson et al., 2017), the ocean's impact on the Arctic interior sea-ice cover should be studied further.

Although the focus region of this dissertation is the Nordic Seas during stadials, the results concerning the sensitivity of the sea ice are highly relevant for the changing Arctic Ocean. The oceanographic settings in the two regions are similar with a cyclonic boundary current of warm Atlantic water at depths. Differences include a larger role for freshwater in the Arctic Ocean. Our results suggest that the increasing Atlantic water temperatures might have profound effects on the sea-ice cover even in the presence of increasing river runoff. If the halocline in the Arctic Ocean is produced by similar processes as those described in Paper II, the small observed increase in Atlantic water temperatures might lead to large and rapid changes in sea-ice cover as the fresh surface layer might disappear.

Greenland temperatures have been sensitive to changes in Nordic Seas ice cover in the past, and perhaps also to the changing sea-ice cover of the Arctic. With the already increased temperatures due to global warming, a 10 degree warming on Greenland due to sea-ice changes would have profound implications for the ice-sheet balance.

Chapter 6

Scientific Results

I

Paper I

6.1 The interaction between sea ice and salinity-dominated ocean circulation: implications for halocline stability and rapid changes of sea ice cover

Jensen, M. F., J. Nilsson, and K. H. Nisancioglu (2016), *Climate Dynamics* **47**, 3301–3317, doi:10.1007/s00382-016-3027-5

Clim Dyn (2016) 47:3301–3317
DOI 10.1007/s00382-016-3027-5

The interaction between sea ice and salinity-dominated ocean circulation: implications for halocline stability and rapid changes of sea ice cover

Mari F. Jensen[1,2] · Johan Nilsson[3] · Kerim H. Nisancioglu[1,2]

Received: 12 June 2015 / Accepted: 6 February 2016 / Published online: 23 February 2016

Abstract Changes in the sea ice cover of the Nordic Seas have been proposed to play a key role for the dramatic temperature excursions associated with the Dansgaard–Oeschger events during the last glacial. In this study, we develop a simple conceptual model to examine how interactions between sea ice and oceanic heat and freshwater transports affect the stability of an upper-ocean halocline in a semi-enclosed basin. The model represents a sea ice covered and salinity stratified Nordic Seas, and consists of a sea ice component and a two-layer ocean. The sea ice thickness depends on the atmospheric energy fluxes as well as the ocean heat flux. We introduce a thickness-dependent sea ice export. Whether sea ice stabilizes or destabilizes against a freshwater perturbation is shown to depend on the representation of the diapycnal flow. In a system where the diapycnal flow increases with density differences, the sea ice acts as a positive feedback on a freshwater perturbation. If the diapycnal flow decreases with density differences, the sea ice acts as a negative feedback. However, both representations lead to a circulation that breaks down when the freshwater input at the surface is small. As a consequence, we get rapid changes in sea ice. In addition to low freshwater forcing, increasing deep-ocean temperatures promote instability and the disappearance of sea ice. Generally, the unstable state is reached before the vertical density difference disappears, and the temperature of the deep ocean do not need to increase as much as previously thought to provoke abrupt changes in sea ice.

Keywords Sea ice feedbacks · Halocline dynamics · Salinity-dominated ocean circulation · Conceptual model · Dansgaard–Oeschger events

✉ Mari F. Jensen
mari.f.jensen@uib.no

[1] Department of Earth Science, University of Bergen, Bergen, Norway

[2] Bjerknes Centre for Climate Research, Bergen, Norway

[3] Department of Meteorology, Stockholm University, Stockholm, Sweden

1 Introduction

The mechanism behind Dansgaard–Oeschger (D–O) events, the abrupt climate changes which occurred repeatedly during the last glacial period, is still debated. One of the hypothesized mechanisms involves a retreating North Atlantic sea ice cover (Broecker 2000; Gildor and Tziperman 2003; Masson-Delmotte et al. 2005; Li et al. 2005). Due to the ice-albedo feedback, the strong insulating effect, and impact on the atmospheric circulation, a changing sea ice cover in the Nordic Seas is a likely agent for the abrupt warming observed on Greenland during D–O events (e.g. Dansgaard et al. 1993; Severinghaus and Brook 1999). Thus, a retreating sea ice cover can explain the transition from cold stadial conditions to warmer, interstadial conditions on Greenland and in the northern North Atlantic (Li et al. 2005). In addition, a changing sea ice cover can explain several other features of the abrupt climate events, including precipitation changes (e.g. Peterson et al. 2000; Li et al. 2005, 2010), and changes in dust content (Mayewski et al. 1997). Here, we investigate the interactions between sea ice and a salinity-dominated ocean circulation in a conceptual model of the Nordic Seas to explore the possible role of sea ice in the abrupt warming associated with D–O events.

Internal instability in the oceanic thermohaline circulation, or the Atlantic Meridional Overturning Circulation

(AMOC) has also been suggested as a mechanism for rapid climate change (Broecker et al. 1990; Tziperman 1997; Marotzke 2000; Ganopolski and Rahmstorf 2001). Broecker et al. (1990) first suggested internal oscillations in the volume transport of the AMOC as a mechanism for D–O events. The idea is that a strong circulation transports more heat from the South Atlantic to the North Atlantic, thereby warming the atmosphere at high latitudes. A weak, or an off state of the AMOC could lead to less heat import to the North Atlantic causing cold stadial conditions. Several modeling studies have simulated an AMOC with a strong and a weak state (e.g. Stocker and Wright 1991; Fanning and Weaver 1997; Manabe and Stouffer 1995; Stouffer et al. 2006). However, paleoclimatic reconstructions have shown active formation of North Atlantic Deep Water also during stadials (Yu et al. 1996). Latitudinal shifts in the North Atlantic Deep Water formation site is also hypothesized to account for the D–O events (Ganopolski and Rahmstorf 2001; Arzel et al. 2010; Colin de Verdiere and Raa 2010; Sevellec and Fedorov 2015). Freshwater forcing has typically been the agent to force the different states of the circulation, and the duration of the cold and the warm states generally depend on the duration of the freshwater forcing (Ganopolski and Rahmstorf 2002). On the other hand, Marotzke (1989), Winton (1993) and Winton and Sarachik (1993) found self-sustaining oscillations with strong and weak overturning due to increasing deep-ocean temperatures. Their idea is that freshwater input at the poles causes a strong, vertical salinity gradient (halocline) which suppresses deep-water formation. The stability of the high latitude halocline breaks down as diffusion from the south heats the deep ocean. Deep-water formation becomes active again, and warm, light water is transported to the high latitudes which then again stabilizes the water column. These deep-decoupling oscillations bear resemblances to the D–O stadial and interstadials (Timmermann et al. 2003). Seen in isolation, a changing AMOC gives a temperature response on Greenland which is too slow and too small compared to the observations. However, the addition of a responsive sea ice cover in the Nordic Seas would enhance the temperature response to small internal oscillations in the ocean.

Paleoclimatic reconstructions support a warming of the subsurface Nordic seas during cold stadial conditions (Dokken and Jansen 1999; Rasmussen and Thomsen 2004; Dokken et al. 2013). In particular, it has been proposed that the warming of the subsurface ocean during cold stadial conditions could explain the rapid retreat of sea ice in the Nordic Seas at the start of each interstadial (Dokken et al. 2013). From a marine sediment core from the Faeroe-Shetland channel, Dokken et al. (2013) showed systematic changes in the hydrography of the Nordic Seas during cold stadials and warm interstadials. During stadial conditions, the hydrography was similar to the Arctic Ocean today, with a cold, fresh surface layer above a warmer Atlantic layer. A sharp halocline marks the transition between the two different water masses, protecting the surface layer from the heat below. The authors proposed that the vertical density gradient and the halocline would gradually weaken due to a slow warming of the deep ocean. Eventually, as the vertical density difference disappeared, the stability of the water column would break down. When the halocline is gone, the Atlantic layer would mix to the surface, melting the sea ice cover. This scenario is dependent on a mechanism that gradually increases the temperature of the Atlantic layer.

A different scenario involves slow changes in the freshwater supply to the ocean. By using an analytical two-layer ocean model, Nilsson and Walin (2010) showed that the salinity-dominated (estuarine) circulation and halocline can break down even before the vertical density gradient vanishes. If this is also true for ice-covered conditions, which can entail additional feedbacks, the convective overturning proposed by Dokken et al. (2013) could occur at low freshwater inputs, even before the vertical density gradient disappears. This would be highly relevant for cold, dry glacial climates. An interesting question is at what point the halocline disappears given a constant temperature below the halocline.

However, the properties of thermohaline circulations are dependent on the relation between flow strength and density differences. In thermohaline models which include vertical mixing, the flow strength is sensitive to how the vertical velocity is represented (Lyle 1997; Huang 1999; Nilsson and Walin 2001). Assuming a fixed external energy supply to the small scale mixing, Nilsson and Walin (2010) represented the vertical velocity with a stratification-dependent vertical diffusivity. The result is a diapycnal velocity which decreases with increasing stratification and an ocean circulation which acts in the same way. If instead, diapycnal velocity is represented with a constant diffusivity, the ocean circulation increases with increasing stratification (e.g. Bryan 1986; Zhang et al. 1999; Nilsson and Walin 2001). As the classical box model by Stommel (1961) involves a flow which speeds up with increasing density difference, the latter representation bears resemblances to the typical Stommel model.

Thus, the stability of the salinity-dominated circulation depends on the assumed properties of the diapycnal mixing. In the conceptual model by Nilsson and Walin (2010) the authors found that there is a minimum freshwater input below which the halocline solution no longer exists. In models where the flow strength increases with density differences, there exists a solution for all freshwater forcing for the salinity-dominated circulation (Zhang et al. 1999; Longworth et al. 2005). If this is the case, other factors, such as increasing subsurface temperatures, are needed to

initiate convective overturning. However, Longworth et al. (2005) and Guan and Huang (2008) showed that the presence of wind-driven, horizontal salt transport destabilizes the thermohaline circulation, and removes the equilibria at weak freshwater supplies. Therefore, additional factors may have the potential to introduce convective overturning due to low freshwater forcing in models with a constant diffusivity as well.

As the proposed mechanism by Dokken et al. (2013) involves a sea ice covered Nordic Seas, we add the sea ice model from Thorndike (1992) to the simple two-layer ocean model of Nilsson and Walin (2010). The aim of the study is to investigate how the presence of sea ice affects the dynamics and stability of the salinity-dominated circulation as the climatic conditions are varied. As the detailed features of the diapycnal mixing are not well known, we will in this study examine the two different vertical mixing representations discussed above. The experiments are divided into an "energy-constrained model", where we retain the diapycnal velocity from Nilsson and Walin (2010), and a "constant-diffusivity model" where the diapycnal velocity is parametrized with a constant diffusivity. The vertical mixing is expected to change with a changing sea ice cover and climate. Therefore, even though the first case is more physically consistent, it is useful to study different representations of the vertical mixing.

Interactions between sea ice and thermally-dominated thermohaline circulation have been studied in conceptual models by for instance Yang and Neelin (1993, 1997) and Jayne and Marotzke (1999). Using a Stommel-type box model coupled to an energy-balance representation of the atmosphere, Jayne and Marotzke (1999) found that sea ice related feedbacks destabilized the thermally-dominated mode of the thermohaline circulation. In their model, feedbacks between sea ice, meridional temperature gradients and atmospheric moisture transport were of key importance, whereas brine rejection associated with sea ice formation played a more central role in the box model of Yang and Neelin (1993). However, less attention has been paid to how sea ice feedbacks affect a salinity-dominated thermohaline circulation. Stigebrandt (1981) developed a process-oriented two-layer model of the Arctic Ocean, which incorporates inflows and outflows, air-sea heat exchange, and sea ice dynamics. Interestingly, Stigebrandt found that the sea ice cover in the model vanished abruptly when the freshwater supply to the Arctic Ocean was reduced below some threshold value. In fact, Nilsson and Walin (2010) essentially used the same geostrophic flow representation as Stigebrandt (1981). However, Stigebrandt's model contains additional complexities which makes it difficult to examine the sea ice related feedbacks in more detail.

In this study, we develop a conceptual model that is simple enough to admit analytical analyses of the key feedbacks. First, the two-layer ocean model by Nilsson and Walin (2010) and the simplified sea ice model from Thorndike (1992) will be presented in Sect. 2. We review the response of the model to freshwater forcing in the absence of sea ice in Sect. 3. Then, the response of the model to freshwater forcing in the presence of sea ice is presented in Sect. 4. We compare the stabilizing effect of sea ice in the energy-constrained model with the constant-diffusivity model in Sect. 4.2. In Sect. 5, we investigate the effect of increasing deep-ocean temperatures on the stability of the system. In Sect. 6, we discuss the impact of the results on the Dokken et al. (2013) hypothesis.

2 Model formulation

Here we will show how the conceptual two-layer ocean model from Nilsson and Walin (2010) can be coupled to the simplified sea ice model from Thorndike (1992). The two model components are presented below, and the coupled ocean–ice system can be seen in Fig. 1. Variables that are not defined in the text can be found in Table 1. The simplified ocean and ice models used here are well established and used in numerous studies. The novelty of this study is to examine the physics that results from their coupling. Useful background information on the physical motivation and derivation of two-layer ocean models can be found in e.g. Gnanadesikan (1999), Nilsson and Walin (2001) and Johnson et al. (2007). Bitz and Roe (2004) provide a concise derivation of the sea ice model from Thorndike (1992).

The ocean model consists of a cold, light surface layer, and a warmer, homogeneous deeper layer with the same hydrography as the open ocean. The circulation is that of a salinity-dominated regime, in the sense that supply of freshwater at the surface establishes a stable stratification. The topography is that of a semi-enclosed basin (Fig. 1). The basin receives freshwater from river run-off, precipitation, and ice-import, together denoted as F_{riv}. The ocean flow consists of the diapycnal flow M_D, and the horizontal geostrophic outflow M_G. The diapycnal flow increases the depth of the light surface layer H, while M_G thins the surface layer.

The subsequent derivations follow Nilsson and Walin (2010). By applying a time-dependent version of the Knudsen's relations (Knudsen 1900), the conservation of volume and salinity can be written as

$$A\frac{dH}{dt} = M_D - M_G + F_{net}, \tag{1}$$

$$A\frac{dHS}{dt} = S_A M_D - S M_G, \tag{2}$$

Table 1 Definitions of variables for the model

	Variables	
A	Area of surface layer (Nordic Seas)	2.5×10^{12} m^2
A_{ex}	Area export	2.5×10^4 m^{2}s^{-1}
A_i	Coefficient of linearized Stefan Boltzmann's law σT_f^4, $T_f = 273K$	320 W m^{-2}
A_s	Stability matrix	
B	Coefficient of linearized Stefan Boltzmann's law $4\sigma T_f^3$	4.6 W m^{-2}K^{-1}
D	Ice melt	Variable (m)
E	Sea ice export	Variable (m)
F_{atm}	Atmospheric meridional heat advection	100 W m^{-2}
F_{ice}	Sea ice export	Variable (Sv)
F_{net}	Net freshwater forcing	Forcing parameter (Sv)
F_{riv}	Freshwater input	Forcing parameter (Sv)
F_{sw}	Shortwave radiation	175 W m^{-2}
G	Ice growth	Variable (m)
H	Surface layer depth	Variable (m)
L	Latent heat of fusion	3×10^8 J m^{-3}
M	Steady-state flow	Variable (Sv)
Q	Heat flux from ocean to sea ice	Variable (W m^{-2})
S	Surface layer salinity	Variable (psu)
S_A	Atlantic water salinity	35 psu
T	Surface layer temperature	$-1.8\,^\circ$C
T_A	Atlantic water temperature	Forcing parameter ($^\circ$C)
T_i	Ice temperature	Variable ($^\circ$C)
c_p	Heat capacity of sea water	4000 J kg$^{-1}\,^\circ$C^{-1}
f	Coriolis parameter	1.37×10^{-4} s^{-1}
g	Acceleration of gravity	9.81 m s^{-2}
h	Ice thickness	Variable (m)
k	Thermal conductivity	2 W m^{-1} K^{-1}
$n_{w,s}$	Optical depth for winter or summer	2.5 or 3.25
α	Sea ice albedo	0.65
β	Haline expansion coefficient	Variable (psu^{-1})
ϵ	The rate of work against the buoyancy force associated with the vertical mixing	1×10^{-3} W m^{-2}
κ	Vertical diffusivity (constant-diffusivity model)	1×10^{-3} m^{2}s^{-1}
ρ_0	Constant density reference	1000 kg m^{-3}
τ	One half year	

1 Sv $= 10^6$ m^{3}s^{-1}

where S is the salinity of the surface layer, S_A is the salinity of the Atlantic layer, $F_{net} = F_{riv} - F_{ice}$ is the net freshwater input to the surface, F_{ice} is the sea ice export, and A is the area of the Nordic Seas. Note that in steady-state, the above equations become the classical Knudsen's relations.

By combining Eqs. 1 and 2, we get

$$AH\frac{d\Delta S}{dt} = -\Delta S M_D + (S_A - \Delta S)F_{net}, \tag{3}$$

where $\Delta S = S_A - S$, and S_A is a constant. This equation can be simplified further: In the open ocean, away from coastal regions, one typically finds that $S_A \sim 35$ and $\Delta S \sim 3$. Therefore, $\Delta S/S_A$ is significantly smaller than unity. This is widely used in oceanography to derive the Boussinesq approximation equations (Vallis 2006) where the surface freshwater flux is substituted by a virtual salt flux boundary condition and the freshwater flux is neglected in the volume conservation equation. We exploit this and derive

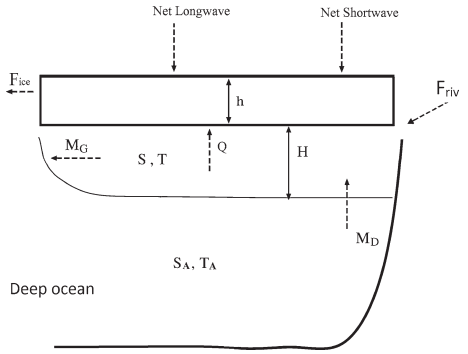

Fig. 1 A sketch of the coupled model. S and T are the surface layer salinity and temperature, respectively, while S_A and T_A are the salinity and temperature of the deeper, Atlantic layer. M_D and M_G are the diapycnal flow and geostrophic outflow, respectively. F_{riv} denote the freshwater input while F_{ice} denote the sea ice export. The surface layer depth is represented by H, the ocean heat flux by Q, and the sea ice thickness by h

simplified equations formally valid in the limit where $\Delta S/S_A \ll 1$. Note that the restriction $\Delta S/S_A \ll 1$ also implies that F_{net} is small compared to the volume flows M_D and M_G. This is consistent with the Boussinesq approximation. We can demonstrate this by examining the steady-state version of Eq. 3 in the limit $\Delta S/S_A \ll 1$, which yields $\Delta S M_D \sim S_A F_{net}$, or equivalently $F_{net}/M_D \sim \Delta S/S_A \ll 1$. From the steady-state volume conservation equation it follows that $M_D \sim M_A \gg F_{net}$. Therefore, when $\Delta S/S_A \ll 1$, we obtain the following approximate relations

$$A\frac{dH}{dt} = -M_G + M_D, \tag{4}$$

$$AH\frac{d\Delta S}{dt} = -\Delta S M_D + S_A F_{net}. \tag{5}$$

These equations yield a model that is simpler to analyse analytically, without changing the results qualitatively.

To derive representations of the flows M_G and M_D, we rely on physical reasoning based on the classical thermocline scaling (e.g. Welander 1971, 1986). To begin with, the horizontal flow, related to M_G, is taken to be in geostrophic and hydrostatic balance, which leads to the thermal wind balance. Further, we assume that the outflow for our "Nordic Seas" domain occurs in a baroclinic boundary current attached to a meridional boundary; analogously to how the low-salinity Arctic surface water exits from the Nordic Seas in the East Greenland Current today (e.g. Nilsson et al. 2008). Thus, we assume that the basic north–south density variation is similar to the east–west density variation in the outflow region (see e.g. Gnanadesikan 1999; Park and Bryan 2000; Nilsson and Walin 2001; Johnson et al. 2007, for further discussion). By applying the thermal wind balance to compute the volume transport in a two-layer baroclinic frontal current, one obtains (e.g. Nilsson and Walin 2001)

$$M_G = \frac{g\Delta\rho H^2}{2f\rho_0}, \tag{6}$$

where

$$\Delta\rho = \rho_0\beta\Delta S - \Delta\rho_T, \tag{7}$$

and $\Delta\rho_T$ is the density difference due to the temperature difference between the two ocean layers.

Previous studies have shown that the resulting dynamics of the ocean model is sensitive to the assumed physical features of the diapycnal flow M_D (e.g. Lyle 1997; Guan and Huang 2008; Nilsson and Walin 2001). Therefore, we examine two different representations of M_D that yield different dynamical behaviours of the model. Following the classical thermocline scaling, we assume that the vertical stratification is governed by an advective-diffusive balance (Munk 1966). Conservation of buoyancy is now used to obtain the scaling of M_D. By taking the two-layer model variables H and $\Delta\rho$ to represent the vertical scale and density variation of the stratification, respectively, the advective–diffusive balance suggests the following relation (Welander 1971, 1986)

$$M_D = \frac{A\kappa}{H}, \tag{8}$$

where κ is a constant vertical turbulent diffusivity. However, a strong background stratification tends generally to suppress the turbulent diffusivity (e.g. Huang 1999). If the turbulent diffusivity is taken to be constrained by the energy input from tides and winds, one can argue for the following expression for κ (Nilsson and Walin 2001)

$$\kappa = \frac{\epsilon}{g\Delta\rho}, \tag{9}$$

where ϵ is the rate of work against the buoyancy force associated with the vertical mixing. In this formula, κ decreases with increasing density stratification. Using the diffusivity formula (Eq. 9) in Eq. 8, we obtain the following alternative expression for the diapycnal flow

$$M_D = \frac{A\epsilon}{g\Delta\rho H}. \tag{10}$$

We note that this is essentially the formula from Kato and Phillips (1969), describing the entrainment rate across a mixed layer with a density jump at its base. Kato and Phillips derived their formula by equating a constant

mechanical energy input with the rate of increase in potential energy caused by the entrainment.

We are interested in the steady-state solutions where $M = M_D = M_G$ and $\Delta SM = S_A F_{net}$. We get the steady-state flow and surface layer depth by combining Eq. 6 with Eqs. 8 or 10. For the energy-constrained model, we get;

$$M = \left(\frac{A^2 \epsilon^2}{g 2 \rho_0 f \Delta \rho} \right)^{1/3}, \tag{11}$$

$$H = \left(\frac{A \epsilon 2 \rho_0 f}{g^2 \Delta \rho^2} \right)^{1/3}. \tag{12}$$

For the constant-diffusivity model;

$$M = \left(\frac{A^2 \kappa^2 g \Delta \rho}{2 f \rho_0} \right)^{1/3}, \tag{13}$$

$$H = \left(\frac{A \kappa 2 \rho_0 f}{g \Delta \rho} \right)^{1/3}. \tag{14}$$

2.1 Sea ice model

For the sea ice component, we follow Bitz and Roe (2004) and Thorndike (1992) which estimated equilibrium sea ice thickness h by assuming a quasi-steady balance between sea ice growth G and decay D. The sea ice thickness is estimated with only the main essential elements included; the net atmospheric flux incident at the top of the ice, and the heat flux Q from the ocean at the base of the ice. Making use of steady-state heat conduction through sea ice, and an atmosphere which is in thermal radiative equilibrium with the sea ice, we calculate G and D following Bitz and Roe (2004);

$$G(h) = \frac{\tau}{L} \left[\frac{A_i + B T_i(h)}{n_w} - \frac{F_{atm}}{2} - Q \right], \tag{15}$$

$$D = \frac{\tau}{L} \left[-\frac{A_i}{n_s} + \frac{F_{atm}}{2} + Q + (1 - \alpha) F_{sw} \right], \tag{16}$$

where the temperature of the ice T_i is given by

$$T_i(h) = \left(\frac{n_w h}{k n_w + B h} \right) \left(-\frac{A_i}{n_w} + \frac{F_{atm}}{2} \right). \tag{17}$$

F_{atm} is the atmospheric meridional heat advection, F_{sw} is the shortwave insolation, A_i and B are the coefficients of the linearized Stefan Boltzmann's law, Q is the heat flux from the ocean to the ice, α is the sea ice albedo, τ is one half year, L is the latent heat of fusion, k is the thermal conductivity, while n_w and n_s are the optical depths for winter and summer, respectively.

During summer, $T_i = 0\,^{\circ}\mathrm{C}$ is assumed, while $F_{sw} = 0$ during winter. F_{sw} is defined as the annual input of shortwave radiation, distributed over the melting season. The growth and melting seasons are each estimated as half of the year.

Decay melt is independent of h, while $\partial G / \partial h < 0$. Thin ice grows faster than thick ice, and as a consequence thick ice is more sensitive to changes in the forcing (Bitz and Roe 2004). Bitz and Roe (2004) showed that the change in thickness increases approximately quadratically with sea ice thickness as thicker ice needs to thin more to establish a new equilibrium.

In this study, we keep the atmospheric and solar energy fluxes constant; see Bitz and Roe (2004) and Stranne and Björk (2012) for the effect of variations in F_{sw} and F_{atm}, respectively. Therefore, variations of the steady-state sea ice thickness are controlled by the ocean heat flux, which is a function of the steady-state flow in the ocean;

$$Q = \frac{c_p \rho_0 M \Delta T}{A}, \tag{18}$$

where $\Delta T = T_A - T, T_A$ is the Atlantic layer temperature, and T is the temperature of the surface layer. A positive heat flux is directed upward into the ice.

Following Stranne and Björk (2012), we include a thickness dependent ice export E in the sea ice model,

$$E = \frac{2 \tau A_{ex} h}{A}, \tag{19}$$

where A_{ex} is the areal export. As we study changes in the sea ice thickness on time scales longer than seasonal, we can write;

$$2\tau \frac{dh}{dt} = G - D - E. \tag{20}$$

The equilibrium sea ice thickness can be found by solving for $G(h) - D = E(h)$. Hence, Eqs. 15–17 and 19 can be combined to one equation which can be solved for the unknown h.

When the ocean-model is coupled to the sea ice-model, the ice-export transports freshwater out of the system. Therefore,

$$F_{net} = F_{riv} - F_{ice}, \tag{21}$$

where[1]

$$F_{ice} = \frac{(G - D)A}{2\tau}. \tag{22}$$

[1] For simplicity, the salt content of the sea ice is ignored in the freshwater budget. This could be accounted for by multiplying F_{ice} with $(S_A - S_{ice})/S_A$, where S_{ice} is the sea ice salinity.

3 Model response to freshwater in absence of sea ice

In this section, we study the features of the model in the absence of sea ice. When the diapycnal flow decreases with increasing stratification, the steady-state flow decreases with increasing density differences (Eq. 11). As freshwater inputs at the surface increase the density difference, the flow decreases with freshwater input in the energy-constrained case (Fig. 2c). The surface layer depth also decreases with freshwater forcing (Fig. 2b). Thus, in the limit of small freshwater input, the low salinity surface layer becomes very deep, implying that the upper limit of the warmer Atlantic water layer is displaced to greater depths; a feature which may have relevance for the glacial Arctic Ocean stratification (Jakobsson et al. 2010; Cronin et al. 2012).

Nilsson and Walin (2010) showed that the salinity-dominated circulation does not have a solution below a threshold value of F_{riv}. The steady-state solution becomes unstable at small salinity contrasts (Fig. 2, stippled lines). To illustrate the underlying physics, we consider the feedbacks acting on a positive salinity perturbation, which decreases the vertical density difference. As we will show in Sect. 4.2, the mean flow always stabilizes, advecting away perturbations. However, the reduced vertical density difference is associated with a positive perturbation in the diapycnal flow (Eq. 10), which increases the salt transport to the upper layer. This further reduces the vertical salinity and density contrast, resulting in a positive feedback. For sufficiently small salinity contrasts, the positive feedback becomes larger than the negative feedback, and the system becomes unstable. In the more detailed stability analysis presented in the next section, it is shown that the flow becomes unstable when $\rho_o \beta \Delta S < 1.5 \Delta \rho_T$. As this limit is approached, the halocline solution breaks down and the surface layer is suggested to extend toward great depths (Fig. 2b). Additional physics need to be incorporated into the model to study this regime.

In contrast to the energy-constrained model, the constant-diffusivity model does have a solution for all density differences (Fig. 3). By applying a constant vertical diffusivity, the flow increases with density differences (Eq. 13). Since $H \propto \Delta\rho^{-1/3}$, the surface layer depth decreases with freshwater forcing also in this case (Fig. 3b). From Eq. 8 and 6, we see that M_D and M_G increases and decreases, respectively, with a reduced H. However, because M_G increases with $\Delta\rho$ and this response dominates that of H, the flow increases with freshwater forcing (Fig. 3c).

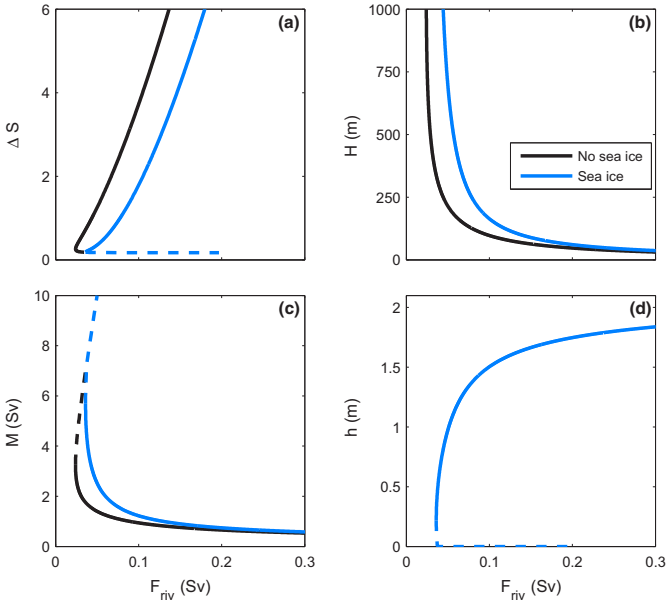

Fig. 2 Salinity contrast ΔS, surface layer depth H, steady-state flow M, and ice thickness h as a function of freshwater input F_{riv} in an energy-constrained model. An Atlantic water temperature of 1 °C is used. The *results* are shown both in the presence and absence of sea ice, specified in legend. *Full and stippled lines* represent the stable and unstable solutions, respectively. The *stippled line* ends where the vertical density difference vanishes

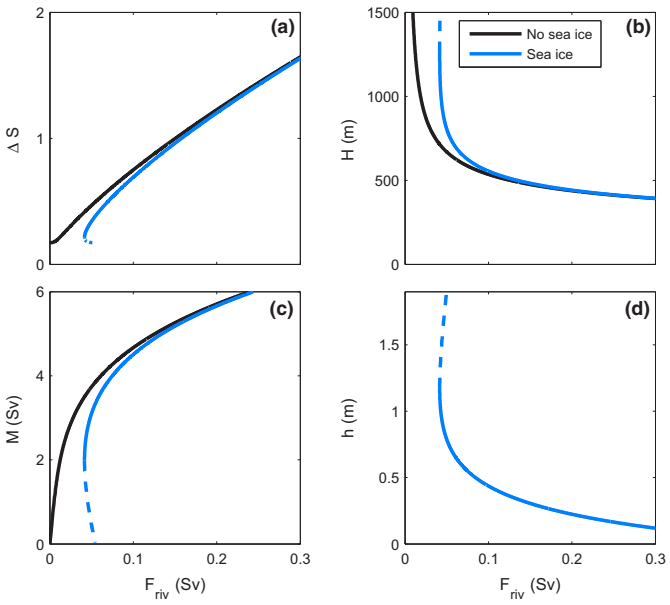

Fig. 3 Salinity contrast ΔS, surface layer depth H, steady-state flow M, and ice thickness h as a function of freshwater input F_{riv} in a constant-diffusivity model. An Atlantic water temperature of 1 °C is used. The *results* are shown both in the presence and absence of sea ice, specified in legend. *Full and stippled lines* represent the stable and unstable solutions, respectively. *The stippled line* ends where the vertical density difference vanishes

4 Model response to freshwater in presence of sea ice

4.1 The steady-state response of sea ice thickness to changes in freshwater supply

Here, we focus on the impact of freshwater supply on the steady-state sea ice thickness. The sea ice is linked to the freshwater supply via the heat flux from the ocean to the ice. The heat flux is proportional to M (Eq. 18). In essence, a stronger steady-state heat flux results in thinner sea ice. However, the thickness-dependent sea ice export affects the net freshwater forcing of the ocean. Therefore, the sea ice is dynamically coupled to the ocean circulation.

The energy-constrained model shows increasing sea ice thickness with increasing freshwater forcing (Fig. 2d). It is also evident that the steady-state sensitivity of the sea ice thickness depends on the strength of freshwater supply. At large freshwater inputs, the sea ice thickness is rather insensitive and large changes in the freshwater forcing are needed to change the sea ice thickness. On the other hand, for small freshwater inputs, only small changes in the freshwater forcing are needed to change the sea ice thickness drastically. It is worth noting that in the uncoupled sea ice model, thick sea ice is more sensitive to a given change in the forcing than thin ice (Bitz and Roe 2004). The same basic physics still applies here, which reflects the fact that thinner ice grows faster. However, the sensitivity of the ocean heat flux becomes so strong at low freshwater supplies that it dominates over the thickness-dependent effect of sea ice growth.

Figure 2a shows that for a given external freshwater input the salinity difference is lower in the presence of sea ice, i.e. the salinity of the upper layer is higher. This is a consequence of the sea ice export, which carries away part of the external freshwater input. For the energy-constrained model which only has steady-state solutions above a threshold value of the net freshwater input, the sea ice tends to extend the range of steady-states. However, the sea ice export actually limits the steady-states with respect to F_{riv} (Fig. 2). Figure 4 illustrates how the net freshwater supply and freshwater exported by sea ice vary with the external freshwater input. For large inputs of F_{riv}, the role of the sea ice in the freshwater budget is small. However, for small inputs of F_{riv}, sea ice plays a leading order role for the freshwater budget.

In the constant-diffusivity case the sea ice response is essentially reversed. Here, the sea ice thins as the freshwater supply increases (Fig. 3d). For a sufficiently large freshwater input, the sea ice will vanish. This transition to an ice-free state is gradual and continuous, and presumably requires too large freshwater inputs to be relevant in

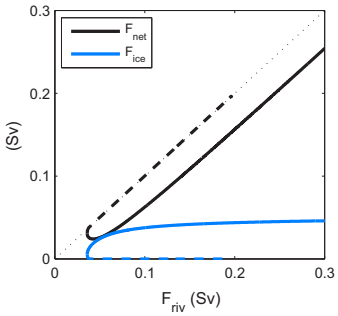

Fig. 4 Net freshwater input F_{net}, and sea ice export F_{ice} as a function of F_{riv} in the energy-constrained case. An Atlantic water temperature of 1 °C is used. *Full and stippled lines* represent the stable and unstable solutions, respectively

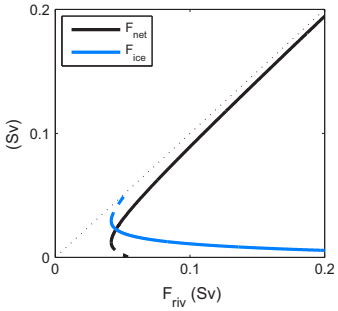

Fig. 5 Net freshwater input F_{net}, and sea ice export F_{ice} as a function of F_{riv} in the constant-diffusivity model. An Atlantic water temperature of 1 °C is used. *Full and stippled lines* represent the stable and unstable solutions, respectively

the present context. More interestingly, Fig. 3 shows that there is no longer a steady-state solution for arbitrary small freshwater inputs when sea ice is present. The underlying physics are illustrated in Fig. 5: As the freshwater supply reduces, the sea ice thickness and export increase. Thus, a critical state is approached where the net freshwater supply vanishes. However, as can be inferred from Figs. 3 and 5, the steady-state solution branch becomes unstable well before the net freshwater supply reaches zero. A formal stability analysis is performed in the next section. However, the physics is straightforward and tied to a positive feedback between the salinity difference and the ice export. If the upper layer becomes more saline (i.e. ΔS decreases), the flow and the heat flux diminish. This causes the sea ice thickness and export to increase, which amplifies the negative perturbation in ΔS. This positive feedback excludes solutions below a threshold value of F_{riv} and introduces an unstable steady-state for which the ice-export nearly balances the freshwater input.

Thus, the sea ice thickness responds differently to freshwater forcing in the two cases. The sea ice thickness increases with freshwater forcing in the energy-constrained model and decreases with freshwater forcing in the constant-diffusivity model.

4.2 The effect of sea ice on ocean circulation

Because the presence of sea ice affects the ocean, it also changes the stability of the system. The following analysis shows the stabilizing effect of sea ice on a freshwater perturbation in both the energy-constrained and constant-diffusivity case.

4.2.1 Stability analysis

Here we examine the feedbacks between ocean circulation and sea ice. The main physical features can be studied with a simplified set of equations, where we neglect the time-rate of change in the equation for H (Eq. 4), but keep it in the salinity equation (Eq. 5). Thus, we assume that the halocline depth adjusts almost instantaneously to yield $0 \approx -M_G + M_D$. As a result, we can write the strength of the circulation as $M = M(\Delta S)$ where $M(\Delta S)$ is the steady-state version of the circulation (Eqs. 11, 13). Whereas this approximation is not formally justifiable, it is reasonable as the approximation yields the correct stability criteria in the case without sea ice interaction (Nilsson and Walin 2010).

The simplified salinity equation (Eq. 5) now becomes

$$AH\frac{d\Delta S}{dt} = -\Delta S M + S_A F_{riv} - S_A F_{ice}. \tag{23}$$

We also assume that perturbations to the sea ice thickness (Eq. 20) are small, and linearize Eqs. 20 and 23 around a steady-state. We obtain

$$A\overline{H}\frac{d\Delta S'}{dt} = -\Delta S'\overline{M} - \overline{\Delta S}M' - S_A F'_{ice}, \tag{24}$$

$$2\tau\frac{dh'}{dt} = G' - D' - E', \tag{25}$$

where the overbar and primed variables denote steady-state and perturbation quantities, respectively.

Before performing the stability analysis, we provide a qualitative understanding of the three different terms on the right hand side of Eq. 24. The first term on the right-hand side represents a negative feedback due to the mean flow, acting to attenuate salinity perturbations.

The feedbacks from the remaining two terms are determined by the dependence of the flow and the ice export on the salinity perturbation. The flow perturbation is related to the salinity perturbation as

$$M' = \left(\frac{\partial \overline{M}}{\partial \overline{\Delta S}}\right)\Delta S'. \tag{26}$$

This makes the second term on the right-hand side of Eq. 24 a positive feedback for the energy-constrained case where $\left(\frac{\partial \overline{M}}{\partial \overline{\Delta S}}\right) < 0$. On the other hand, for the constant-diffusivity case, the feedback becomes negative as $\left(\frac{\partial \overline{M}}{\partial \overline{\Delta S}}\right) > 0$.

We now consider the feedback from the last term in Eq. 24; the sea ice export dependence on the salinity perturbation. Equation 22 relates F_{ice} and $G - D$. The growth and decay depends indirectly on the salinity via the ocean heat flux which is proportional to M (Eq. 18). Therefore,

$$F'_{ice} = -\frac{c_p \rho_0 \Delta T}{L} M' = -\frac{c_p \rho_0 \Delta T}{L}\left(\frac{\partial \overline{M}}{\partial \overline{\Delta S}}\right)\Delta S'. \tag{27}$$

Equation 27 shows that a positive flow perturbation, associated with increased ocean heat flux, yields negative perturbations in the ice export. We thus find that the sea ice export results in a positive feedback in the constant-diffusivity model where a positive perturbation in ΔS is associated with a positive perturbation in the flow. This reduces the sea ice export, which increases the net amount of freshwater retained in the surface layer. The reverse is true for the energy-constrained model where the sea ice export results in a stabilizing feedback.

As we now have a qualitatively feel for the different responses of Eq. 24 to salinity perturbations, we move on to the proper linear stability analysis to find out whether the equilibrium solutions are stable or not. The equations governing small perturbations in sea ice thickness and salinity differences, Eqs. 24 and 25, can be written

$$\frac{d}{dt}\begin{pmatrix} H' \\ \Delta S' \end{pmatrix} = \begin{pmatrix} a & b \\ c & d \end{pmatrix}\begin{pmatrix} H' \\ \Delta S' \end{pmatrix} \tag{28}$$

where a, b, c, and d are the coefficients of the stability matrix A_s, given by the partial derivatives of the right hand side of Eqs. 24 and 25. To perform a stability analysis which is valid for both mixing representations considered in this study, we write

$$\overline{M} = c\overline{\Delta\rho}^{\gamma}, \tag{29}$$

where c is a constant, $\gamma = -1/3$ for the energy-constrained case, and $\gamma = 1/3$ for the constant-diffusivity case. This gives,

$$a = \left(\frac{\partial (G-E)}{\partial h}\right)\frac{1}{2\tau}, \quad b = -\frac{c_p \Delta T \rho_0}{L}\frac{\overline{M}\gamma\beta\rho_0}{A\overline{\Delta\rho}},$$
$$c = -\left(\frac{\partial G}{\partial h}\right)\frac{S_A}{2\tau\overline{H}}, \quad d = -\frac{\overline{M}}{A\overline{H}}\left[1 + \frac{\gamma\beta\rho_0}{\overline{\Delta\rho}}\left(\overline{\Delta S} - S_A\frac{c_p\Delta T\rho_0}{L}\right)\right]. \tag{30}$$

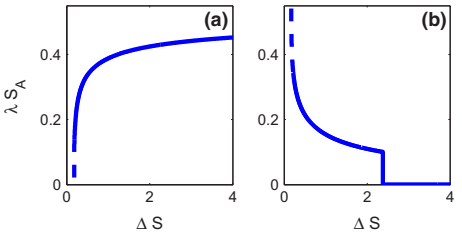

Fig. 6 The parameter λS_A as a function of the salinity contrast ΔS for the **a** energy-constrained and **b** constant-diffusivity model

where a results from $\partial D/\partial h = 0$ (Eq. 16), and b results from $\partial E/\partial Q = 0$ (Eq. 19). c is found given that only the last term in Eq. 24 is a function of h, and d is found making use of Eqs. 26 and 27.

An equilibrium solution is stable provided that the real parts of the eigenvalues of the stability matrix are negative. We are looking for solutions on the form $\exp(xt)$. Therefore, the eigenvalues can be found by solving $\det(A_s - Ix) = 0$. This gives us

$$x_{1,2} = \frac{a+d}{2} \pm \left(\left(\frac{a+d}{2}\right)^2 + bc - ad\right)^{1/2}. \tag{31}$$

The eigenvalues are negative and an equilibrium solution is stable provided that $bc - ad < 0$ and $a + d < 0$. The first constraint, $bc - ad < 0$, gives

$$\overline{\Delta S} > \frac{\Delta\rho_T}{\beta\rho_0(1+\gamma)} + \frac{\gamma S_A \lambda}{1+\gamma}, \tag{32}$$

where

$$\lambda \equiv \begin{cases} -\frac{c_p\Delta T\rho_0}{L}\left(\frac{\partial E}{\partial h}\right)\left(\frac{\partial (G-E)}{\partial h}\right)^{-1} & \text{for} \quad h > 0 \\ 0 & \text{for} \quad h = 0. \end{cases} \tag{33}$$

The second constraint, $a + d < 0$, gives

$$\overline{\Delta S} > \frac{\Delta\rho_T(1+\phi)}{\beta\rho_0(1+\gamma+\phi)} + \frac{\gamma S_A}{1+\gamma+\phi}\frac{c_p\Delta T\rho_0}{L}, \tag{34}$$

where

$$\phi = -\frac{A\overline{H}}{\overline{M}2\tau}\left(\frac{\partial (G-E)}{\partial h}\right). \tag{35}$$

Note that $\frac{\partial (G-E)}{\partial h} < 0$, and that the stability criteria are not analytical solutions as $\lambda = \lambda(\Delta S)$ and $\phi = \phi(\Delta S)$.

The parameter λ controls the sea ice feedback in this model. It depends mainly on the ice thickness, which is indirectly linked to the ocean state which is determined mainly by the salinity contrast (Fig. 6). The parameter λ attains a maximum value of $c_p\Delta T\rho_0/L$ when

$\left(\frac{\partial \overline{E}}{\partial \overline{h}}\right) \gg \left(\frac{\partial \overline{G}}{\partial \overline{h}}\right)$. For $T_A = 1$°C, that value is 0.0372. Due to the thermodynamics of sea ice, the rate of sea ice growth decreases for thick ice, and λ approaches its maximum for very thick sea ice. If sea ice export is insensitive to sea ice thickness, λ is zero.

The parameter ϕ is essentially the ratio of the time scales for the response of the salinity and the sea ice. In the limit of fast sea ice response, ϕ approaches infinity, and the second stability criterion (Eq. 34) yields $\overline{\Delta S} > \Delta\rho_T/\beta\rho_0$ which is always satisfied. In the limit of slow sea ice response, $\phi = 0$. In this case, the second stability criterion is stricter when $\gamma > 0$. The first criterion applies for $\gamma < 0$. For both representations of the diapycnal flow considered in this study, the first criterion determines where the solution becomes unstable.

For the energy-constrained case where $\gamma < 0$, the sea ice feedback from the last term in Eq. 32 is negative, confirming sea ice as a negative feedback. As the presence of sea ice stabilizes the circulation, while flow perturbations destabilize, it is interesting to see whether the presence of sea ice compensates for the destabilizing effects in the energy-constrained model. We get the stability criterion for the energy-constrained model $\overline{\Delta S_E}$ by inserting $\gamma = -1/3$ in Eq. 32;

$$\overline{\Delta S_E} > \frac{3\Delta\rho_T}{2\rho_0\beta} - \frac{S_A\lambda}{2}. \tag{36}$$

The critical salinity contrast where the vertical density difference vanishes $\overline{\Delta S_T}$ is given by $\overline{\Delta S_T} = \Delta\rho_T/(\beta\rho_o)$. For $\overline{\Delta S} > S_A\lambda$ the critical salinity $\overline{\Delta S_E}$ is reached before the vertical density difference disappears. As a consequence, the equilibrium becomes unstable in the energy-constrained model before the vertical density difference disappears for high Atlantic water temperatures and thin sea ice. This is always true for the parameters used in this study (Fig. 7a).

For the constant-diffusivity model where $\gamma > 0$, Eq. 32 shows that the sea ice feedback is positive; the presence of sea ice increases the salinity difference where the solution becomes unstable. The stability criterion for the constant-diffusivity model $\overline{\Delta S_S}$ becomes;

$$\overline{\Delta S_S} = \frac{3\Delta\rho_T}{4\rho_0\beta} + \frac{S_A\lambda}{4}. \tag{37}$$

For $\overline{\Delta S} < S_A\lambda$ the salinity contrast $\overline{\Delta S_S}$ is reached before $\overline{\Delta S_T}$. Hence, the equilibrium solution becomes unstable before the vertical density difference disappears. Concluding, the constant-diffusivity model becomes unstable before the vertical density difference disappears for low Atlantic water temperatures, thick sea ice, or large ice exports. As h decreases with F_{riv}, this occurs at small freshwater supplies (Fig. 7b). Given the parameters in Table 1, and a freshwater input of 0.5 Sv, the system becomes unstable before the vertical density difference disappears for Atlantic water temperatures below 2 °C.

5 Quasi-steady response to increasing Atlantic water temperatures

We have now established how the system responds to freshwater perturbations in the presence of sea ice. As the hypothesis from Dokken et al. (2013) involves a destabilization of the vertical stratification through increasing subsurface temperatures, we here investigate how increasing the Atlantic water temperature affects the steady-state solutions. Increasing Atlantic water temperatures decreases the vertical density difference and increases the heat flux from the ocean to the ice. As these two variables are indirectly coupled, the response of the steady-state solution is not straightforward, and will be examined in the following sections.

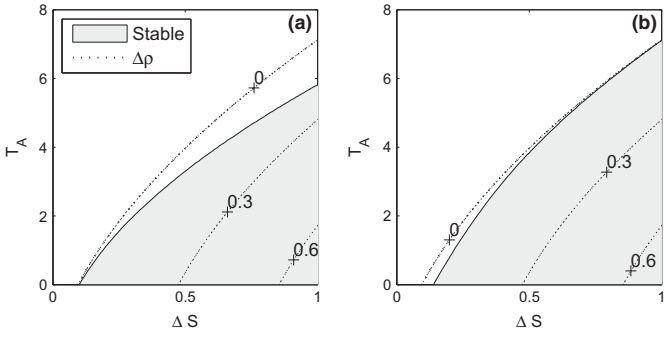

Fig. 7 Stability criteria for the **a** energy-constrained and **b** constant-diffusivity model for given Atlantic water temperatures T_A and salinity contrasts ΔS. *Shaded areas* represent the stable parts of the system. *Dotted, black lines* mark the vertical density difference $\Delta\rho$

5.1 Energy-constrained case

First, we study the dynamic response of the steady-state flow to increasing T_A. We recall that M intensifies with decreasing density differences in the energy-constrained case (Eq. 11).

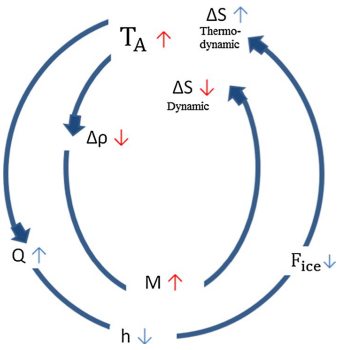

Fig. 8 The isolated effect of Atlantic water temperatures T_A on salinity differences ΔS. The thermodynamic response (*outer loop*) is valid for both models, while the dynamic response is only valid for the energy-constrained model (*inner loop*). $\Delta\rho$ is the density difference, M the steady-state flow, Q the heat flux from the ocean to the ice, h the sea ice thickness and F_{ice} the sea ice export.

The stronger ocean flow advects more saline water into the surface layer, thereby reducing the salinity contrast (Fig. 8, inner loop). In addition, the value of the critical salinity contrast increases with Atlantic water temperatures (Eq. 36). The dynamic response to increasing Atlantic water temperatures is therefore to decrease the stability of the system by driving the system toward the critical salinity contrast where the steady-state solution becomes unstable.

Figure 9a shows instead that the salinity difference predominantly increases with T_A for a given freshwater forcing. This is linked to the thermodynamic sea ice response and the following decrease in sea ice thickness. As the heat flux from the ocean to the ice is proportional to the temperature contrast between the two ocean layers, $\Delta T = T_A - T$, and T is taken to be fixed, ΔT increases linearly with T_A. Therefore, the sea ice thins when the Atlantic water temperature increases (Fig. 9d). The following melting of sea ice (or decrease in sea ice export) freshens the upper layer, thereby enhancing ΔS (Fig. 8, outer loop).

When sea ice is present, the dynamic and thermodynamic effects of increasing T_A have opposing effects on the density contrast. The sea ice melt buffers the system's response to increasing T_A. The result is that $\Delta\rho$ is nearly constant, and as a consequence, the steady-state flow is close to invariant to changes in T_A (Fig. 9c). Therefore, the heat flux from the ocean to the ice is mainly determined by

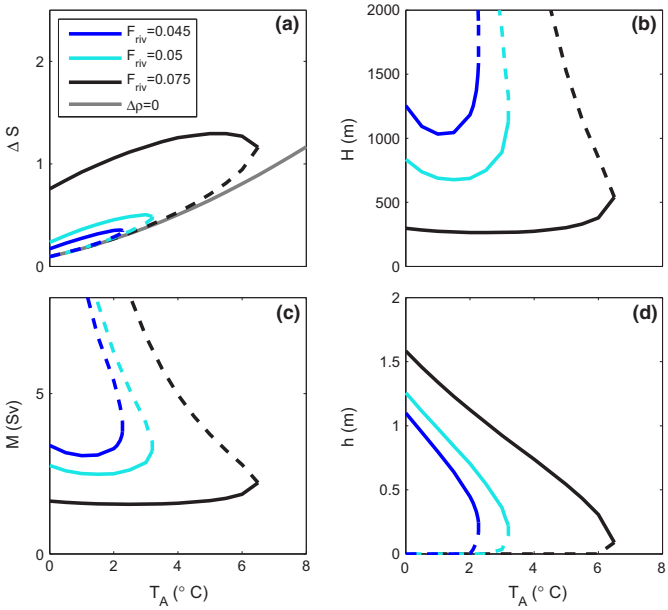

Fig. 9 Salinity contrast ΔS, surface layer depth H, steady-state flow M, and ice thickness h as a function of Atlantic water temperature T_A in an energy-constrained model. F_{riv} is specified in legend (Sv). The salinity contrast where the density difference disappears is shown by the *grey line*. *Full and stippled lines* represent the stable and unstable solutions, respectively

ΔT in the energy-constrained case. However, when the sea ice thins sufficiently, the effect of melting is too small to balance the increase in T_A with respect to the density contrast. At that point, $\Delta\rho$ decreases with T_A. Therefore, as h approaches zero, M increases sharply with T_A. As a consequence, the salinity contrast decreases with Atlantic water temperatures when h is small (Fig. 9a, d). At this point, high Atlantic water temperatures destabilize the system. The sea ice feedback, which is controlled by λ (Eq. 33), is not strong enough to balance the destabilizing effect of the flow.

Due to the destabilizing effect of the flow, the steady-state solution becomes unstable at high Atlantic water temperatures (Fig. 9). For low freshwater inputs, this occurs at salinity contrasts where sea ice still is present. As a consequence, the sea ice abruptly disappears (Fig. 9d). For higher freshwater inputs, the steady-state solution turns unstable as the sea ice disappears due to the removal of the stabilizing effect of the sea ice (not shown). For all values, the system turns unstable before the vertical density difference disappears (Fig. 7).

5.2 Constant-diffusivity case

The thermodynamic response of sea ice thickness to increasing Atlantic water temperatures is independent of the mixing representation. The increase in the temperature contrast increases the ocean heat flux, and hence decrease the sea ice thickness in the constant-diffusivity model as well (Fig. 8, outer loop). The consequent melting from the sea ice (or decrease in ice-export) leads to an increase in the salinity contrast.

On the other hand, as the flow slows down with increasing T_A in the constant-diffusivity case (Eq. 13), the dynamic response differs from the response of the energy-constrained case. A weaker flow enhances ΔS, thereby stabilizing the system. However, at low temperatures and freshwater inputs, the steady-state flow actually speeds up with increasing Atlantic water temperatures (Fig. 10c). The reason why is related to the thick sea ice which is more sensitive to changes in the forcing than thin ice. The sea ice decreases rapidly with increasing heat flux. Therefore, the strong sea ice melt leads to an increase in the salinity contrast which dominates the changes in the temperature contrast. As a consequence, the density difference increases and hence the steady-state flow speeds up. However, as the melting effect exceeds the anomalous advective salt transport, the positive flow perturbation freshens the upper layer. Therefore, this intermediate increase in flow with T_A does not change the stabilizing effect of the Atlantic temperatures; the salinity contrast still increases with Atlantic water temperatures (Fig. 10a).

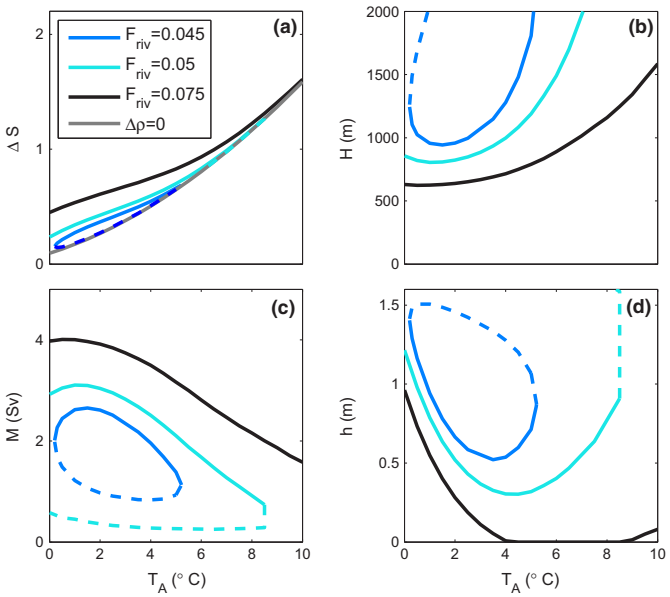

Fig. 10 Salinity contrast ΔS, surface layer depth H, steady-state flow M, and ice thickness h as a function of Atlantic water temperature T_A in a constant-diffusivity model. F_{riv} is specified in legend (Sv). The salinity contrast where the density difference disappears is shown by the *grey line*. *Full and stippled lines* represent the stable and unstable solutions, respectively

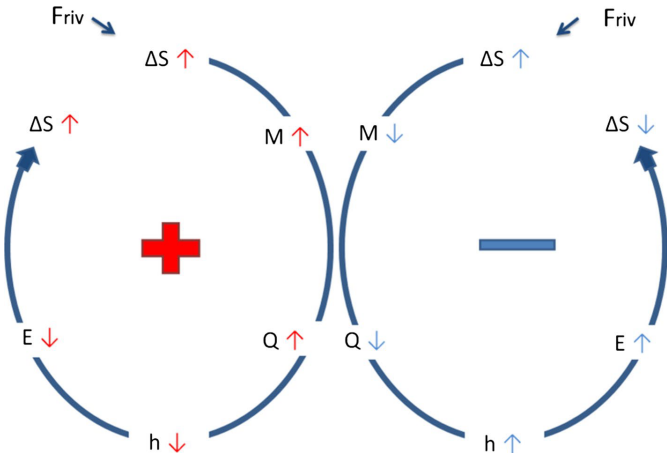

Fig. 11 The stabilizing effect of sea ice on a freshwater perturbation. *Left/red* part of the figure represents the constant-diffusivity case, while the *right/blue* part represents the energy-constrained case. F_{riv} is the freshwater input at the surface, ΔS the salinity contrast, M the steady-state flow, Q the heat flux from the ocean to the ice, h the sea ice thickness and E the sea ice export

In the constant-diffusivity case, the sea ice thickness response depends on the competing effects of the dynamic and thermodynamic responses to increasing T_A. The heat flux is proportional to ΔTM, and the two terms have opposing effects on the heat flux as the steady-state flow mainly decreases with T_A (Fig. 10c). Interestingly, we get a local minimum in sea ice thickness with increasing T_A (Fig. 10d). This occurs when the decrease in M balances the increase in ΔT, i.e., when the dynamic and thermodynamic effects are equal. When the decrease in the steady-state flow is large enough to dominate changes in the temperature contrast, the heat flux decreases with increasing T_A. The result is an increase in h with increasing Atlantic water temperatures at large T_A (Fig. 10d).

The change in the response of the sea ice to increasing Atlantic water temperatures changes the stability properties of the system. At low freshwater inputs the steady-state solution becomes unstable at low Atlantic water temperatures (Fig. 10, blue line, and Fig. 7). This is due to the thick sea ice and large ice-export which removes most of the freshwater introduced to the surface layer. By increasing T_A, steady-state solutions are introduced as the sea ice melt stabilizes the system. However, at higher Atlantic water temperatures, where sea ice thickens with T_A, the sea ice growth acts destabilizing. At high Atlantic water temperatures, the ice export dominates the freshwater input and flow perturbations, and the system becomes unstable. Note that the salinity contrast still increases at high temperatures due to a weaker flow (Fig. 10a). However, due to thicker sea ice and a larger λ, so does the salinity contrast where the steady-state solution becomes unstable (Eq. 37). Interestingly, the system becomes unstable at both high and low Atlantic water temperatures for low freshwater inputs (Fig. 10, blue line). For high freshwater inputs, the system stays stable until the vertical density difference disappears (Fig. 7).

We have shown that the system can turn unstable at high Atlantic water temperatures for both mixing representations, depending on the freshwater input. What happens at this point goes beyond the physics contained in the present version of our model. Still, it is fair to assume that the sea ice suddenly disappears as a new regime is established.

6 Discussion

The dynamical effect of sea ice on a freshwater perturbation is seen to depend on the representation of vertical mixing. In a system where the diapycnal flow increases with density differences (constant-diffusivity case), sea ice destabilizes against a freshwater perturbation (Fig. 11, red part) and introduces unstable solutions. If the diapycnal flow decreases with density differences (energy-constrained case), the presence of sea ice stabilizes the system (Fig. 11, blue part). In this case, the presence of sea ice extends the range of stable steady-state solutions. However, the stabilizing effect is not strong enough to allow for stable solutions for arbitrarily small freshwater inputs.

As the salinity-dominated circulation state abruptly becomes unstable for threshold values of freshwater input and deep-ocean temperature, the model suggests that the halocline and sea ice cover in the Nordic Seas could break down abruptly in response to a slow gradual change of the climatic conditions. The systematic stratification changes between cold stadials and warm interstadials as observed in the Nordic Seas by e.g. Dokken and Jansen (1999),

Rasmussen and Thomsen (2004) and Dokken et al. (2013) can be explained by a reduction in the freshwater supply to the Nordic Seas. This is highly relevant for a cold, glacial climate with a weaker hydrological cycle. Generally, we expect reduced input of freshwater to the Nordic Seas during cold, stadial conditions. In this case, only a small change in the freshwater supply is needed to initiate large and abrupt changes in both sea ice and ocean stratification (Fig. 2). This can be contrasted to the traditional freshwater hosing experiments where a large additional freshwater forcing of about 1 Sv to the North Atlantic is applied to maintain cold stadial conditions with extensive sea ice cover (e.g. Manabe and Stouffer 1995; Stouffer et al. 2006). In this case, an abrupt termination of the freshwater forcing is required to trigger a transition to a warm interstadial with weak stratification and reduced sea ice (Liu et al. 2009).

The abrupt changes in sea ice and ocean stratification at small freshwater supplies can occur independently of a change in subsurface temperature. However, the simple model also transitions to an unstable solution with a removal of sea ice when the temperature of the subsurface Atlantic water is increased (Fig. 9d). This is similar to the hypothesized transition from cold stadial states to warm interstadials triggered by warm Atlantic water as in Dokken et al. (2013). Interestingly, the unstable state is reached before the vertical density difference disappears. This is mainly true for the energy-constrained case. For the constant-diffusivity case, the stable solutions disappear for both high and low Atlantic water temperatures when the freshwater supply is low. At higher freshwater supplies, the system stays stable until the vertical density difference disappears. However, we recall that the constant-diffusivity model may be a less realistic representation of the system and is not thought of as a good analogue for the Nordic Seas/Arctic.

For the energy-constrained case, at low freshwater inputs, only a small increase in temperature is needed to destabilize the equilibrium state, and as a consequence, sea ice abruptly disappears. As both increasing Atlantic water temperatures and decreasing freshwater inputs promote an unstable system, the removal of the halocline as proposed by Dokken et al. (2013), can occur with smaller changes in Atlantic water temperatures than previously thought.

Our results are highly dependent on the use of a thickness dependent sea ice export. If we instead assume that the ice-export is constant and independent of the ice thickness (not shown), then the sea ice related feedbacks on the flow and the salinity stratification vanish. The equilibrium states become unstable at the same salinity contrast as when sea ice is absent. However, as the ice-export reduces the salinity contrast for a given freshwater input, the system with stability-dependent mixing still becomes unstable at a larger freshwater input in the presence of sea ice.

As the present conceptual model is highly simplified and essentially one-dimensional, it neglects several processes that could be of importance for the dynamics of the halocline and sea ice. In particular, the model does not represent effects of wind forcing on either the ocean circulation or the sea ice export. Possible impacts of ice mechanics are also ignored in the parametrization of the sea ice export, which simply is taken as proportional to the sea ice thickness. Note further that even though the sea ice model crudely represents an annual growth and melt cycle, effects of seasonal changes in the freshwater storage due to growth and melt of sea ice are not accounted for in the model. Adding representations of seasonality and natural variability can obviously change the stability range of the steady-state solutions examined here. Reductions in air-sea momentum exchange for high sea ice concentrations could also affect the stability properties of the system. In the presence of sea ice, the energy input from the atmosphere to oceanic mixing via e.g. internal wave generation should diminish (Rainville and Woodgate 2009). Thus, the energy supply to the vertical mixing ϵ would hence decrease. In the energy-constrained model this would introduce a feedback between the strength of the flow and the sea ice concentration, with ensuing impacts on the stability of the system.

The results from our simple model suggest a mechanism for how a reduction in freshwater input to the Nordic Seas could initiate large changes in the sea ice cover. Due to the instability at small freshwater supplies, small changes in the freshwater input or increases in subsurface temperatures could terminate the salinity-dominated mode with sea ice, and allow for a less stratified regime without sea ice. This could aid in explaining why the sea ice and hydrography of the Nordic Seas were highly variable during the last glacial cycle. Our simple model only accounts for the retreat of the sea ice cover, and does not provide any mechanism for the re-appearance of sea ice in the Nordic Seas.

7 Conclusion

The main results from the examination of the conceptual model of sea ice-ocean-circulation feedbacks are:

- The presence of sea ice stabilizes against a freshwater perturbation when the vertical velocity is represented with a constant energy-supply to the diffusivity.
- The presence of sea ice destabilizes against a freshwater perturbation when the vertical velocity is represented with a constant diffusivity.
- For sufficiently weak freshwater supply and irrespective of the representation of the vertical mixing, the salinity-dominated circulation becomes unstable.

– The sea ice is highly sensitive to changes in subsurface Atlantic water temperatures.
– The results from the simple conceptual model suggest that during cold glacial conditions, with reduced input of freshwater to the Nordic Seas, relatively small changes in freshwater or Atlantic water temperature could have triggered abrupt transitions in sea ice cover.

Acknowledgments The research was supported by the Centre for Climate Dynamics at the Bjerknes Centre. The research leading to these results is part of the ice2ice project funded by the European Research Council under the European Community's Seventh Framework Programme (FP7/2007-2013)/ERC Grant Agreement No. 610055. J. Nilsson acknowledges support from the Swedish National Space Board, the Knut and Alice Wallenberg Foundation (via the SWERUS-C3 program), and the Bolin Centre for Climate Research at Stockholm University. We thank the anonymous reviewers for their constructive comments which greatly improved the manuscript.

References

Arzel O, Colin de Verdiere A, England MH (2010) The role of oceanic heat transport and wind stress forcing in abrupt millennial-scale climate transitions. J Clim 23:2233–2256

Bitz CM, Roe GH (2004) A mechanism for high rate of sea ice thinning in the Arctic Ocean. J Clim 17:3623–3632

Broecker WS (2000) Abrupt climate change: casual constraints provided by the paleoclimate record. Earth-Sci Rev 51:137–154

Broecker WS, Bond G, Klas M (1990) A salt oscillator in the glacial Atlantic? 1: the concept. Paleoceanography 5:469–477

Bryan F (1986) High-latitude salinity effects and interhemispheric thermohaline circulations. Nature 323:301–323

Colin de Verdiere A, Raa LT (2010) Weak oceanic heat transport as a cause of the instability of glacial climates. Clim Dyn 35(7–8):1237–1256. doi:10.1007/s00382-009-0675-8

Cronin TM, Dwyer GS, Farmer J, Bauch HA, Spielhagen RF, Jakobsson M, Nilsson J, Briggs WM, Stepanova A (2012) Deep Arctic Ocean warming during the last glacial cycle. Nat Geosci 5:631–634

Dansgaard W, Johnsen SJ, Clausen HB, Dahl-Jensen D, Gundestrup NS, Hammer CU, Hvidberg CS, Steffensen JP, Sveinbjörnsdottir AE, Jouzel J, Bond G (1993) Evidence for general instability of past climate from a 250-kyr ice-core record. Nature 364:218–220

Dokken T, Jansen E (1999) Rapid changes in the mechanism of ocean convection during the last glacial period. Nature 401:458–461

Dokken TM, Nisancioglu KH, Li C, Battisti DS, Kissel C (2013) Dansgaard–Oeschger cycles: interactions between ocean and sea intrinsic to the Nordic Seas. Paleoceanography 28:491–502

Fanning AF, Weaver AJ (1997) Temporal-geographical meltwater influences on the North Atlantic conveyor: implications for the younger dryas. Paleoceanography 12:307–320

Ganopolski A, Rahmstorf S (2001) Rapid changes of glacial climate simulated in a coupled climate model. Nature 409:153–158

Ganopolski A, Rahmstorf F (2002) Abrupt glacial climate changes due to stochastic resonance. Phys Rev Lett 88:038501

Gildor H, Tziperman E (2003) Sea-ice switches and abrupt climate change. Philos Trans R Soc London Ser A 361:1935–1944

Gnanadesikan A (1999) A simple predictive model for the structure of the oceanic pycnocline. Science 283:2077–2079

Guan YP, Huang RX (2008) Stommel's box model of thermohaline circulation revisited: the role of mechanical energy supporting mixing and the wind-driven gyration. J Phys Oceanogr 38:909–917

Huang R (1999) Mixing and energetics of the oceanic thermohaline circulation. J Phys Oceanogr 29(4):727–746

Jakobsson M, Nilsson J, Oregan M, Backman J, Lowemark L, Dowdeswell JA, Mayer L, Polyak L, Colleoni F, Anderson LG, Björk G, Darby D, Eriksson B, Hanslik D, Hell B, Marcussen C, Sellen E, Wallin A (2010) An Arctic Ocean ice shelf during MIS 6 constrained by new geophysical and geological data. Quat Sci Rev 29:3505–3517

Jayne SR, Marotzke J (1999) A destabilizing thermohaline circulation-atmosphere-sea ice feedback. J Clim 12:642–651

Johnson HL, Marshall DP, Sproson DAJ (2007) Reconciling theories of a mechanically driven meridional overturning circulation and multiple equilibria. Clim Dyn 29:821–836

Kato H, Phillips OM (1969) On the penetration of a turbulent layer into stratified fluid. J Fluid Mech 37:643–655

Knudsen M (1900) Ein hydrographischer lehrsatz. Ann Hydrogr Maritimen Meteor 28:316–320

Li C, Battisti DS, Schrag DP, Tziperman E (2005) Abrupt climate shifts in Greenland due to displacements of the sea ice edge. Geophys Res Lett 32(L19):702. doi:10.1029/2005GL023,492

Li C, Battisti DS, Bitz CM (2010) Can North Atlantic sea ice anomalies account for Dansgaard-Oeschger climate signals? J Clim 23:5457–5475

Liu Z, Otto-Bliesner B, He F, Brady E, Tomas R, Clark P, Carlson A, Lynch-Stieglitz J, Curry W, Brook E, Erickson D, Jacob R, Kutzbach J, Cheng J (2009) Transient simulation of last deglaciation with a new mechanism for bølling-allerød warming. Science 325:310–314

Longworth H, Marotzke J, Stocker TF (2005) Ocean gyres and abrupt climate change in the thermohaline circulation: a conceptual analysis. J Clim 18:2403–2416

Lyle M (1997) Could early Cenozoic thermohaline circulation have warmed the poles? Paleoceanography 12:161–167

Manabe S, Stouffer RJ (1995) Simulation of abrupt climate change induced by freshwater input to the North Atlantic Ocean. Nature 378:165–167

Marotzke J (1989) Instabilities and multiple steady states of the thermohaline circulation. In: Anderson DLT, Willebrand J (eds) Oceanic circulation models: Combining data and dynamics. Springer, Netherlands, pp 501–511

Marotzke J (2000) Abrupt climate change and the thermohaline circulation: mechanisms and predictability. P Natl Acad Sci USA 97:1347–1350

Masson-Delmotte V, Jouzel J, Landais A, Stievenard M, Johnsen SJ, White JWC, Werner M, Sveinbjornsdottir A, Fuhrer K (2005) GRIP deuterium excess reveals rapid and orbital-scale changes in Greenland moisture origin. Science 309:118–121

Mayewski PA, Meeker LD, Twickler MS, Whitlow SI, Yang Q, Lyons WB, Prentice M (1997) Major features and forcing of high latitude northern hemisphere atmospheric circulation over the last 110,000 years. J Geophys Res 102:26,345–26,366

Munk WH (1966) Abyssal recipes. Deep-Sea Res 13:707–730

Nilsson J, Walin G (2001) Freshwater forcing as a booster of thermohaline circulation. Tellus 53A:629–641

Nilsson J, Walin G (2010) Salinity-dominated thermohaline circulation in sill basins: Can two stable equilibria exist? Tellus 62A:123–133

Nilsson J, Björk G, Rudels B, Winsor P, Torres D (2008) Liquid freshwater transport and polar surface water characteristics in the East Geenland current during the AO-02 Oden expedition. Prog Oceanogr 78:45–57

Park YG, Bryan K (2000) Comparison of thermally driven circulation from a depth-coordinate model and an isopycnal model. part i: scaling-law sensitivity to vertical diffusivity. J Phys Oceanogr 30:590–605

Peterson LC, Haug GH, Hughen KA, Rohl U (2000) Rapid changes in the hydrologic cycle of the tropical Atlantic during the last glacial. Science 290:1947–1951

Rainville L, Woodgate RA (2009) Observations of internal wave generation in the seasonally ice-free arctic. Geophys Res Lett 36(23):L23,604. doi:10.1029/2009GL041291

Rasmussen TL, Thomsen E (2004) The role of the North Atlantic Drift in the millennial timescale glacial climate fluctuations. Palaeogeogr Palaeoclimatol Palaeoecol 210:101–116

Sevellec F, Fedorov AV (2015) Unstable AMOC during glacial intervals and millennial variability: the role of mean sea ice extent. Earth Planet Sci Lett 429:60–68. doi:10.1016/j.epsl.2015.07.022

Severinghaus JP, Brook EJ (1999) Abrupt climate change at the end of the last glacial period inferred from trapped air in polar ice. Science 286:930–934

Stigebrandt A (1981) A model for the thickness and salinity of the upper layer in the Arctic Ocean and the relationship between the ice thickness and some external parameters. J Phys Oceanogr 11:1407–1422

Stocker TF, Wright DG (1991) Rapid transitions of the ocean's deep circulation induced by changes in surface water fluxes. Nature 351:729–732

Stommel HM (1961) Thermohaline convection with two stable regimes of flow. Tellus 13:224–230

Stouffer RJ, Yin J, Gregory JM, Dixon KW, Spelman MJ, Hurlin W, Weaver AJ, Eby M, Flato GM, Hasumi H, Hu A, Jungclaus JH, Kamenkovich IV, Levermann A, Montoya M, Murakami S, Nawrath S, Oka A, Peltier WR, Robitaille DY, Sokolov A, Vettoretti G, Weber SL (2006) Investigating the causes of the response of the thermohaline circulation to past and future climate changes. J Clim 19(8):1365–1387. http://dx.doi.org/10.1175/JCLI3689.1

Stranne C, Björk G (2012) On the Arctic Ocean ice thickness response to changes in the external forcing. Clim Dyn 39:3007–3018

Thorndike AS (1992) A toy model linking atmospheric thermal radiation and sea ice growth. J Geophys Res 97:9401–9410

Timmermann A, Gildor H, Schulz M, Tziperman E (2003) Coherent resonant millennial-scale climate oscillations triggered by massive meltwater pulses. J Clim 16:2569–2585

Tziperman E (1997) Inherently unstable climate behaviour due to weak thermohaline ocean circulation. Nature 386:592–595

Vallis GK (2006) Atmospheric and oceanic fluid dynamics: fundamentals and large-scale circulation, 1st edn. Cambridge University Press, Cambridge

Welander P (1971) The thermocline problem. Philos Trans R Soc Lond A 270:415–421

Welander P (1986) Thermohaline effects in the ocean circulation andrelated simple models. In: Willebrand J, Anderson DLT (eds) Large-scale transport processes in the oceans and atmosphrere. D.Reidel, Holland

Winton M (1993) Deep decoupling oscillations of the oceanic thermohaline circulation, in Ice in the climate system. Springer Verlag, Berlin

Winton M, Sarachik ES (1993) Thermohaline oscillations induced by strong steady salinity forcing of ocean general circulation models. J Phys Oceanogr 23:1389–1410

Yang J, Neelin JD (1993) Sea-ice interaction with the thermohaline circulation. Geophys Res Lett 20:217–220

Yang J, Neelin JD (1997) Sea-ice interaction and the stability of the thermohaline circulation. Atmos-Ocean 35(4):433–469

Yu EF, Francois F, Bacon M (1996) Similar rates of modern and last-glacial ocean thermohaline circulation inferred from radiochemical data. Nature 379:689–694

Zhang J, Schmitt RW, Huang RX (1999) The relative influence of diapycnal mixing and hydrological forcing on the stability of thermohaline circulation. J Phys Oceanogr 29:1096–1108

Paper III

6.3 A spatio-temporal reconstruction of sea-surface temperatures in the North Atlantic during Dansgaard-Oeschger events 5-8

Jensen M. F., A. Nummelin, S. B. Nielsen, H. Sadatzki, E. Sessford, B. Risebrobakken, C. Andersson, A. Voelker, W. H. G. Roberts, and A. Born, *Clim. Past Discuss.*, doi:10.5194/cp-2017-103. Under review for Climate of the Past.

Clim. Past Discuss., https://doi.org/10.5194/cp-2017-103
Manuscript under review for journal Clim. Past
Discussion started: 24 August 2017

Climate of the Past Discussions

A spatio-temporal reconstruction of sea-surface temperatures in the North Atlantic during Dansgaard-Oeschger events 5-8

Mari F. Jensen[1], Aleksi Nummelin[2], Søren B. Nielsen[3], Henrik Sadatzki[1], Evangeline Sessford[1], Bjørg Risebrobakken[4], Carin Andersson[4], Antje Voelker[5], William H. G. Roberts[6], and Andreas Born[7,1]

[1]Department of Earth Science, University of Bergen and Bjerknes Centre for Climate Research, Bergen, Norway
[2]Geophysical Institute, University of Bergen and Bjerknes Centre for Climate Research, Bergen, Norway and Department of Earth and Planetary Sciences, Johns Hopkins University, Baltimore, USA
[3]Climate and Geophysics, Niels Bohr Institute, University of Copenhagen, Copenhagen, Denmark
[4]Uni Research Climate, Bjerknes Centre for Climate Research, Bergen, Norway
[5]Instituto Português do Mar e da Atmosfera, Lisbon, and Centre of Marine Sciences (CCMAR), University of Algarve, Faro, Portugal
[6]University of Bristol, Bristol, England
[7]Institute of Physics and Oeschger Centre for Climate Research, University of Bern, Bern, Switzerland

Correspondence to: M. F. Jensen (mari.f.jensen@uib.no)

Abstract. Here we establish a spatio-temporal evolution of the sea-surface temperatures in the North Atlantic over Dansgaard Oeschger (DO) events 5-8 (c. 30-40 ka) using the proxy surrogate reconstruction method. Proxy data suggest a large variability in North Atlantic sea-surface temperatures during the DO-events of the last glacial period. However, proxy data availability is limited and cannot provide a full spatial picture of the oceanic changes. Therefore, we combine fully coupled, general circulation model simulations with planktic foraminifera based sea-surface temperature reconstructions to obtain a broader spatial picture of the ocean state during DO-events 5-8. The resulting spatial sea-surface temperature patterns agree over a number of different general circulation models and simulations. We find that sea-surface temperature variability over the DO-events is characterized by colder conditions in the subpolar North Atlantic during stadials than during interstadials, and the variability is linked to changes in the Atlantic Meridional Overturning circulation, and in the sea-ice cover. Forced simulations are needed to capture the strength of the temperature variability and to reconstruct the variability in other climatic records not directly linked to the sea-surface temperature reconstructions. Our results are robust to uncertainties in the age models of the proxy data, the number of available temperature reconstructions, and over a range of climate models.

1 Introduction

The Dansgaard-Oeschger (DO) events of the last glacial are some of the most prominent climate variations known from the past. Ice cores from Greenland show multiple temperature excursions during the last glacial period as the climate over Greenland alternated between cold stadial (Greenland Stadial, GS), and warmer interstadial (Greenland Interstadial, GI) conditions with

Clim. Past Discuss., https://doi.org/10.5194/cp-2017-103
Manuscript under review for journal Clim. Past
Discussion started: 24 August 2017

a period of roughly 1500 years (Grootes and Stuiver, 1997). Each DO-event is characterised by an initial temperature rise of 10±5°C toward GI conditions in a few decades, a more gradual cooling over the following several hundreds of years, and a relatively rapid temperature drop back to GS at the end of most of the events (Johnsen et al., 1992; Dansgaard et al., 1993; North-Greenland-Ice-Core-project members, 2004; Kindler et al., 2014). DO-events are manifested not only in Greenland, but around the world. Concurrent with warm GIs, proxies show a warmer and wetter climate in Europe, an intensified Asian summer monsoon, and a cooling of parts of the Southern Hemisphere (Voelker, 2002; Rahmstorf, 2002, for overviews).

With its proximity to Greenland, much attention has been paid to the North Atlantic in reconstructing the millennial-scale GS/GI climate cycles. Reconstructions from Marine Isotope Stage 3 (MIS3, 24-59 ka), during which about 15 DO-events occurred, suggest a large variability in sea-surface and sub-surface temperatures in the North Atlantic coincident with the temperature variability on Greenland. Elliot et al. (2002) and Bond et al. (1993) show significant decreases in sea-surface temperatures (SST) in the North Atlantic during GSs. In the Nordic Seas, on the other hand, sub-surface temperatures are found to increase during the same periods (Rasmussen and Thomsen, 2004; Dokken et al., 2013; Ezat et al., 2014). Large movements of the oceanic temperature fronts are associated with the variability (Voelker and de Abreu, 2013; Eynaud et al., 2009) and Rasmussen et al. (2016) recently suggested a gradual northward movement of warm subsurface waters during GSs compared to GIs in the North Atlantic. New studies also suggest variability in the sea-ice cover of the Nordic Seas with expanded sea-ice cover during GSs compared to GIs when the sea-ice cover retreated. These changes coincide with the temperature variability on Greenland (Dokken et al., 2013; Hoff et al., 2016). However, expanded sea-ice cover during GIs compared to GSs has also been suggested based on dinoflagellate cyst assemblages (Eynaud et al., 2002; Wary et al., 2016).

Several mechanisms involving the North Atlantic have been proposed to explain the GS/GI cycles. These include latitudinal shifts in the North Atlantic Deep Water formation site (Labeyrie et al., 1995; Ganopolski and Rahmstorf, 2001; Arzel et al., 2010; Colin de Verdiere and Raa, 2010; Curry et al., 2013; Sevellec and Fedorov, 2015); changes in the heat transport to the North Atlantic due to either internal instabilities in the Atlantic Meridional Overturning circulation (AMOC, Broecker et al., 1990; Tziperman, 1997; Marotzke, 2000; Ganopolski and Rahmstorf, 2001) or a salt oscillator (Peltier and Vettoretti, 2014; Vettoretti and Peltier, 2016); changes in the sea-ice cover of the Nordic Seas (Broecker, 2000; Gildor and Tziperman, 2003; Masson-Delmotte et al., 2005; Li et al., 2005; Dokken et al., 2013; Petersen et al., 2013). However, the mechanisms behind the DO-events are still debated, and it is not clear whether the events are forced by internal ice-sheet instabilities, if they originate from variability within the ocean-atmosphere system, or from a combination of both.

To understand the dynamics behind the DO-events, integrating climate modelling and paleo-reconstructions is necessary. While modelling studies can demonstrate feasibility of all of the above mentioned mechanisms for DO variability, proxy data should be used to assess the realism of such scenarios. However, due to limited proxy data and computing resources, model-data integration poses a challenge to the community. Although the North Atlantic region contains much information from the last glacial period, marine paleoclimatic reconstructions are still confined to suitable locations for coring, making the information sparse and spatially limited. In addition, the marine proxy records that cover MIS3 have variable temporal resolution, and even the best resolved marine reconstructions are of much lower resolution than the ice core records from Greenland. Although there are a number of idealized attempts to simulate the full MIS3 period (e.g., Brandefelt et al., 2011; Van Meerbeeck et al., 2009;

Clim. Past Discuss., https://doi.org/10.5194/cp-2017-103
Manuscript under review for journal Clim. Past
Discussion started: 24 August 2017

Peltier and Vettoretti, 2014) the lack of high resolution coupled climate model simulations (including interactive ice-sheets) is arguably another limiting factor for our understanding of the mechanisms behind DO-events.

The model-data integration for the recent past has been performed using various techniques. One example is regression models that base on the relationship between climate model variables or observations, and are applied (directly) to proxy reconstructions (e.g., Rahmstorf et al., 2015). While using regression models is computationally efficient, it inherently assumes the same linear relationships between variables in the past as for the present; an assumption which might not be true, especially when investigating a glacial climate. Regression models have also been applied using climate models with MIS3 boundary conditions (Zhang et al., 2015), however, linearity between the model variables is still assumed and this assumption may be invalid during the abrupt non-linear DO-events. Another example is data-assimilation and inversion techniques which are becoming more frequently used for paleoclimate studies. For example, Kurahashi-Nakamura et al. (2014) and Gebbie et al. (2015) have used these techniques to investigate the ocean circulation during the last glacial maximum (LGM). However, due to the lack of proxy data, these studies often focus on reconstructing a relatively stable climate state, which allows for aggregating a large number of proxy records over a long timespan. While data-assimilation would be an ideal method for confining model simulations, it is not feasible in the transient case of MIS3 where the proxy data coverage is very sparse. Due to their individual restrictions, both regression methods as well as data-assimilation, together with long coupled climate model simulations, appear sub-optimal for studying the non-linear changes over the long time period of MIS3.

In this study, we combine the physically consistent output of model simulations with the temporally accurate information from proxy data in the North Atlantic by applying the proxy surrogate reconstruction (PSR) method. This method has recently undergone sensitivity tests and has been successfully applied in reconstructing European atmospheric temperatures over the last 200 years (Franke et al., 2011), and the observed global decadal temperature variability of the last century (Gómez-Navarro et al., 2017). Although Graham et al. (2007) used one coastal SST reconstruction together with terrestrial records to reconstruct US climate back to 500 AD, the PSR method has, to our knowledge, never been applied to ocean data before. Also, the PSR method has never before been used for the MIS3 time period. Here, we use the SST variability in the North Atlantic during the last glacial period as a test-case for the PSR method to see whether the method can widen our knowledge of spatial patterns back in time. In doing so, we also aim to learn about the underlying DO variability in the North Atlantic region.

Our analysis shows that the surrogate reconstruction is a good solution for combining model simulations and proxy data without having to assume the same climatic changes at all locations. In the North Atlantic, where the data coverage during MIS3 severely limits the usefulness of other data-assimilation and inversion techniques, the PSR method is an especially useful method. As the method allows for the full non-linearity of the climate system, as represented by the coupled model simulations, we are able to capture a large part of the glacial variability in the ocean during MIS3 and also on Greenland. The method is an efficient offline data assimilation technique which allows for the quantification of uncertainty, unlike expensive transient simulations, which makes it a good first step for understanding the spatial variability of the climate changes seen during MIS3. Until such time as full complexity models are capable of simulating the full transient evolution of the climate over long periods, such simplified approaches will be crucial to our understanding of the climate.

Clim. Past Discuss., https://doi.org/10.5194/cp-2017-103
Manuscript under review for journal Clim. Past
Discussion started: 24 August 2017

Climate of the Past Discussions

We present the PSR method together with the proxy-based temperature reconstructions and model simulations in Sect. 2, test the method in Sect. 3, show the results of the method in Sect. 4, and discuss the results in Sect. 5.

2 Materials and Methods

2.1 Proxy Surrogate Reconstruction

We use the PSR method which was first introduced by Graham et al. (2007) to combine sparse proxy data and spatially complete and physically consistent climate model output. In this way we can produce a climate reconstruction that is complete in both space and time. This approach was first introduced for weather forecasting by Lorenz (1969).

Briefly, the PSR method is as follows (see below for details). A collection of years from one or several model simulations are treated as a pool of possible "climate states" (see Sect. 2.3 for details). Then, for any time period in which we have a set of proxy data, we find the climate state from the model pool that best matches the proxy data: an "analog". This is done using an objective cost function. By repeating this and finding analogs for all time steps in the proxy data, we compile a set of climate states from the model pool which are consistent with the proxy data. We thus have a time series of modelled climate states with a complete spatial coverage which are the best fit to the spatially sparse proxy data. Furthermore, since the model simulates variables other than those that are used in the matching, we can also reconstruct variables for which no paleo-reconstruction exist.

We follow the PSR implementation introduced by Franke et al. (2011). First, we find the model grid cells that are closest to the proxy record locations and extract the modelled temperature for each climate state from those locations. Results are not sensitive to this choice as picking the four closest grid cells yield virtually identical results. Second, we define a cost function for deciding which of the climate states will represent a given proxy time step. For this we use the root mean square error (RMSE) in temperature space as a distance measure:

$$d(T^p, T^m) = \sqrt{\frac{\sum_{i=1}^{I} w_i (T_i^p - T_i^m)^2}{I}}, \tag{1}$$

where T_i^p and T_i^m are the proxy and model temperature anomaly records at location i, respectively. The anomalies are calculated from the temporal mean of the proxy data and each individual model simulation, respectively (see. Sect. 3.2.3). I is the total number of core locations with a proxy-based reconstructed temperature value at the given time step, ranging from 12-14 in this study. w_i is a weight which one could apply to reduce the bias toward areas with large variability. However, we decided not to use any weight ($w_i = 1$), because the spatial differences in interannual variability in the ocean are much smaller than spatial differences in monthly variability in the atmosphere (which is what motivated Franke et al. (2011) to use w_i). We did test several different weighting options, however, no weighting function impacted the final results, further justifying our choice of setting $w_i = 1$.

As a final step, we create a composite T^c consisting of several analogs; the model climate states with the smallest d. We choose to form the composite based on the 10 analogs (N=10) with the smallest RMSE, and weight the analogs by a function

Clim. Past Discuss., https://doi.org/10.5194/cp-2017-103
Manuscript under review for journal Clim. Past
Discussion started: 24 August 2017

of the RMSE;

$$T^c(x,y,t=k) = \sum_{n=1}^{N} W_n T_n^m(x,y) \tag{2}$$

where x and y are the two spatial dimensions, t is time dimension (on the proxy time axis), k marks a given year in the proxy record, n is a specific analog from the model pool, T_n^m is the model temperature field for analog n, and the weight scalar W_n is defined to be inversely proportional to the RMSE distance d_n:

$$W_n = \frac{\left(\sum_{n=1}^{N} d_n\right) - d_n}{\sum_{n=1}^{N}\left[\left(\sum_{n=1}^{N} d_n\right) - d_n\right]}. \tag{3}$$

Note that because the sum of W is scaled to be 1, the composite is not very sensitive to the increase in number of analogs (N) as usually analogs beyond $n = 10$ are assigned with very small weights. The choice of number of analogs in the composite is further discussed in Sect. 3.2.1.

As we repeat this algorithm for each proxy time step, we construct a three-dimensional dataset of the composites; the surrogate reconstruction c_i. We either present the results as a surrogate time series or as composite maps of the surrogate reconstruction.

2.2 Data Pool

We compiled proxy-based SST reconstructions from 14 marine sediment cores located in the North Atlantic for the time interval from 30 to 40 kyr (GS/GI cycle 5-8) (Table 1, Fig. 1). For 10 of the cores (Table 1), we calculate SST estimates based on assemblage counts of planktic foraminifera and the Maximum Likelihood technique (ML) (ter Braak and Looman, 1986; ter Braak and Prentice, 1988; ter Braak and van Dam, 1989). We use the North Atlantic core top calibration dataset developed within the MARGO framework (Kucera et al., 2005). The calibration uses modern SST values for 10 m water depth during summer (July, August, September, JAS) taken from the World Ocean Atlas version 2 (WOA, 1998). The choice of transfer function is most often based on the RMSE between the measured and inferred variable, used to access the predictive power of the transfer function. Choosing a transfer function with low RMSE will in a statistical sense provide the best transfer function model. The estimation of the predictive power of transfer functions assumes that the test sites are independent from the modelling sites. However, autocorrelation is common in ecological data. Using an independent dataset, Telford and Birks (2005) explored and quantified how autocorrelation affects the statistical performance of different transfer functions. They concluded that the true RMSE is approximately twice the value of previously published estimates for some methods, e.g., the modern analog technique. In this study we have chosen the ML transfer function technique which is based on a unimodal species response. We base this decision on the results by Telford and Birks (2005) that suggest that this method, and other methods based on the assumption of an unimodal species-environment response model, is more robust with regards to spatial structure in the data. For the ML technique the RMSE is 1.78°C, based on cross-validation using bootstrapping.

Clim. Past Discuss., https://doi.org/10.5194/cp-2017-103
Manuscript under review for journal Clim. Past
Discussion started: 24 August 2017

For the remaining four cores from which the full planktic foraminifera assemblage counts are not available, we use records of the percentage of the polar planktic foraminifera *Neogloboquadrina pachyderma* (%NP, formerly known as N. pachyderma sinistral) to reconstruct the SST variations. We include these four additional records to increase the spatial coverage of SST reconstructions. SST estimates based on %NP rely on a linear relationship between SST at 10 m water depth and %NP as described by Govin et al. (2012), where

$$\mathrm{SST} = -0.06\%\mathrm{NP} + 12.26. \tag{4}$$

As the linear relationship in Eq. (4) is only valid for %NP values between 10 and 94%, we exclude values out of this range. Cores 5 and 9 have all values within the interval, while for cores 6 and 10 we have excluded parts of the record.

We use the original age model of each core and linearly interpolate between existing data to obtain data points at consistent steps of 20 years. The absolute temperatures are shown in Fig. 2, but note that we use the temperature anomalies from the temporal mean over the 30-40 kyr interval in the PSR method. The age models of all but three cores are defined by correlating SST or Ice Rafted Debris (IRD) signals to the DO signals in the GISP2 ice core record, or magnetic susceptibility signals to those in the NGRIP record (Table 1). In the Greenland ice cores the transitions between stadials and interstadials occur in less than 50 years (Rasmussen et al., 2014). The difference between the original GISP2 and NGRIP chronologies is up to 300 years in between 40 and 30 kyr (Svensson et al., 2008). The transitions between the stadials and interstadials are rapid, large scale features that can easily be identified. However, when the respective marine property records are tuned to the Greenland isotopes, an added uncertainty to the relative relation between the dated records is expected. Taking into account the various sources of age model uncertainties, we argue that a $\pm$500 years relative age uncertainty in between the records that have been tuned to Greenland ice core records is a conservative estimate. As the PSR method is sensitive to relative dating differences, we test how our results are influenced when assuming a $\pm$500 year age uncertainty. We note that the original age models of cores 3, 4 and 14 were solely based on ^{14}C dates (Table 1), and the age uncertainty for these cores, relative to the ages of the other cores, is considered larger.

2.3 Model Pool

We base the surrogate reconstruction on a number of different GCM simulations. The main model pool consists of model output from the Hadley Centre coupled model version 3 (HadCM3, Gordon et al., 2000; Singarayer and Valdes, 2010), spanning 8 simulations at different times. There are 6 time slices from MIS3; at 30, 32, 34, 36, 38, and 40 kyr. In addition, a time slice at 21 kyr (LGM), and a pre-industrial (PI) simulation are included. Each simulation is initialised from a PI simulation and run for 500 years, and the last 200 years are included in the pool. The simulations are performed with prescribed orbital forcing (Berger and Loutre, 1991), ice sheet configuration and greenhouse gases (Petit et al., 1999; Loulergue et al., 2008; Spahni et al., 2005) corresponding to the respective ages. Since there are no ice sheet reconstructions for MIS3, which is before the LGM, we use ice sheets that are a linear rescaling of their LGM topography. To do this rescaling, we multiply the LGM ice sheet height by the fraction of the total LGM ice sheet volume that is realised at each time slice. We use the ICE-5G LGM ice sheet reconstruction (Peltier, 2004) and assume that for all MIS3 time slices the ice sheet extent is as for the LGM: it is

Clim. Past Discuss., https://doi.org/10.5194/cp-2017-103
Manuscript under review for journal Clim. Past
Discussion started: 24 August 2017

only the ice sheet height that varies. See (Singarayer and Valdes, 2010) for further details. Additionally, we add 99 years from two simulations (32 and 38 kyr) where 1 Sv of freshwater is added to the Atlantic between 50°N and 70°N to mimic Heinrich events (for more details, see Singarayer and Valdes, 2010). For this study, we continue these two simulations for 250 years with the freshwater forcing turned off. The horizontal grid of the ocean is 1.25°× 1.25°. These 10 simulations constitute the main model pool, but we also perform sensitivity experiments with the PSR method using the 8 unforced simulations only ("HadCM3 nohose").

Additionally, we experiment with the Community Climate System Model version 4 (CCSM4) data from a 1300 year long PI simulation and a 200 year long LGM (only 1000 and 100 years, respectively, included in the model pool) simulation of the 1°× 1° version (Gent et al., 2011; Danabasoglu et al., 2012; Brady et al., 2013) as well as a 1000 year long PI simulation with a 2°× 2° atmosphere model (Kleppin et al., 2015; Born and Stocker, 2014). Including the 2° atmosphere version of CCSM4 adds new model states to the pool as the simulation has been shown to have cold GS-like, and warm GI-like conditions (Kleppin et al., 2015).

As the proxy data are calibrated to 10 m depth and represent a summer temperature average, the model pools consist of temperatures from the upper vertical grid cell averaged over the months JAS. As the proxy data in essence represents an integrated signal of temperatures over several years, the JAS averages from the model output are low-pass filtered using a 4th order Butterworth filter with a cut off frequency of $0.2\,\mathrm{yrs}^{-1}$, thus each member of the model pool is a 10 year average of model data. For all GCM simulations, we remove the temporal mean of each simulation to obtain temperature anomalies for the PSR method. This is also done for all other variables when using anomalies. Different ways of defining the anomalies are discussed in Sect. 3.2.3.

The model pools are summarized in Table 2 where the main model pool, HadCM3, is highlighted.

3 Testing the PSR method

Here, we test the PSR method, first with synthetic data (Sect. 3.1), and then with the proxy data and model pools (Sect. 3.2) introduced in Sects. 2.2 and 2.3.

3.1 Synthetic PSR-study

Before applying the PSR method on the proxy reconstructions, we perform a test with synthetic data. The synthetic data are 30 random climate states (as explained above) of the HadCM3 model output at the proxy locations. The remaining climate states from the model output serve as the model data pool. We follow the PSR method as described in Sect. 2.1 with the final surrogate reconstruction based on an average of 10 analogs. We perform such a reconstruction 1000 times in order to obtain robust statistics, and find the distance between the PSR output and the original model output at each grid cell. This is presented as offsets in Fig. 3 at the 5, 50, and 95 percentile.

The good agreement between the PSR output and the original model output (Fig. 3) demonstrates that the spatially sparse synthetic data at the proxy locations can effectively recover the simulated ocean state. The correlation between the surrogate

Clim. Past Discuss., https://doi.org/10.5194/cp-2017-103
Manuscript under review for journal Clim. Past
Discussion started: 24 August 2017

reconstruction and the original model output exceeds 0.8 in the North Atlantic, except along the eastern coast of Greenland and along 35°N where the correlation still exceeds 0.6. Practically all of the variability is captured in the eastern subpolar gyre. The reconstructed temperatures are generally within ± 0.1°C of the model output (Fig. 3b), but some of the reconstructed values are up to 1°C from the real value. These offsets are mainly found in the Nordic Seas region and along the coast of North America (Fig. 3c,d). This reflects the fact that the proxy locations do not provide enough information for the PSR method to fully recover the model output in these areas. Using the CCSM4-model pool as the observations and the HadCM3 as the model data pool, the largest offsets are 1.5°C (not shown). In general, these results act as a guide as we proceed to the proxy data.

3.2 Proxy data testing

3.2.1 Number of analogs

Several climate states from the model pools might match the proxy-reconstructions well at the core locations, but differences away from the core sites might be large as different climate states can produce similar RMSE at the core locations (Fig. 4). Therefore, to ensure a consistent surrogate reconstruction, the composites are an average of a number of analogs with the smallest RMSE. As the number of analogs (N) increases, each additional member has less and less effect on the final 2D pattern. As noted by Gómez-Navarro et al. (2017), the correlation between the proxy and the surrogate time series increases with N, while the standard deviation of the surrogate time series decreases with it. In our case, choosing N much larger than 10 results only in a small increase in correlation, but in a large decrease in the standard deviation of the surrogate time series (Fig. 5a). On the other hand, choosing N less than 10 decreases the correlation of the time series. In addition, the lowest RMSE is obtained around N=10, the number of analogs which we use for the remainder of this study.

3.2.2 Model pool

The correlation between the surrogate reconstructions and the corresponding proxy data is largely independent of the model pool, while the amplitude (standard deviation) of the variability depends on it (Fig. 5b). The surrogate reconstruction based on the full HadCM3 model pool outperforms the others with regard to the standard deviation and RMSE (Fig. 5b), which is why it is the main model pool in this study. The mean correlation between the proxy record and the surrogate time series at the core locations does not change when excluding the two hosing simulations from the model pool. However, the mean standard deviation of the surrogate time series at the core locations decreases from 0.98 with the main HadCM3 model pool to 0.64 with HadCM3 nohose. If the CCSM4 pool is used instead, the variability of the surrogate time series decreases further.

For all model pools, the JAS average of the model data gives better results than annual means. As expected, unfiltered data give a larger variability of the surrogate time series than filtered data. However, as the proxy data consist of temperature signals integrated over several years, only filtered data are used hereafter.

Clim. Past Discuss., https://doi.org/10.5194/cp-2017-103
Manuscript under review for journal Clim. Past
Discussion started: 24 August 2017

Climate of the Past Discussions
Open Access
EGU

3.2.3 Model-proxy distance

Ideally, if the full model pool captures the variability of the proxy record, the best analogs are scattered among all possible climate states represented in the model pool and have equally low RMSE (Eq. (1)) throughout the surrogate reconstruction. This is not the case throughout the record (Fig. 4) as generally colder periods are better captured by the model pool than warmer periods. The worst fit between the model and proxy data is found during the time interval 36.9-38.3 kyr (same for all models; not shown). During this interval the RMSE is large and the best analogs are constructed from very few different climate states which mainly belong to the hosing simulations. One could argue that this is an artifact that depends on the baseline from which we calculate the anomalies for both proxy and model data. Indeed, the mean of the proxy data is closest to stadial temperatures and the amplitudes of the warm interstadials are larger than the cold stadials in the proxy data. Therefore a large RMSE during interstadials does not necessarily indicate that the model state is furthest from the interstadials, but rather that the model pool does not capture the full variability of the proxy record.

Nevertheless, because choosing a baseline from which we compute the anomalies is not trivial, we test three plausible alternatives.

For the original approach, we simply compute anomalies from the temporal mean;

$$\begin{aligned} T_i^{p'} &= T_i^p - \overline{T_i^p}, \\ T_i^{m'} &= T_i^m - \overline{T_i^m}, \end{aligned} \tag{5}$$

where the overline ($\bar{\cdot}$) represents the mean, and the prime ($'$) the anomaly (excluded in the other sections of the text for simplicity). Note that for the model pool the anomalies are with respect to each individual model simulation, not the full model pool.

One could argue that a reasonable way to calculate the proxy and model anomalies would be to compare them to PI (Holocene) conditions in order to avoid the bias toward stadial times. We have temperature reconstructions of PI conditions for 9 of the cores for which we use the mean of the past 10 kyr as the baseline. We omit the proxy records for which we do not have this information. For the model pools we use the mean of the PI control simulations. The anomalies become:

$$\begin{aligned} T_i^{p'} &= T_i^p - \overline{T_i^p}(0-10\,\mathrm{kyr}), \\ T_i^{m'} &= T_i^m - \overline{T_i^m}(\mathrm{PI}). \end{aligned} \tag{6}$$

Using the PSR method with these anomalies we find that the RMSE between the proxy data and the model simulations increases, and the mean correlation between the surrogate and proxy reconstructions at the core locations drops by 35% (compared to the original definition, but with only 9 cores), and very few different model years are chosen for the analogs.

Finally, one could argue that a reasonable choice would be to use the stadial conditions as the baseline. Here we compute the anomalies as;

$$\begin{aligned} T_i^{p'} &= T_i^p - \overline{T_i^p}(38.2-39.9\,\mathrm{kyr}), \\ T_i^{m'} &= T_i^m - \overline{T_i^m}(\mathrm{MIS3\,no\,hose\,sim.}). \end{aligned} \tag{7}$$

Clim. Past Discuss., https://doi.org/10.5194/cp-2017-103
Manuscript under review for journal Clim. Past
Discussion started: 24 August 2017

As a result, the RMSE increases, and the mean correlation and standard deviation of the resulting surrogate reconstruction and proxy data at the core locations decrease. Neither the hosing simulations, nor the PI or LGM simulations are chosen for the analogs. This is also true if Eq. (7) is normalized by the standard deviation of the stadial time period in addition. The definition of the anomaly is clearly important for the PSR method, but since the original definition performs the best, the following discussion will focus on it.

4 The proxy surrogate reconstruction

We now look at the results of the PSR both as time series at the core locations and as composite maps. Our interpretation of the results is found in Sect. 5.

4.1 Reconstruction at proxy locations

The performance of the surrogate time series at the different proxy locations differs between sites (Fig. 6, r=0.47-0.92; A=0.32-1.24, where A is the ratio between the standard deviation of the surrogate and proxy data time series). The surrogate time series matches the proxy time series best in the central North Atlantic and in the subpolar gyre (cores 5,6,8,10,12, and 14; r^2=0.64-0.92; A=0.52-1.01). Surrogate time series taking into account possible uncertainties in the age models produce a confidence interval that generally follows the proxy time series. This is especially true for the long lasting GS9 and GI8 where most of the surrogate time series produced with the original age models agree with the age model uncertainties at the core locations. We therefore focus on GS9 and GI8 when studying the spatial patterns using composite maps of the surrogate time series over these periods.

The surrogate reconstruction proves to be relatively independent of a single proxy time series. By excluding one core at a time before performing the PSR method, we can estimate the importance of each core in the full reconstruction. The mean correlation between the proxy data and the surrogate time series hardly changes and slightly improves in some cases ($\overline{r} = 0.71 - 0.78$) as there are fewer constraints on the surrogate reconstruction. By doing this, we can also assess the agreement between the proxy data and the surrogate time series at the location where the core was excluded (i.e., bootstrapping). Once again, the performance differs between sites, but the agreement between the two records is on average $r = 0.35$.

4.2 Reconstructed spatial patterns

The surrogate reconstruction based on the full HadCM3 model pool shows colder SSTs during GS9 than during GI8 throughout the subpolar North Atlantic (Fig. 7). Notable exceptions are the subtropical-subpolar gyre boundary off the coast of North America which shows warmer conditions during GS9 than during GI8, and the eastern subpolar gyre and the northern Nordic Seas which show little to no temperature change. We note that the synthetic test in Sect. 3.1 showed that the variability in the subtropical-subpolar gyre boundary off the coast of North America was poorly represented by the variability at the core locations. During GI8, the subpolar gyre is warmer than normal with especially strong warming near the Greenland-Scotland

Clim. Past Discuss., https://doi.org/10.5194/cp-2017-103
Manuscript under review for journal Clim. Past
Discussion started: 24 August 2017

ridge and the coast of western Europe. Except for the magnitude of the warming in the eastern North Atlantic, the results are robust to differences in age models and do not depend on single cores (see details in Fig. 7).

The spatial SST patterns are largely consistent with the surrogate reconstructions produced using the other model pools. Both the CCSM4 pool and the HadCM3 nohose-model pool produce comparable surrogate time series, albeit lacking the amplitude present in the main HadCM3 model pool. The temperature patterns are similar (Figs. 8, 9), although the Nordic Seas are warmer during GS9 than GI8, which is not clearly seen when the HadCM3 model pool is used. We note that the general SST pattern holds when PI control simulations with NorESM and IPSL are used as the model pools (not shown). The similarity in reconstructed ocean patterns suggests that the ocean variability is based on physical mechanisms present in a wide range of simulations.

4.3 Extending the information to other climate variables

Given the reasonable agreement with the reconstructed SSTs and the original proxy record, we expand our analysis to other climate variables. We note that none of these variables are constrained by the PSR method, other than by being linked to the changing SSTs over the North Atlantic. Using the HadCM3 model pool, the ice core temperature record from NGRIP (Kindler et al., 2014) and the reconstructed atmospheric temperature from the closest grid location to NGRIP in the surrogate time series are highly correlated (Fig. 7d, Table 3). Despite the high correlation, the amplitude of the temperature variability is lower in the PSR record than in the ice core. However, since we are not able to capture the full amplitude of the temperature variability in the ocean, we do not expect to capture the full temperature variability on Greenland either.

While the HadCM3 model pool produces reasonable agreement with ice core record at NGRIP, less of the NGRIP temperature variability is captured with the HadCM3 nohose and CCSM4 pools (Figs. 8d, 9d, Table 3). The results of NGRIP are comparable if the surrogate reconstructions are compared to temperature reconstructions from the GISP2 ice core instead (Table 3, Cuffey and Clow, 1997; Alley, 2004).

The agreement between the reconstructed temperatures from ice cores on Greenland and the surrogate reconstruction shows that the PSR method has skill at reconstructing the climate in areas away from the core locations and in variables that are not directly linked to the SST-proxies. Therefore, we now look at more variables and outside the core locations for GS9/GI8. Even though we do not aim to fully understand the dynamics of the variability, other variables might elucidate the mechanisms behind the oceanic variability we see.

We start by examining the ocean circulation with the AMOC variability of the surrogate reconstruction based on the HadCM3 model pool (Fig. 10), in which AMOC mostly varies with the strong freshwater forcing. The surrogate reconstruction consists of years from different states of the hosing runs: GS9 is best represented by the hosed conditions with weak AMOC, whereas GI8 is best represented by years just before or after the hosing. The beginning of GI8 tends to be best represented by the end of the hosing simulation as the AMOC resumes, while the end of the GI8 tends to be best represented by the beginning of the hosing simulations when the AMOC weakens (Fig. 4).

The overturning streamfunction output was not available for all of the HadCM3 simulations, but we were able to continue the simulations lacking the output for another 100 years to recover the streamfunction output (note that these are simulations with

Clim. Past Discuss., https://doi.org/10.5194/cp-2017-103
Manuscript under review for journal Clim. Past
Discussion started: 24 August 2017

constant forcing and we do not expect the AMOC properties to change from the original data). These simulations form a new model pool HadCM3⋆ (Table 2) which enables a full AMOC reconstruction. We note that the PSR based on the HadCM3⋆ and HadCM3 are comparable (Fig. 5, similar RMSE and surrogate time series at core locations; not shown). The AMOC reconstruction shows a stronger overturning circulation during GI8 than during GS9; the whole upper cell of the streamfunction is weaker during GS9, apart from a negative cell in the Southern Ocean which behaves the opposite way (Fig. 10d). There is hardly any change in the overturning in the Nordic Seas. The same analysis with the HadCM3 nohose and CCSM4 model pools show a generally stronger AMOC during GI8 than during GS9 (Figs. 12d, 11d). Interestingly, the HadCM3 nohose model pool shows a stronger overturning circulation over the Greenland-Scotland ridge during GI8 than GS9, but a weaker Southern Ocean cell during GS9 than GI8. However, the HadCM3 nohose and CCSM4 model pools lead to AMOC changes that are generally very small. Due to the uncertainties in age models of the oceanic proxies, it is difficult to conclude whether the AMOC signal leads or lags the transitions between the GSs and GIs.

Sea-ice changes are largest for the main HadCM3 pool which includes hosing. There is a ∼25% decrease in the annual sea-ice concentration in the subpolar gyre region between GS9 and GI8. The sea-ice edge retreats north-west during GI8, with largest change in the winter sea-ice edge (Fig. 10c). Close to the Greenland-Scotland ridge, the annual mean sea-ice concentration changes are even larger (>50%) as the area is perennially ice covered during GS9, but ice-free almost the whole year during GI8. For the model pools without the hosing simulations the changes in the sea-ice cover are small (Figs. 11c, 12c) and mostly visible as a shift in the summer sea-ice edge.

Consistent with the sea-ice changes and the freshwater forcing, the surrogate reconstruction shows a much fresher surface in the North Atlantic during GS9 than GI8 (Fig. 10b). Indeed, the surrogate time series consist of model years taken from the beginning and end of the hosing simulations during GS9 and GI8, respectively (Fig. 4). Interestingly, the unforced simulations also produce a fresher subpolar gyre during GS9 (Figs. 11b, 12b), although the freshening does not extend to the Nordic Seas as in the freshwater forced simulations.

Changes in the atmospheric temperature are similar to the changes in the SSTs. The HadCM3 model pool results in a colder atmosphere during GS9 than GI8 over much of the North Atlantic, with the cold conditions extending to Greenland, western Europe and northern Africa (Fig. 10a). However, in the subtropical-subpolar gyre boundary and in the southern Atlantic, the atmosphere is warmer during GS9 than GI8, consistent with the AMOC changes. The strongest atmospheric anomalies are found near the Greenland-Scotland ridge where the sea-ice changes are the largest. When the HadCM3 nohose and CCSM4 model pools are used, the atmospheric temperature signals are mostly confined to the North Atlantic ocean and do not extend over land, except to parts of western Europe and Eastern North America (Figs. 11a, 12a). For both model pools, the subpolar gyre region is colder during GS9 than GI8, but for the Nordic Seas and the subtropical-subpolar gyre boundary where the atmosphere is warmer during GS9 than GI8 (consistent with the SST changes).

Clim. Past Discuss., https://doi.org/10.5194/cp-2017-103
Manuscript under review for journal Clim. Past
Discussion started: 24 August 2017

5 Discussions

The PRS method is tested for the first time with proxy data from MIS3. We are able to produce a new time series which agrees with the information from the proxy data, although being dependent on the relative dating between records. We have addressed the uncertainties in the age models for the different proxy records, however, each individual test could be further evaluated. We also note that the method gives quantitatively similar results when individual proxy records are excluded, suggesting that one poor age model would not throw off the results. Further testing could include the addition of noise to the records to see how robust the PSR is to errors in the proxy data. The method is also sensitive to how the anomalies used to compare proxy data and model output are defined, and care should be taken in finding the right analogs. One obvious limitation is the lack of long LGM and glacial simulations with different forcings, however, such simulations can easily be included in the model pool should they come available. In general, expanding the model pool is straightforward and would be a natural next step when new simulations become available, for example through the Climate Model Intercomparison Project Phase 6 (CMIP6).

We have shown that the PSR leads to a pattern of SST change from GS9 to GI8 which is largely independent of the underlying model pool. However, the results suggest that forced simulations are needed to capture the magnitude of the SST variability and the temperature signal on Greenland. We suggest that these results have two interesting implications.

First, the pattern of SST variability can be reproduced across a wide range of model simulations including some without external forcing. This suggests that DO-events create SST patterns that are not unlike those of modern internal variability. In the case of the HadCM3 model pool, this mode is excited by freshwater forcing. However, we suggest that in the case of HadCM3 nohose and CCSM4 model pools a somewhat similar pattern results from an ocean response to a shift in the North Atlantic Oscillation (NAO), a prominent mode of atmospheric variability. This interpretation is backed up by earlier studies that show almost identical SST (Delworth and Zeng, 2016; Delworth et al., 2017) and sea-ice (Ukita et al., 2007) patterns as a response to changing NAO, but this does not exclude the possibility for other trigger mechanisms. It is clear that the oceanic changes associated with the NAO are not large enough to explain the amplitude of the ocean variability during DO-events

Second, the PSR from the HadCM3 model pool is the only reconstruction where the GS9 to GI8 temperature difference is visible much beyond the North Atlantic Ocean. Previous literature (Broecker, 2000; Gildor and Tziperman, 2003; Masson-Delmotte et al., 2005; Li et al., 2005, 2010; Dokken et al., 2013; Hoff et al., 2016) suggests that changes in the sea-ice cover amplify the temperature response on Greenland over the DO-transition. We suggest that the lack of sea-ice change in the HadCM3 nohose and CCSM4 model pool based PSRs is the primary reason for the weak temperature signal over Greenland in the surrogate reconstructions. Similarly, the weaker than observed temperature variability in the HadCM3 based PSR on Greenland is probably partly dependent on the amplitude and location of the changes in the sea-ice cover. Sea-ice reductions in the Nordic Seas have been shown to produce a larger temperature response on Greenland than sea-ice reductions in the subpolar gyre (Li et al., 2010) which is where we see the largest sea-ice changes. We also note that for the HadCM3 model pool, the largest changes in the sea-ice cover take place in winter, consistent with studies suggesting that winter sea-ice change is needed to capture the Greenland temperature variability (Li et al., 2005; Denton et al., 2005). However, for HadCM3 nohose and CCSM4, the change in the summer sea ice tends to be larger than the change in the winter sea ice.

Clim. Past Discuss., https://doi.org/10.5194/cp-2017-103
Manuscript under review for journal Clim. Past
Discussion started: 24 August 2017

While our results suggest that changes in the freshwater input to the North Atlantic could explain large parts of the glacial temperature variability in the North Atlantic and on Greenland, this does not necessarily imply that freshwater input is the only possible forcing of the glacial variability. Since the internal variability reproduces the patterns of glacial SST variability, it could be that any forcing that can excite such internal modes of variability could possibly contribute to the DO type of temperature change if the boundary conditions (e.g., sea ice) are right. The results suggest that even in the absence of freshwater forcing, GS9 is linked to anomalously fresh conditions in the cold subpolar gyre (Figs. 11b, 12b). Such fresh conditions provide a positive feedback that slows down the circulation and further cools the gyre, a feedback mechanism found to be important in both decadal and millennial climate variability (Born et al., 2010b; Born and Levermann, 2010a; Born et al., 2013; Moffa-Sánchez et al., 2014; Born et al., 2015). Therefore, even if the freshwater is not a primary forcing needed for glacial variability, internal freshwater feedbacks like the subpolar-gyre response can still be an important amplifier in the glacial variability. Extending the model pool to simulations forced with other possible mechanisms could be used to further explore the importance of the freshwater forcing.

6 Conclusions

We have applied, for the first time, the proxy surrogate reconstruction method to oceanic proxy data from MIS3. The results are robust to different sensitivity tests and relatively independent of the underlying model data and proxy locations.

Our results imply that the patterns of oceanic variability in the glacial climate can be well represented by patterns of short term variability intrinsic to the climate system. We find consistent patterns of variability in sea-surface temperature, sea-surface salinity, and atmospheric temperature in two different climate models and in different background climates. However, to fully capture the amplitude of the North Atlantic sea-surface temperature variability, and the surface air temperature variability on Greenland, forced simulations, in our case forced by freshwater, are required.

Our results further suggest that the sea-ice cover could play an amplifying role during DO-events. We see a clear reduction in sea-ice concentration between stadial and interstadial conditions when the forced simulations are included in the proxy-surrogate reconstruction, likely contributing to the temperature signal on Greenland. Indeed, the lack of a sea-ice signal might be one of the reasons why the unforced model results lack the amplitude of the DO variations, especially on Greenland.

Finally, we are well aware of the limitations of the methodology and the validation so far back in time. Therefore, we see this study as an encouraging first attempt to apply the PSR method to oceanic variability during MIS3 and believe it should be further developed for an ideal implementation. A straightforward next step would be to expand the model pool with simulations from different models and with different boundary conditions.

Data availability. All proxy records used (with exception of the MD95-2010 record) are previously published, and we refer to the original publications for details regarding availability of these records. The record MD95-2010 is currently under publication processes, and details

will be added when they become available. For access to the model output from HadCM3 please contact Dr. William H. G. Roberts directly (William.Roberts@bristol.ac.uk). The model output from the CCSM4 can be found at e.g., http://pcmdi9.llnl.gov/.

Competing interests. The authors declare that they have no conflict of interest

Acknowledgements. The research leading to these results is part of the ice2ice project funded by the European Research Council under the European Community's Seventh Framework Programme (FP7/2007-2013)/ERC Grant Agreement No. 610055. The research was supported by the Centre for Climate Dynamics at the Bjerknes Centre. We thank Paul Valdes and Joy Singarayer for the use of their HadCM3 model simulations. The HadCM3 model simulations were carried out using the computational facilities of the Advanced Computing Research Centre, University of Bristol - http://www.bris.ac.uk/acrc/. We acknowledge the World Climate Research Programme's Working Group on Coupled Modelling, which is responsible for CMIP, and we thank the National Center for Atmospheric Research for producing and making available their model output.

Clim. Past Discuss., https://doi.org/10.5194/cp-2017-103
Manuscript under review for journal Clim. Past
Discussion started: 24 August 2017

References

Alley, R.: GISP2 Ice Core Temperature and Accumulation Data, iGBP PAGES/World Data Center for Paleoclimatology Data Contribution Series 2004-013, NOAA/NGDC Paleoclimatology Program, Boulder CO, USA, 2004.

Arzel, O., Colin de Verdiere, A., and England, M. H.: The Role of Oceanic Heat Transport and Wind Stress Forcing in Abrupt Millennial-Scale Climate Transitions, J. Clim, 23, 2233–2256, 2010.

Bard, E., Rostek, F., and Ménot-Combes, G.: Radiocarbon calibration beyond 20,000 14C yr B.P. by means of planktonic foraminifera of the Iberian Margin, Quaternary Research, 61, 204 – 214, doi:https://doi.org/10.1016/j.yqres.2003.11.006, http://www.sciencedirect.com/science/article/pii/S0033589403001698, 2004.

Barker, S., Chen, J., Gong, X., Jonkers, L., Knorr, G., and Thornalley, D.: Icebergs not the trigger for North Atlantic cold events, Nature, 520, 333–336, 2015.

Berger, A. and Loutre, M. F.: Insolation values for the climate of the last 10 million years, Quaternary Science Reviews, 10(4), 297–317, 1991.

Bond, G., Broecker, W., Johnsen, S., McManus, J., Labeyrie, L., Jouzel, J., and Bonani, G.: Correlations between climate records from North Atlantic sediments and Greenland ice, Nature, 365, 143–147, 1993.

Bond, G. C., Showers, W., Elliot, M., Evans, M., Lotti, R., Hajdas, I., Bonani, G., and Johnson, S.: The North Atlantic's 1-2 Kyr Climate Rhythm: Relation to Heinrich Events, Dansgaard/Oeschger Cycles and the Little Ice Age, pp. 35–58, American Geophysical Union, doi:10.1029/GM112p0035, http://dx.doi.org/10.1029/GM112p0035, 2013.

Born, A. and Levermann, A.: The 8.2 ka event: Abrupt transition of the subpolar gyre toward a modern North Atlantic circulation, Geochemistry, Geophysics, Geosystems, 11, n/a–n/a, doi:10.1029/2009GC003024, http://dx.doi.org/10.1029/2009GC003024, q06011, 2010a.

Born, A. and Stocker, T. F.: Two Stable Equilibria of the Atlantic Subpolar Gyre, Journal of Physical Oceanography, 44, 246–264, 2014.

Born, A., Nisancioglu, K. H., and Braconnot, P.: Sea ice induced changes in ocean circulation during the Eemian, Climate Dynamics, 35, 1361–1371, doi:10.1007/s00382-009-0709-2, https://doi.org/10.1007/s00382-009-0709-2, 2010b.

Born, A., Stocker, T. F., Raible, C. C., and Levermann, A.: Is the Atlantic subpolar gyre bistable in comprehensive coupled climate models?, Clim Dyn, 40, 2993–3007, 2013.

Born, A., Mignot, J., and Stocker, T. F.: Multiple Equilibria as a Possible Mechanism for Decadal Variability in the North Atlantic Ocean, Journal of Climate, 28, 8907–8922, doi:10.1175/JCLI-D-14-00813.1, https://doi.org/10.1175/JCLI-D-14-00813.1, 2015.

Brady, E. C., Otto-Bliesner, B. L., Kay, J. E., and Rosenbloom, N.: Sensitivity to Glacial Forcing in the CCSM4, Journal of Climate, 26, 1901–1925, doi:10.1175/JCLI-D-11-00416.1, http://dx.doi.org/10.1175/JCLI-D-11-00416.1, 2013.

Brandefelt, J., Kjellström, E., Näslund, J.-O., Strandberg, G., Voelker, A. H. L., and Wohlfarth, B.: A coupled climate model simulation of Marine Isotope Stage 3 stadial climate, Climate of the Past, 7, 649–670, 2011.

Broecker, W. S.: Abrupt climate change: casual constraints provided by the paleoclimate record, Earth-Sci. Rev., 51, 137–154, 2000.

Broecker, W. S., Bond, G., and Klas, M.: A salt oscillator in the glacial Atlantic? 1. The concept, Paleoceanography, 5, 469–477, 1990.

Colin de Verdiere, A. and Raa, L. T.: Weak oceanic heat transport as a cause of the instability of glacial climates, Clim. Dyn., 35, 1237–1256, doi:10.1007/s00382-009-0675-8, 2010.

Cuffey, K. and Clow, G.: Temperature, accumulation, and ice sheet elevation in central Greenland through the last deglacial transition, Journal of Geophysical Research, 102, 26 383–26 396, 1997.

Clim. Past Discuss., https://doi.org/10.5194/cp-2017-103
Manuscript under review for journal Clim. Past
Discussion started: 24 August 2017

Curry, W. B., Marchitto, T. M., Mcmanus, J. F., Oppo, D. W., and Laarkamp, K. L.: Millennial-scale Changes in Ventilation of the Thermocline, Intermediate, and Deep Waters of the Glacial North Atlantic, pp. 59–76, American Geophysical Union, doi:10.1029/GM112p0059, http://dx.doi.org/10.1029/GM112p0059, 2013.

Danabasoglu, G., Bates, S. C., Briegleb, B. P., Jayne, S. R., Jochum, M., Large, W. G., Peacock, S., and Yeager, S. G.: The CCSM4 Ocean Component, J. Clim, 25, 1361–1389, 2012.

Dansgaard, W., Johnsen, S. J., Clausen, H. B., Dahl-Jensen, D., Gundestrup, N. S., Hammer, C. U., Hvidberg, C. S., Steffensen, J. P., Sveinbjörnsdottir, A. E., Jouzel, J., and Bond, G.: Evidence for general instability of past climate from a 250-kyr ice-core record, Nature, 364, 218–220, 1993.

de Abreu, L., Shackleton, N. J., Schönfeld, J., Hall, M., and Chapman, M.: Millennial-scale oceanic climate variability off the Western Iberian margin during the last two glacial periods, Marine Geology, 196, 1 – 20, doi:https://doi.org/10.1016/S0025-3227(03)00046-X, http://www.sciencedirect.com/science/article/pii/S002532270300046X, 2003.

Delworth, T. L. and Zeng, F.: The Impact of the North Atlantic Oscillation on Climate through Its Influence on the Atlantic Meridional Overturning Circulation, Journal of Climate, 29, 941–962, doi:10.1175/JCLI-D-15-0396.1, http://dx.doi.org/10.1175/JCLI-D-15-0396.1, 2016.

Delworth, T. L., Zeng, F., Zhang, L., Zhang, R., Vecchi, G. A., and Yang, X.: The Central Role of Ocean Dynamics in Connecting the North Atlantic Oscillation to the Extratropical Component of the Atlantic Multidecadal Oscillation, Journal of Climate, 30, 3789–3805, doi:10.1175/JCLI-D-16-0358.1, https://doi.org/10.1175/JCLI-D-16-0358.1, 2017.

Denton, G. H., Alley, R. B., Comer, G. C., and Broecker, W. S.: The role of seasonality in abrupt climate change, Quaternary Science Reviews, 24, 1159 – 1182, doi:http://dx.doi.org/10.1016/j.quascirev.2004.12.002, http://www.sciencedirect.com/science/article/pii/S027737910500003X, 2005.

Dokken, T. and Jansen, E.: Rapid changes in the mechanism of ocean convection during the last glacial period, Nature, 401, 458–461, 1999.

Dokken, T. M., Nisancioglu, K. H., Li, C., Battisti, D. S., and Kissel, C.: Dansgaard-Oeschger cycles: interactions between ocean and sea intrinsic to the Nordic Seas, Paleoceanography, 28, 491–502, 2013.

Elliot, M., Labeyrie, L., Bond, G., Cortijo, E., Turon, J.-L., Tisnerat, N., and Duplessy, J.-C.: Millennial-scale iceberg discharges in the Irminger Basin during the Last Glacial Period: Relationship with the Heinrich events and environmental settings, Paleoceanography, 13, 433–446, doi:10.1029/98PA01792, http://dx.doi.org/10.1029/98PA01792, 1998.

Elliot, M., Labeyrie, L., and Duplessy, J.-C.: Changes in North Atlantic deep-water formation associated with the Dansgaard-Oeschger temperature oscillations (60-10 ka), Quaternary Science Reviews, 21, 1153–1165, 2002.

Eynaud, F., Turon, J. L., Matthiessen, J., Kissel, C., Peypouquet, J. P., de Vernal, A., and Henry, M.: Norwegian sea-surface palaeoenvironments of marine oxygen-isotope stage 3: the paradoxical response of dinoflagellate cysts, Journal of Quaternary Science, 17, 349–359, doi:10.1002/jqs.676, http://dx.doi.org/10.1002/jqs.676, 2002.

Eynaud, F., de Abreu, L., Voelker, A., SchÃ¶nfeld, J., Salgueiro, E., Turon, J.-L., Penaud, A., Toucanne, S., Naughton, F., SÃ¡nchez GoÃ±i, M. F., MalaizÃ©, B., and Cacho, I.: Position of the Polar Front along the western Iberian margin during key cold episodes of the last 45 ka, Geochemistry, Geophysics, Geosystems, 10, doi:10.1029/2009GC002398, http://dx.doi.org/10.1029/2009GC002398, q07U05, 2009.

Ezat, M. M., Rasmussen, T. L., and Groeneveld, J.: Persistent intermediate water warming during cold stadials in the southeastern Nordic seas during the past 65 k.y., Geology, 42, 663–666, doi:10.1130/G35579.1, 2014.

Clim. Past Discuss., https://doi.org/10.5194/cp-2017-103
Manuscript under review for journal Clim. Past
Discussion started: 24 August 2017

Franke, J., González-Rouco, J. F., Frank, D., and Graham, N. E.: 200 years of European temperature variability: insights from and tests of the proxy surrogate reconstruction analog method, Climate Dynamics, 37, 133–150, doi:10.1007/s00382-010-0802-6, http://dx.doi.org/10.1007/s00382-010-0802-6, 2011.

Ganopolski, A. and Rahmstorf, S.: Rapid changes of glacial climate simulated in a coupled climate model, Nature, 409, 153–158, 2001.

Gebbie, G., Peterson, C. D., Lisiecki, L. E., and Spero, H. J.: Global-mean marine δ13C and its uncertainty in a glacial state estimate, Quaternary Science Reviews, 125, 144 –159, doi:https://doi.org/10.1016/j.quascirev.2015.08.010, 2015.

Gent, P. R., Danabasoglu, G., Donner, L. J., Holland, M. M., Hunke, E. C., Jayne, S. R., Lawrence, D. M., Neale, R. B., Rasch, P. J., Vertenstein, M., Worley, P. H., Yang, Z.-L., and Zhang, M.: The Community Climate System Model Version 4, J. Clim, 24, 4973–4991, 2011.

Gildor, H. and Tziperman, E.: Sea-ice switches and abrupt climate change, Phil. Trans R. Soc. London Ser. A, 361, 1935–1944, 2003.

Gómez-Navarro, J. J., Zorita, E., Raible, C. C., and Neukom, R.: Pseudo-proxy tests of the analogue method to reconstruct spatially resolved global temperature during the Common Era, Climate of the Past, 13, 629–648, doi:10.5194/cp-13-629-2017, 2017.

Gordon, C., Cooper, C., Senior, C. A., Banks, H., Gregory, J. M., Johns, T. C., Mitchell, J. F. B., and Wood, R. A.: The simulation of SST, sea ice extents and ocean heat transports in a version of the Hadley Centre coupled model without flux adjustments, Climate Dynamics, 16, 147–168, doi:10.1007/s003820050010, http://dx.doi.org/10.1007/s003820050010, 2000.

Govin, A., Braconnot, P., Capron, E., Cortijo, E., Duplessy, J.-C., Jansen, E., Labeyrie, L., Landais, A., Marti, O., Michel, E., Mosquet, E., Risebrobakken, B., Swingedouw, D., and Waelbroeck, C.: Persistent influence of ice sheet melting on high northern latitude climate during the early Last Interglacial, Climate of the Past, 8, 483–507, 2012.

Graham, N. E., Hughes, M. K., Ammann, C. M., Cobb, K. M., Hoerling, M. P., Kennett, D. J., Kennett, J. P., Rein, B., Stott, L., Wigand, P. E., and Xu, T.: Tropical Pacific – mid-latitude teleconnections in medieval times, Clim Change, 83, 241–285, doi:10.1007/s10584-007-9239-2, 2007.

Grootes, P. M. and Stuiver, M.: Oxygen 18/16 variability in Greenland snow and ice with 10^3- to 10^5- year time resolution, J. Geophys. Res., 102, 26 455–26 470, 1997.

Hagen, S. and Hald, M.: Variation in surface and deep water circulation in the Denmark Strait, North Atlantic, during marine isotope stages 3 and 2, Paleoceanography, 17, 2002.

Hall, I. R., Colmenero-Hidalgo, E., Zahn, R., Peck, V. L., and Hemming, S. R.: Centennial- to millennial-scale ice-ocean interactions in the subpolar northeast Atlantic 18-41 kyr ago, Paleoceanography, 26, doi:10.1029/2010PA002084, http://dx.doi.org/10.1029/2010PA002084, pA2224, 2011.

Hoff, U., Rasmussen, T. L., Stein, R., Ezat, M. M., and Fahl, K.: Sea ice and millennial-scale climate variability in the Nordic seas 90 kyr ago to present, Nature Communications, 7, doi:doi:10.1038/ncomms12247, 2016.

Johnsen, S. J., Clausen, H. B., Dansgaard, W., Fuhrer, K., Gundestrup, N., Hammer, C. U., Iversen, P., Jouzel, J., Stauffer, B., and Steffensen, J. P.: Irregular glacial interstadials recorded in a new Greenland ice core, Nature, 359, 311–313, 1992.

Kiefer, T.: Produktivität und Temperaturen im subtropischen Nordatlantik: zyklische und abrupte Veränderungen im späten Quartär, Ph.D. thesis, Berichte-Reports Geologisch-Paläontologisches Institut, Univ. Kiel, 1998.

Kindler, P., Guillevic, M., Baumgartner, M., Schwander, J., Landais, A., and Leuenberger, M.: Temperature reconstruction from 10 to 120 kyr b2k from the NGRIP ice core, Climate of the Past, 10, 887–902, doi:10.5194/cp-10-887-2014, 2014.

Kleppin, H., Jochum, M., Otto-Bliesner, B., Shields, C. A., and Yeager, S.: Stochastic atmospheric forcing as a cause of Greenland climate transitions, J. Clim, 28, 7741–7763, 2015.

Kucera, M., Rosell-Mele, A., Schneider, R., Waelbroeck, C., , and Weinelt, M.: Multiproxy approach for the reconstruction of the glacial ocean surface (MARGO), Quarternary Science Reviews, 24, 813–819, 2005.

Kurahashi-Nakamura, T., Losch, M., and Paul, A.: Can sparse proxy data constrain the strength of the Atlantic meridional overturning circulation?, Geoscientific Model Development, 7, 419–432, doi:10.5194/gmd-7-419-2014, 2014.

Labeyrie, L., Vidal, L., Cortijo, E., Paterne, M., Arnold, M., Duplessy, J. C., Vautravers, M., Labracherie, M., Duprat, J., Turon, J. L., Grousset, F., and Weering, T. V.: Surface and Deep Hydrology of the Northern Atlantic Ocean during the past 150 000 Years, Philosophical Transactions of the Royal Society of London B: Biological Sciences, 348, 255–264, doi:10.1098/rstb.1995.0067, http://rstb.royalsocietypublishing.org/content/348/1324/255, 1995.

Labeyrie, L., Leclaire, H., Waelbroeck, C., Cortijo, E., Duplessy, J.-C., Vidal, L., Elliot, M., and Coat, B. L.: Mechanisms of Global Climate Change at Millennial Time Scales, vol. 112, chap. Temporal variability of the Surface and Deep Waters of the North West Atlantic Ocean at Orbital and Millenial Scales, pp. 77–98, Geophysical Monograph Series, 1999.

Li, C., Battisti, D. S., Schrag, D. P., and Tziperman, E.: Abrupt climate shifts in Greenland due to displacements of the sea ice edge, Geophys. Res. Lett., 32, L19 702, doi:10.1029/2005GL023 492, 2005.

Li, C., Battisti, D. S., and Bitz, C. M.: Can North Atlantic Sea Ice Anomalies Account for Dansgaard-Oeschger Climate Signals?, J. Clim, 23, 5457–5475, 2010.

Lorenz, E. N.: Atmospheric Predictability as Revealed by Naturally Occuring Analogues, Journal of the Atmospheric Sciences, 26, 636–646, 1969.

Loulergue, L., Schilt, A., Spahni, R., Masson-Delmotte, V., Blunier, T., Lemieux, B., Barnola, J.-M., Raynaud, D., Stocker, T. F., and Chappellaz, J.: Orbital and millennial-scale features of atmospheric CH4 over the past 800,000 years., Nature, 453, doi:10.1038/nature06950, 2008.

Marotzke, J.: Abrupt climate change and the thermohaline circulation: mechanisms and predictability, P. Natl. Acad. Sci. U.S.A., 97, 1347–1350, 2000.

Masson-Delmotte, V., Jouzel, J., Landais, A., Stievenard, M., Johnsen, S. J., White, J. W. C., Werner, M., Sveinbjornsdottir, A., and Fuhrer, K.: GRIP deuterium excess reveals rapid and orbital-scale changes in Greenland moisture origin,, Science, 309, 118–121, 2005.

Moffa-Sánchez, P., Born, A., Hall, I. R., Thornalley, D. J. R., and Barker, S.: Solar forcing of North Atlantic surface temperature and salinity over the past millennium, Nature Geoscience, 7, 275–278, doi:doi:10.1038/ngeo2094, 2014.

North-Greenland-Ice-Core-project members: High-resolution record of Northern Hemisphere climate extending into the last interglacial period, Nature, 431, 147–151, 2004.

Peck, V. L., Hall, I. R., Zahn, R., Grousset, F., Hemming, S. R., and Scourse, J. D.: The Relationship of Heinrich events and their Europe precursors over the past 60 ka BP: a multi-proxy ice-rafted debris provenance study in the North East Atlantic, Quarternary Science Reviews, 26, 862–875, 2007.

Peltier, W.: Global Glacial Isostasy and the Surface of the Ice-Age Earth: The ICE-5G (VM2) Model and GRACE, Annual Review of Earth and Planetary Sciences, 32, 111–149, doi:10.1146/annurev.earth.32.082503.144359, https://doi.org/10.1146/annurev.earth.32.082503.144359, 2004.

Peltier, W. R. and Vettoretti, G.: Dansgaard-Oeschger oscillations predicted in a comprehensive model of glacial climate: A “kicked” salt oscillator in the Atlantic, Geophysical Research Letters, 41, 7306–7313, doi:10.1002/2014GL061413, http://dx.doi.org/10.1002/2014GL061413, 2014GL061413, 2014.

Petersen, S. V., Schrag, D. P., and Clark, P. U.: A new mechanism for Dansgaard-Oeschger cycles, Paleoceanography, 28, 24–30, 2013.

Clim. Past Discuss., https://doi.org/10.5194/cp-2017-103
Manuscript under review for journal Clim. Past
Discussion started: 24 August 2017

Petit, J., Jouzel, J., Raynaud, D., Barkov, N., Barnola, J., Basile, I., Bender, M., Chappellaz, J., Davis, M., Delaygue, G., Delmotte, M., Kotlyakov, V., Legrand, M., Lipenkov, V., Lorius, C., Pepin, L., Ritz, C., Saltzman, E., and Stievenard, M.: Climate and atmospheric history of the past 420,000 years from the Vostok ice core, Antarctica, Nature, 399, 429–436, doi:10.1038/20859, 1999.

Rahmstorf, S.: Ocean circulation and climate during the past 120,000 years, Nature, 419, 207–214, 2002.

Rahmstorf, S., Box, J. E., Feulner, G., Mann, M. E., Robinson, A., Rutherford, S., and Schaaernicht, E. J.: Exceptional twentieth-century slowdown in Atlantic Ocean overturning circulation, Nature Climate Change, pp. 475–480, doi:10.1038/NCLIMATE2554, 2015.

Rasmussen, S. O., Bigler, M., Blockley, S. P., Blunier, T., Buchardt, S. L., Clausen, H. B., Cvijanovic, I., Dahl-Jensen, D., Johnsen, S. J., Fischer, H., Gkinis, V., Guillevic, M., Hoek, W. Z., Lowe, J. J., Pedro, J. B., Popp, T., Seierstad, I. K., Steffensen, J. P., Svensson, A. M., Vallelonga, P., Vinther, B. M., Walker, M. J., Wheatley, J. J., and Winstrup, M.: A stratigraphic framework for abrupt climatic changes during the Last Glacial period based on three synchronized Greenland ice-core records: refining and extending the INTIMATE event stratigraphy, Quaternary Science Reviews, 106, 14 – 28, doi:http://dx.doi.org/10.1016/j.quascirev.2014.09.007, 2014.

Rasmussen, T. L. and Thomsen, E.: The role of the North Atlantic Drift in the millennial timescale glacial climate fluctuations, Palaeogeogr. Palaeoclimatol. Palaeoecol., 210, 101–116, 2004.

Rasmussen, T. L., Thomsen, E., and Moros, M.: North Atlantic warming during Dansgaard-Oeschger events synchronous with Antarctic warming and out-of-phase with Greenland climate, Sci. Rep., 6, 2016.

Salgueiro, E., Voelker, A., de Abreu, L., Abrantes, F., Meggers, H., and Wefer, G.: Temperature and productivity changes off the western Iberian margin during the last 150 ky, Quaternary Science Reviews, 29, 680–695, doi:http://dx.doi.org/10.1016/j.quascirev.2009.11.013, http://www.sciencedirect.com/science/article/pii/S0277379109003862, 2010.

Sánchez Goñi, M. F., Landais, A., Fletcher, W. J., Naughton, F., Desprat, S., and Duprat, J.: Contrasting impacts of Dansgaard-Oeschger events over a western European latitudinal transect modulated by orbital parameters, Quaternary Science Reviews, 27, 1136 – 1151, doi:http://dx.doi.org/10.1016/j.quascirev.2008.03.003, http://www.sciencedirect.com/science/article/pii/S0277379108000759, 2008.

Sevellec, F. and Fedorov, A. V.: Unstable AMOC during glacial intervals and millennial variability: The role of mean sea ice extent, Earth and Planetary Science Letters, 429, 60–68, doi:10.1016/j.epsl.2015.07.022, 2015.

Shackleton, N. J., Hall, M. A., and Vincent, E.: Phase relationships between millennial-scale events 64,000-24,000 years ago, Paleoceanography, 15, 565–569, doi:10.1029/2000PA000513, http://dx.doi.org/10.1029/2000PA000513, 2000.

Singarayer, J. S. and Valdes, P. J.: High-latitude Climate sensitivity to ice-sheet forcing over the last 120 kyr, Quaternary Science Reviews, 29, 43–55, 2010.

Spahni, R., Chappellaz, J., Stocker, T. F., Loulergue, L., Hausammann, G., Kawamura, K., Flückiger, J., Schwander, J., Raynaud, D., Masson-Delmotte, V., and Jouzel, J.: Atmospheric Methane and Nitrous Oxide of the Late Pleistocene from Antarctic Ice Cores, Science, 310, 1317–1321, doi:10.1126/science.1120132, 2005.

Svensson, A., Andersen, K., Bigler, M., Clausen, H., Dahl-Jensen, D., Davies, S., Johnsen, S., Muscheler, R., Parrenin, F., Rasmussen, S., Rothlisberger, R., Seierstad, I., Steffensen, J., and Vinther, B.: A 60 000 year Greenland stratigraphic ice core chronology, Climate of the Past, 4, 47–57, 2008.

Telford, R. J. and Birks, H. J. B.: The secret assumption of transfer functions: problems with spatial autocorrelation in evaluating model performance, Quarternary Science Reviews, 24, 2173–2179, 2005.

ter Braak, C. and Looman, C.: Weighted averaging, logistic regression and the Gaussian response model, Vegetatio, 65, 3–11, 1986.

ter Braak, C. J. F. and Prentice, I.: A theory of gradient analysis, Adv. Ecol. Res., 18, 271–317, 1988.

ter Braak, C. J. F. and van Dam, H.: Inferring pH from diatoms: a comparison of old and new calibration methods, Hydrobiologia, 178, 209–223, 1989.

Tziperman, E.: Inherently unstable climate behaviour due to weak thermohaline ocean circulation, Nature, 386, 592–595, 1997.

Ukita, J., Honda, M., Nakamura, H., Tachibana, Y., Cavalieri, D. J., Parkinson, C. L., Koide, H., and Yamamoto, K.: Northern Hemisphere sea ice variability: lag structure and its implications, Tellus A, 59, 261–272, doi:10.1111/j.1600-0870.2006.00223.x, http://dx.doi.org/10.1111/j.1600-0870.2006.00223.x, 2007.

van Kreveld, S., Sarnthein, M., Erlenkeuser, H., Grootes, P., Jung, S., Nadeau, M. J., Pflaumann, U., and Voelker, A.: Potential links between surging ice sheets, circulation changes, and the Dansgaard-Oeschger Cycles in the Irminger Sea, 60-18 Kyr, Paleoceanography, 15, 425–442, doi:10.1029/1999PA000464, http://dx.doi.org/10.1029/1999PA000464, 2000.

Van Meerbeeck, C., Renssen, H., Roche, D., et al.: How did Marine Isotope Stage 3 and Last Glacial Maximum climates differ?–perspectives from equilibrium simulations, Climate of the Past, 5, 33–51, 2009.

Vettoretti, G. and Peltier, W. R.: Thermohaline instability and the formation of glacial North Atlantic super polynyas at the onset of Dansgaard-Oeschger warming events, Geophysical Research Letters, 43, 5336–5344, doi:10.1002/2016GL068891, http://dx.doi.org/10.1002/2016GL068891, 2016GL068891, 2016.

Voelker, A. H.: Global distribution of centennial-scale records for Marine Isotope Stage (MIS) 3: a database, Quaternary Science Reviews, 21, 1185–1212, 2002.

Voelker, A. H. L. and de Abreu, L.: A Review of Abrupt Climate Change Events in the Northeastern Atlantic Ocean (Iberian Margin): Latitudinal, Longitudinal, and Vertical Gradients, pp. 15–37, American Geophysical Union, doi:10.1029/2010GM001021, http://dx.doi.org/10.1029/2010GM001021, 2013.

Waelbroeck, C., Duplessy, J.-C., Michel, E., Labeyrie, L., Paillard, D., and Duprat, J.: The timing of the last deglaciation in North Atlantic climate records, Nature, 412, 724–727, 2001.

Wary, M., Eynaud, F., Rossignol, L., Lapuyade, J., Gasparotto, M.-C., Londeix, L., Malaizé, B., Castéra, M.-H., and Charlier, K.: Norwegian Sea warm pulses during Dansgaard-Oeschger stadials: Zooming in on these anomalies over the 35-41 ka cal BP interval and their impacts on proximal European ice-sheet dynamics, Quaternary Science Reviews, 151, 255 – 272, doi:https://doi.org/10.1016/j.quascirev.2016.09.011, http://www.sciencedirect.com/science/article/pii/S0277379116303614, 2016.

Weinelt, M.: Veränderungen der Oberflächenzirkulation im Europäischen Nordmeer während der letzten 60.000 Jahre - Hinweise aus stabilen Isotopen, Berichte aus dem sonderforschungsbereich 313, Christian-Albrechts-Universität, Kiel, 1993.

Weinelt, M., Rosell-Mele, A., Pflaumann, U., Sarnthein, M., and Kiefer, T.: Zur Rolle der Produktivität im Nordostatlantik bei abrupten Klimaänderungen in den letzten 80 000 Jahren (The role of productivity in the Northeast Atlantic on abrupt climate change over the last 80,000 years), Zeitschrift der Deutschen Geologischen Gesellschaft, 154, 47–66, 2003.

Zhang, X., Prange, M., Merkel, U., and Schulz, M.: Spatial fingerprint and magnitude of changes in the Atlantic meridional overturning circulation during marine isotope stage 3, Geophysical Research Letters, 42, 1903–1911, doi:10.1002/2014GL063003, http://dx.doi.org/10.1002/2014GL063003, 2014GL063003, 2015.

Clim. Past Discuss., https://doi.org/10.5194/cp-2017-103
Manuscript under review for journal Clim. Past
Discussion started: 24 August 2017

Climate of the Past Discussions
Open Access
EGU

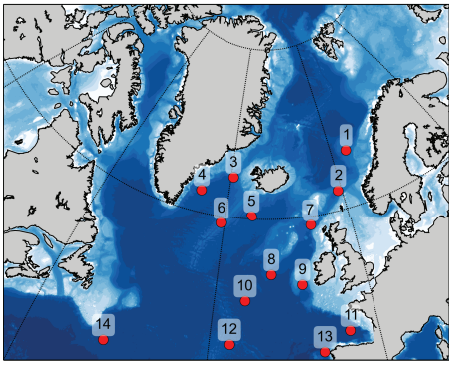

Figure 1. Core locations of the proxy data, numbers correspond to Table 1. Colors indicate bathymetry.

Clim. Past Discuss., https://doi.org/10.5194/cp-2017-103
Manuscript under review for journal Clim. Past
Discussion started: 24 August 2017

Climate of the Past Discussions
Open Access
EGU

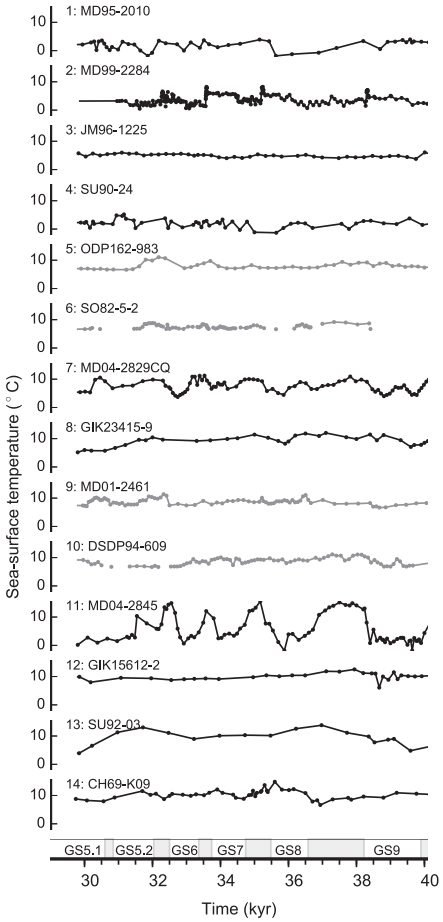

Figure 2. The proxy data. Black time series correspond to ML SSTs while grey time series are produced with %NP. Dots mark a data point. Shaded, grey areas on x-axis mark the GIs, while the GSs are named.

Clim. Past Discuss., https://doi.org/10.5194/cp-2017-103
Manuscript under review for journal Clim. Past
Discussion started: 24 August 2017

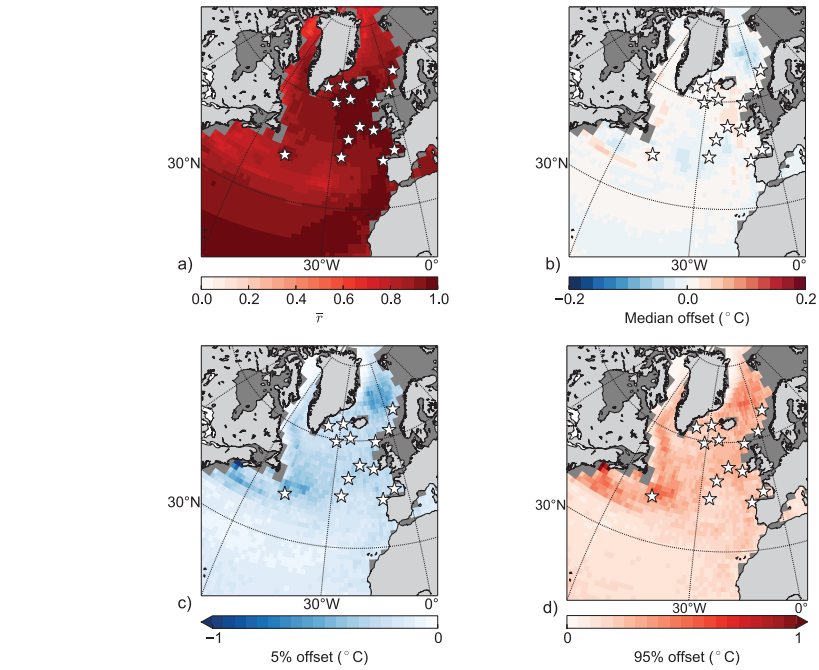

Figure 3. Synthetic PSR-study. Colors show the a) mean correlation coefficient between the synthetic data and the surrogate reconstruction, b) the median, c) the 5% and d) 95% offset between the synthetic value and the reconstructed surrogate value. The synthetic observations are 30 random years from the main HadCM3 model pool at the core locations, the model pool is the HadCM3, synthetic data extracted. This is repeated 1000 times. Grey shading represents the glacial coastline in the tcmoe3 simulation (Table 2, differs slightly between runs), while the white stars mark the core locations.

Clim. Past Discuss., https://doi.org/10.5194/cp-2017-103
Manuscript under review for journal Clim. Past
Discussion started: 24 August 2017

Climate of the Past Discussions
Open Access
EGU

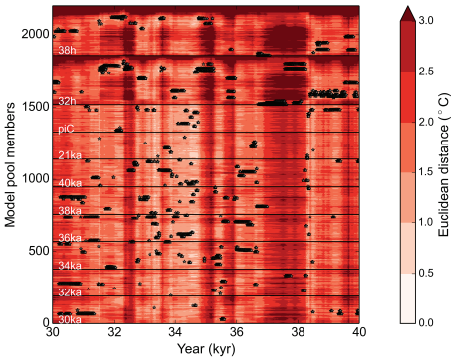

Figure 4. Colors show the RMSE between the main model pool and the SST-proxy data. Black dots indicate the ten model years (analogs) that constitute the composite for a given year in the surrogate reconstruction (i.e., the years with smallest RMSE). Model members and respective simulations are indicated on the y-axis and in white writing, while the proxy time steps are indicated on the x-axis.

Clim. Past Discuss., https://doi.org/10.5194/cp-2017-103
Manuscript under review for journal Clim. Past
Discussion started: 24 August 2017

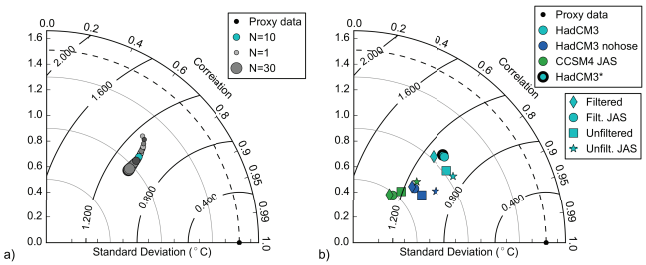

Figure 5. Taylor diagram showing the agreement between the proxy data and the surrogate time series produced using a) different number of analogs (1-30) using the main HadCM3 model pool. Increasing size of circles correspond to increasing analog numbers. N=10 is marked in cyan. b) Different model pools (legend). Dashed, black line indicates the standard deviation of the proxy data. Full, black lines indicate the centered RMS difference (labels, in °C). All values are means over the 14 core locations.

Clim. Past Discuss., https://doi.org/10.5194/cp-2017-103
Manuscript under review for journal Clim. Past
Discussion started: 24 August 2017

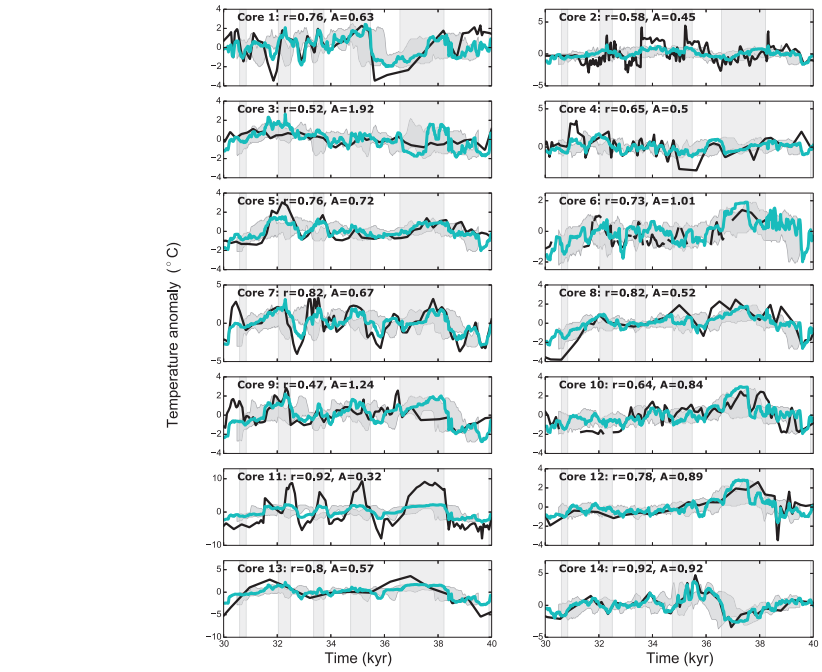

Figure 6. Surrogate time series (cyan) and proxy time series (black) for all 14 core locations. All time series are plotted as anomalies from the mean value of the respective time series. The filtered, JAS averaged SSTs from HadCM3 is used. Core numbers correspond to those shown in Fig. 1 and r is the correlation coefficient of the time series at each location. A is the ratio between the standard deviation of the two shown time series, A=$\sigma(c_i)/\sigma(T_i^p)$. The grey shading around the surrogate time series is the 90% confidence interval produced by shifting each proxy record by $\pm$ 500 years. The vertical bars represent interstadial conditions on Greenland as defined by Rasmussen et al. (2014).

Clim. Past Discuss., https://doi.org/10.5194/cp-2017-103
Manuscript under review for journal Clim. Past
Discussion started: 24 August 2017

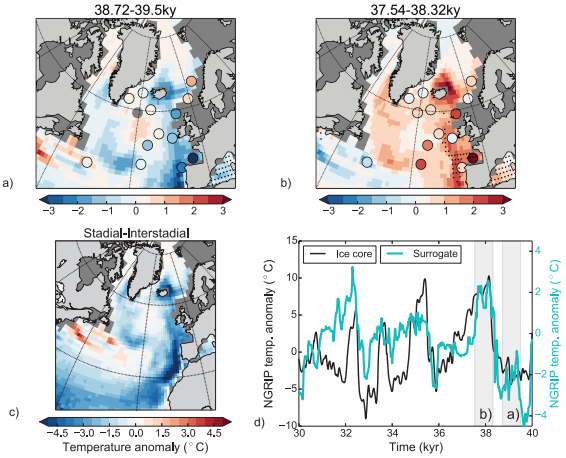

Figure 7. Temporal means of the spatial patterns for a) end of GS9, b) beginning of GI8, and c) GS9-GI8. Background color show the temperature anomalies from the surrogate reconstruction, while colors in circles indicate temperature anomalies from the proxy data (missing values for core 5 in the time-period of a)). Black (yellow) stars mark points where the surrogate reconstruction using the original age models is not within the 90% confidence level using age offsets of 500 years (dropping each core, all values within). Panel d) shows reconstructed NGRIP temperatures from the ice core (black line, right y-axis, Kindler et al., 2014) and the values from the surrogate time series (blue, note different y-axis). The surrogate reconstruction is made using the same analog-years which were picked for the SST reconstruction. The grey, vertical shadings show the time periods used in the other panels.

Clim. Past Discuss., https://doi.org/10.5194/cp-2017-103
Manuscript under review for journal Clim. Past
Discussion started: 24 August 2017

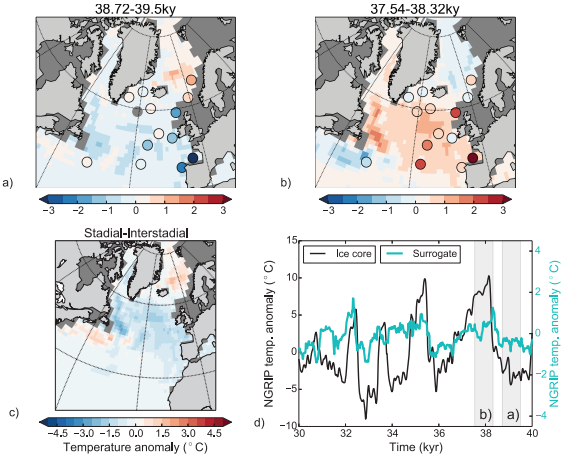

Figure 8. Fig. 7 but for HadCM3 nohose.

Clim. Past Discuss., https://doi.org/10.5194/cp-2017-103
Manuscript under review for journal Clim. Past
Discussion started: 24 August 2017

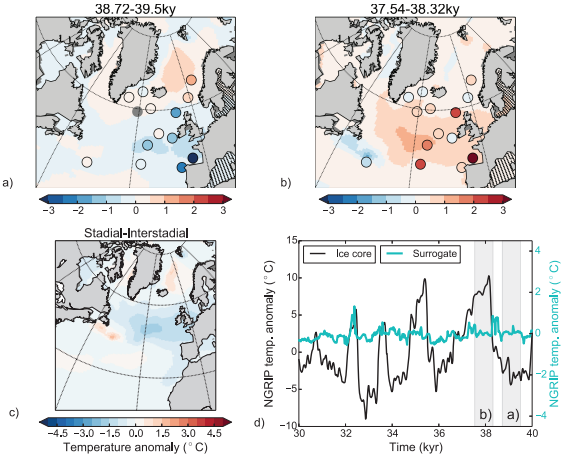

Figure 9. Fig. 7 but for CCSM4 data.

Clim. Past Discuss., https://doi.org/10.5194/cp-2017-103
Manuscript under review for journal Clim. Past
Discussion started: 24 August 2017

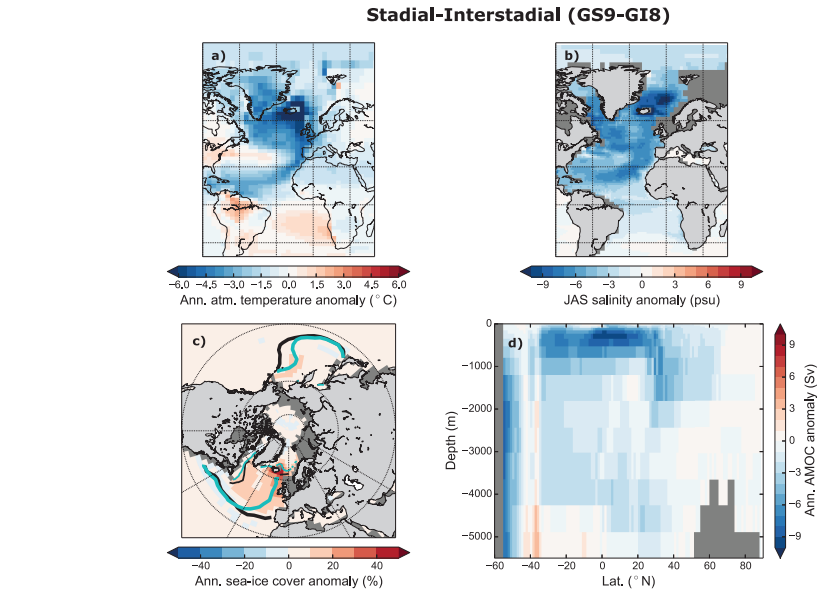

Figure 10. Composite of stadial-interstadial conditions (38.72-39.5 kyr vs. 37.54-38.32 kyr) for the surrogate time series constructed using the analogs picked with SSTs from the HadCM3 pool for a-c and HadCM3⋆ for d. Colors show a) annual atmospheric temperature anomalies, b) JAS ocean salinity anomalies, c) annual sea-ice cover concentration anomalies, and d) annual AMOC anomalies. The black and blue contour lines in panel c are the 0.15 sea-ice concentration lines for stadial and interstadial, respectively, thick for March, thin for September.

Clim. Past Discuss., https://doi.org/10.5194/cp-2017-103
Manuscript under review for journal Clim. Past
Discussion started: 24 August 2017

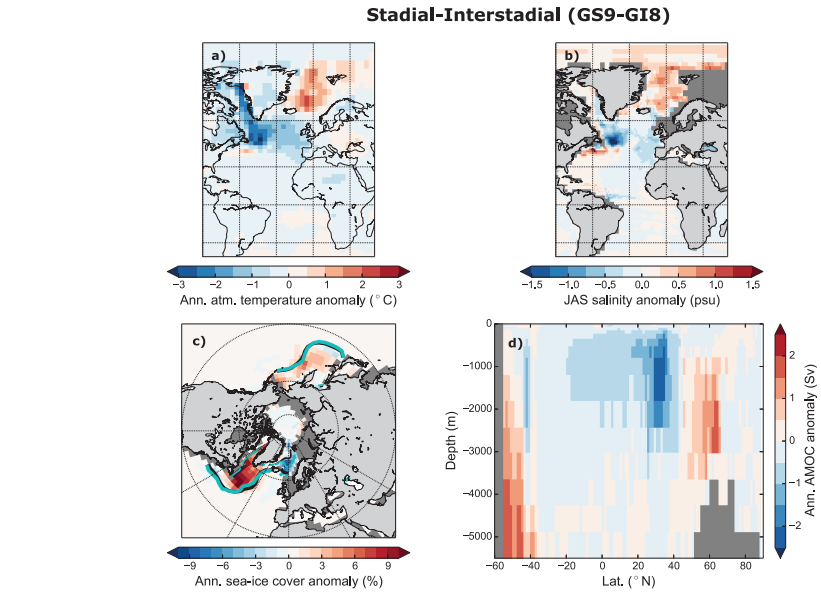

Figure 11. Fig. 10 for the HadCM3 nohose model pool

Clim. Past Discuss., https://doi.org/10.5194/cp-2017-103
Manuscript under review for journal Clim. Past
Discussion started: 24 August 2017

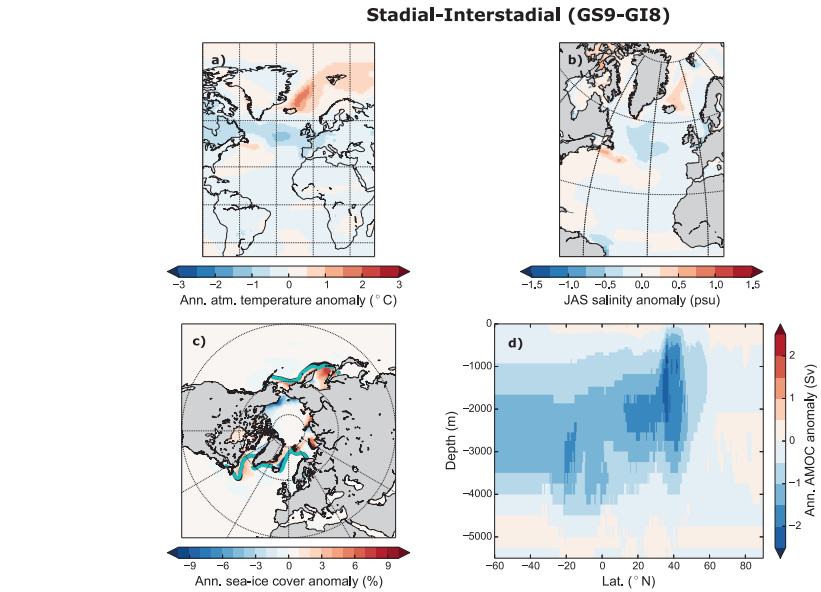

Figure 12. Fig. 10 with the CCSM4 model pool. For clarity, only the contours of the March sea-ice extent are shown.

Clim. Past Discuss., https://doi.org/10.5194/cp-2017-103
Manuscript under review for journal Clim. Past
Discussion started: 24 August 2017

Climate of the Past Discussions

Table 1. Core sites and age model information

Core nr.	Name	Method	Basis for age model 30-40 kyr	Reference
1	MD95-2010	ML	Two age models presented and discussed. 1) Calibrated ^{14}C dates (9), and NAAZ II and Laschamp magnetic excursion. 2) Magnetic Susceptibility (MS) vs. GISP2 δ^{18}O. The deviation between the ^{14}C based and the MS vs. GISP2 δ^{18}O age models are always less than 1 kyr and mostly close to zero	*Unpub. data T. Dokken* Age model: Dokken and Jansen (1999)
2	MD99-2284	ML	Age model are based on Anhysteretic Remanent Magnetism vs NGRIP δ^{18}O and 2 ash horizons (FMAZ III and II). The age model is supported by calibrated ^{14}C dates (5) that are not used as tie points in the established age model, a well as the Laschamp and Mono Lake magnetic excursions	Dokken et al. (2013)
3	JM96-1225	ML	Calibrated ^{14}C dates (2) and ash zone II (at 52 ka)	Hagen and Hald (2002)
4	SU90-24	ML	Uncalibrated ^{14}C dates (7)	Elliot et al. (1998)
5	ODP 983	%NP	Warming at the site are assumed to be synchronous with warming of the wider North Atlantic and these warm events are aligned to a synthetic Greenland record at EDC3 age model.	Barker et al. (2015)
6	SO82-5-2	%NP	Age model based on the combination of information given by δ^{18}O, ^{14}C dates (28), and tuning of SSTs to GISP2 δ^{18}O	van Kreveld et al. (2000)
7	MD04-2829CQ	ML	Age model based on calibrated ^{14}C dates (5), followed by a fine tuning of the %NP, used a SST indicator, to GISP2 δ^{18}O. The Lachamp magnetic excursion is identified	Hall et al. (2011)
8	GIK23415-9	ML	Age model based on correlation of IRD and δ^{18}O to GISP2 and supported by the calibrated ^{14}C dates (6)	Weinelt et al. (2003), Weinelt (1993)
9	MD01-2461	%NP	Age model based on calibrated ^{14}C dates (4), followed by a fine tuning of the %NP, used a SST indicator, to GISP2 δ^{18}O. Ash horizons.	Peck et al. (2007)
10	DSDP 609	%NP	Age model based on tuning the %NP, used a SST indicator, to GISP2 δ^{18}O	Bond et al. (2013)
11	MD04-2845	ML	Identified regional climatic and biostratigraphic events are correlated to the same events identified in MD04-2042. MD04-2042 is tuned to GISP2 δ^{18}O following the assumption that Greenland temperature changes associated with DO-events were synchronous over the North Atlantic region (Bard et al., 2004). Supported by calibrated ^{14}C dates (3). The not used ^{14}C dates deviate from the established age model by 90-1250 years.	Sánchez Goñi et al. (2008)
12	GIK15612-2	ML	IRD maxima related to Heinrich layers are tuned to GISP2 δ^{18}O. The chronology is supported by calibrated ^{14}C dates not used to establish the age model	Kiefer (1998)
13	SU92-03	ML	Age model based on tuning $\delta^{18}O_p$ and %NP to GISP2 δ^{18}O and Heinrich layers. The age model is also compared to MD95-2040 (de Abreu et al., 2003) and MD95-2042 (Shackleton et al., 2000), where also $\delta^{18}O_p$ and SSTs were tuned to GISP2 δ^{18}O	Salgueiro et al. (2010)
14	CH69-K09	ML	Calibrated ^{14}C dates (6)	Labeyrie et al. (1999), Waelbroeck et al. (2001)

Numbers in parenthesis mark number of ^{14}C dates. FMAZ: Faeroe Marine Ash Zone. NAAZ: North Atlantic Ash Zone. IRD: ice-rafted debris

Clim. Past Discuss., https://doi.org/10.5194/cp-2017-103
Manuscript under review for journal Clim. Past
Discussion started: 24 August 2017

Climate of the Past Discussions

Table 2. GCM simulations

Name	Simulated years	Period	Horz. resolution ocean	Hosing	Reference
HadCM3 - tcmqw3	200 (⋆:100)	30 ka	1.25° × 1.25°	NO	Singarayer and
HadCM3 - tcmob3	200 (⋆:100)	32 ka	1.25° × 1.25°	NO	Valdes (2010)
HadCM3 - tcmqv3	200 (⋆:100)	34 ka	1.25° × 1.25°	NO	
HadCM3 - tcmoa3	200 (⋆:100)	36 ka	1.25° × 1.25°	NO	
HadCM3 - tcmqu3	200 (⋆:100)	38 ka	1.25° × 1.25°	NO	
HadCM3 - tcmpu3	200 (⋆:100)	40 ka	1.25° × 1.25°	NO	
HadCM3 - tcmoe3	200 (⋆:100)	LGM	1.25° × 1.25°	NO	
HadCM3 - tcmfa3	200 (⋆:100)	PI	1.25° × 1.25°	NO	
HadCM3 - tcoxj+	99 hosed year +	32 ka	1.25° × 1.25°	YES	This study + Singarayer
	250 non-hosed years	32 ka			and Valdes (2010)
HadCM3 - tcoxk+	99 hosed year +	38 ka	1.25° × 1.25°	YES	
	250 non-hosed years	32 ka			
CCMS4 PI-1	1000	PI	Bipolar 1°	NO	Gent et al. (2011),
					Danabasoglu et al. (2012)
CCMS4 PI-2	1000	PI	Bipolar 1°	NO	Kleppin et al. (2015),
					Born and Stocker (2014)
CCMS4 LGM	101	LGM	Bipolar 1°	NO	Brady et al. (2013)
Model pool	Simulations				
HadCM3 (main)	tcmqw3,	tcmob3,	tcmqv3,	tcmoa3,	tcmqu3,
	tcmpu3,	tcmoe3,	tcmfa3,	tcoxj+,	tcoxk+
HadCM3 nohose	tcmqw3,	tcmob3,	tcmqv3,	tcmoa3,	tcmqu3,
	tcmpu3,	tcmoe3,	tcmfa3		
CCSM4	PI-1,	PI-2,	LGM		
HadCM3⋆	tcmqw3⋆,	tcmob3⋆,	tcmqv3⋆,	tcmoa3⋆,	tcmqu3⋆,
	tcmpu3⋆,	tcmoe3⋆,	tcmfa3⋆,	tcoxj+,	tcoxk+

Clim. Past Discuss., https://doi.org/10.5194/cp-2017-103
Manuscript under review for journal Clim. Past
Discussion started: 24 August 2017

Climate of the Past Discussions

Table 3. The agreement between the PSR and the ice-core record

Ice core	NGRIP			GISP2		
Model pool	r	$r_{36-40\mathrm{kyr}}$	A	r	$r_{36-40\mathrm{kyr}}$	r
HadCM3	0.49	0.81	0.35	0.63	0.84	0.32
HadCM3 nohose	0.47	0.66	0.13	0.63	0.76	0.13
CCSM4	0.25	0.13	0.06	0.31	0.21	0.06

Bibliography

Aagaard, K., and E. C. Carmack (1989), The role of sea ice and other fresh water in the Arctic circulation, *J. Geophys. Res.*, *94*, 14,485–14,498.

Aagaard, K., L. K. Coachman, and E. Carmack (1981), On the halocline of the Arctic Ocean, *Deep-Sea Research*, *28A*, 529–545.

Aagaard, K., J. H. Swift, and E. C. Carmack (1985), Thermohaline circulation in the Arctic Mediterranean Seas, *Journal of Geophysical Research: Oceans*, *90*(C3), 4833–4846, doi:10.1029/JC090iC03p04833.

Alley, R. B., S. Anandakrishnan, and P. Jung (2001), Stochastic resonance in the North Atlantic, *Paleoceanography*, *16*(2), 190–198, doi:10.1029/2000PA000518.

Arzel, O., A. Colin de Verdiere, and M. H. England (2010), The role of oceanic heat transport and wind stress forcing in abrupt millennial-scale climate transitions, *J. Clim*, *23*, 2233–2256.

Berger, A., and M. F. Loutre (1991), Insolation values for the climate of the last 10 million years, *Quaternary Science Reviews*, *10(4)*, 297–317.

Birchfield, G. E., and W. S. Broecker (1990), A salt oscillator in the glacial Atlantic? 2. A "Scale Analysis" Model, *Paleoceanography*, *5*, 835–843.

Bitz, C. M., J. C. H. Chiang, W. Cheng, and J. J. Barsugli (2007), Rates of thermohaline recovery from freshwater pulses in modern, last glacial maximum, and greenhouse warming climates, *Geophysical Research Letters*, *34*(7), doi: 10.1029/2006GL029237.

Blindheim, J., and S. Østerhus (2013), *The Nordic Seas, Main Oceanographic Features*pp.11–37, American Geophysical Union, doi:10.1029/158GM03.

Blunier, T., and E. J. Brook (2001), Timing of Millennial-Scale Climate Change in Antarctica and Greenland During the Last Glacial Period, *Science*, *291*(5501), 109–112, doi:10.1126/science.291.5501.109.

Böning, C. W., M. Scheinert, J. Dengg, A. Biastoch, and A. Funk (2006), Decadal variability of subpolar gyre transport and its reverberation in the North Atlantic overturning, *Geophysical Research Letters*, *33*(21), doi:10.1029/2006GL026906, l21S01.

Bond, G., W. Broecker, S. Johnsen, J. McManus, L. Labeyrie, J. Jouzel, and G. Bonani (1993), Correlations between climate records from North Atlantic sediments and Greenland ice, *Nature*, *365*, 143–147.

Born, A., and A. Levermann (2010), The 8.2 ka event: Abrupt transition of the subpolar gyre toward a modern north atlantic circulation, *Geochemistry, Geophysics, Geosystems*, *11*(6), doi:10.1029/2009GC003024, q06011.

Born, A., J. Mignot, and T. F. Stocker (2015), Multiple equilibria as a possible mechanism for decadal variability in the north atlantic ocean, *Journal of Climate*, *28*(22), 8907–8922, doi:10.1175/JCLI-D-14-00813.1.

Bourke, R. H., A. M. Weigel, and R. G. Paquette (1988), The westward turning branch of the West Spitsbergen Current, *J. Geophys. Res.*, *93*, 14 065–14 077, doi: 10.1029/JC093iC11p14065.

Braun, H., M. Christl, S. Rahmstorf, and A. a. Ganopolski (2005), Possible solar origin of the 1,470-year glacial climate cycle demonstrated in a coupled model, *Nature*, *438*.

Broecker, W. S. (2000), Abrupt climate change: casual constraints provided by the paleoclimate record, *Earth-Sci. Rev.*, *51*, 137–154.

Broecker, W. S., D. M. Peteet, and D. Rind (1985), Does the ocean-atmosphere system have more than one stable mode of operation?, *Nature*, *315*, 21–26.

Broecker, W. S., G. Bond, and M. Klas (1990), A salt oscillator in the glacial Atlantic? 1. The concept, *Paleoceanography*, *5*, 469–477.

Buckley, M. W., and J. Marshall (2016), Observations, inferences, and mechanisms of the Atlantic Meridional Overturning Circulation: A review, *Reviews of Geophysics*, *54*(1), 5–63, doi:10.1002/2015RG000493, 2015RG000493.

Chappell, J., and N. J. Shackleton (2002), Oxygen isotopes and sea level, *Nature*, *324*, 137–140.

Chiang, J. C. H., and C. M. Bitz (2005), Influence of high latitude ice cover on the marine Intertropical Convergence Zone, *Climate Dynamics*, *25*(5), 477–496, doi: 10.1007/s00382-005-0040-5.

Cisewski, G. B., B., and G. Krause (2003), Absolute transport estimates of total and individual water masses in the northern Greenland Sea derived from hydrographic and acoustic Doppler current profiler measurement, *J. Geophys. Res.*, *108*, doi: 10.1029/2002JC001530.

Clement, A. C., M. A. Cane, and R. Seager (2001), An Orbitally Driven Tropical Source for Abrupt Climate Change, *Journal of Climate*, *14*(11), 2369–2375, doi: 10.1175/1520-0442(2001)014<2369:AODTSF>2.0.CO;2.

Coachman, L., and C. Barnes (1963), The movement of Atlantic water in the Arctic Ocean, *Arctic*, *16*(1), 8–16.

Colin de Verdiere, A., and L. T. Raa (2010), Weak oceanic heat transport as a cause of the instability of glacial climates, *Clim. Dyn.*, *35*(7-8), 1237–1256, doi: 10.1007/s00382-009-0675-8.

Crowley, T. J. (1992), North Atlantic Deep Water cools the southern hemisphere, *Paleoceanography*, *7*, 489–497.

Curry, J. A., J. L. Schramm, and E. E. Ebert (1995), Sea ice-albedo climate feedback mechanism, *Journal of Climate*, *8*(2), 240–247, doi:10.1175/1520-0442(1995).

Curry, W. B., and D. W. Oppo (1997), Synchronous, high-frequency oscillations in tropical sea surface temperatures and North Atlantic Deep Water production during the last glacial cycle, *Paleoceanography*, *12*(1), 1–14.

Curry, W. B., T. M. Marchitto, J. F. Mcmanus, D. W. Oppo, and K. L. Laarkamp (2013), *Millennial-scale Changes in Ventilation of the Thermocline, Intermediate, and Deep Waters of the Glacial North Atlantic*pp.59–76, American Geophysical Union, doi: 10.1029/GM112p0059.

Dansgaard, W., H. B. Clausen, N. Gundestrup, C. U. Hammer, S. F. Johnsen, P. M. Kristinsdottir, and N. Reeh (1982), A New Greenland Deep Ice Core, *Science*, *218*(4579), 1273–1277, doi:10.1126/science.218.4579.1273.

Dansgaard, W., S. J. Johnsen, H. B. Clausen, D. Dahl-Jensen, N. S. Gundestrup, C. U. Hammer, C. S. Hvidberg, J. P. Steffensen, A. E. Sveinbjörnsdottir, J. Jouzel, and G. Bond (1993), Evidence for general instability of past climate from a 250-kyr ice-core record, *Nature*, *364*, 218–220.

Deshayes, J., F. Straneo, and M. A. Spall (2009), Mechanisms of variability in a convective basin, *Journal of Marine Research*, *67*, 273–303, doi: doi:10.1357/002224009789954757.

Dickson, B., I. Yashayaev, J. Meincke, B. Turrell, S. Dye, and J. Holfort (2002), Rapid freshening of the deep North Atlantic Ocean over the past four decades, *Nature*, *416*(6883), 832–837.

Dickson, R., J. Lazier, J. Meincke, P. Rhines, and J. Swift (1996), Long-term coordinated changes in the convective activity of the North Atlantic, *Progress in Oceanography*, *38*(3), 241 – 295, doi:http://dx.doi.org/10.1016/S0079-6611(97)00002-5.

Dickson, R. R., and J. Brown (1994), The production of North Atlantic Deep Water: Sources, rates, and pathways, *Journal of Geophysical Research: Oceans*, *99*(C6), 12,319–12,341, doi:10.1029/94JC00530.

Dokken, T., and E. Jansen (1999), Rapid changes in the mechanism of ocean convection during the last glacial period, *Nature*, *401*, 458–461.

Dokken, T. M., K. H. Nisancioglu, C. Li, D. S. Battisti, and C. Kissel (2013), Dansgaard-Oeschger cycles: interactions between ocean and sea intrinsic to the Nordic Seas, *Paleoceanography*, *28*, 491–502.

Dorale, J., R. Edwards, E. Ito, and L. Gonzalez (1998), Climate and vegetation history of the Midcontinent from 75 to 25 ka: a speleothem record from Crevice Cave, Missouri, USA., *Science*, *282*, 1871–1874.

Drange, H., R. Gerdes, Y. Gao, M. Karcher, F. Kauker, and M. Bentsen (2013a), *Ocean General Circulation Modelling of the Nordic Seas*pp.199–219, American Geophysical Union, doi:10.1029/158GM14.

Drange, H., T. Dokken, T. Furevik, R. Gerdes, W. Berger, A. Nesje, K. Arild Orvik, y. Skagseth, I. Skjelvan, and S. Østerhus (2013b), *The Nordic Seas: An Overview*pp.1–10, American Geophysical Union, doi:10.1029/158GM02.

Eldevik, T., J. E. . Nilsen, D. Iovino, K. A. Olsson, A. B. Sandø, and H. Drange (2009), Observed sources and variability of Nordic seas overflow, *Nature Geoscience*, *2*, 406–410, doi:DOI: 10.1038/NGEO518.

Elliot, M., L. Labeyrie, and J.-C. Duplessy (2002), Changes in North Atlantic deep-water formation associated with the Dansgaard-Oeschger temperature oscillations (60-10 ka), *Quaternary Science Reviews*, *21*, 1153–1165.

EPICA Community Members (2006), One-to-one coupling of glacial climate variability in Greenland and Antarctica, *Nature*, *444*, 195–198, doi: doi:10.1038/nature05301.

Eynaud, F., J. L. Turon, J. Matthiessen, C. Kissel, J. P. Peypouquet, A. de Vernal, and M. Henry (2002), Norwegian sea-surface palaeoenvironments of marine oxygen-isotope stage 3: the paradoxical response of dinoflagellate cysts, *Journal of Quaternary Science*, *17*(4), 349–359, doi:10.1002/jqs.676.

Eynaud, F., L. de Abreu, A. Voelker, J. Schönfeld, E. Salgueiro, J.-L. Turon, A. Penaud, S. Toucanne, F. Naughton, M. F. Sánchez Goñi, B. Malaizé, and I. Cacho (2009), Position of the Polar Front along the western Iberian margin during key cold episodes of the last 45 ka, *Geochemistry, Geophysics, Geosystems*, *10*(7), doi: 10.1029/2009GC002398, q07U05.

Ezat, M. M., T. L. Rasmussen, and J. Groeneveld (2014), Persistent intermediate water warming during cold stadials in the southeastern Nordic seas during the past 65 k.y., *Geology*, *42*(8), 663–666, doi:10.1130/G35579.1.

Fer, I., A. K. Peterson, A. Randelhoff, and A. Meyer (2017), One-dimensional evolution of the upper water column in the Atlantic sector of the Arctic Ocean in winter, *Journal of Geophysical Research: Oceans*, *122*(3), 1665–1682, doi: 10.1002/2016JC012431.

Ganopolski, A., and S. Rahmstorf (2001), Rapid changes of glacial climate simulated in a coupled climate model, *Nature*, *409*, 153–158.

Ganopolski, A., and S. Rahmstorf (2002), Abrupt Glacial Climate Changes due to Stochastic Resonance, *Physical Review Letters*, *88*.

Gerdes, R., J. Hurka, M. Karcher, F. Kauker, and C. Köberle (2013), *Simulated History of Convection in the Greenland and Labrador Seas, 1948—2001*pp.221–238, American Geophysical Union, doi:10.1029/158GM15.

Gildor, H., and E. Tziperman (2001a), Physical mechanisms behind biogeochemical glacial-interglacial CO2 variations, *Geophysical Research Letters*, *28*(12), 2421–2424, doi:10.1029/2000GL012571.

Gildor, H., and E. Tziperman (2001b), A sea ice climate switch mechanism for the 100-kyr glacial cycles, *Journal of Geophysical Research: Oceans*, *106*(C5), 9117–9133, doi:10.1029/1999JC000120.

Gildor, H., and E. Tziperman (2003), Sea-ice switches and abrupt climate change, *Phil. Trans R. Soc. London Ser. A*, *361*, 1935–1944.

Gill, A. (1973), Circulation and bottom water production in the Weddell Sea, *Deep Sea Research and Oceanographic Abstracts*, *20*(2), 111 – 140, doi: http://dx.doi.org/10.1016/0011-7471(73)90048-X.

Gottschalk, J., L. C. Skinner, S. Misra, C. Waelbroeck, L. Menviel, and A. Timmermann (2015), Abrupt changes in the southern extent of North Atlantic Deep Water during Dansgaard–Oeschger events, *Nature Geoscience*, *8*, 950–954.

Haine, T. W., B. Curry, R. Gerdes, E. Hansen, M. Karcher, C. Lee, B. Rudels, G. Spreen, L. de Steur, K. D. Stewart, and R. Woodgate (2015), Arctic freshwater export: Status, mechanisms, and prospects, *Global and Planetary Change*, *125*, 13 – 35, doi:https://doi.org/10.1016/j.gloplacha.2014.11.013.

Hansen, B., and S. Østerhus (2000), North Atlantic-Nordic Seas exchanges, *Prog. Oceanogr.*, *45*, 109–208, doi:10.1016/S0079-6611.

Hátún, H., A. B. Sandø, H. Drange, B. Hansen, and H. Valdimarsson (2005), Influence of the Atlantic Subpolar Gyre on the Thermohaline Circulation, *Science*, *309*, doi: 10.1126/science.1114777.

Heinrich, H. (1988), Origin and consequences of cyclic ice rafting in the Northeast Atlantic Ocean during the past 130,000 years, *Quaternary Research*, *29*, 142–152.

Hemming, S. R. (2004), Heinrich events: Massive late Pleistocene detritus layers of the North Atlantic and their global climate imprint, *Rev. Geophys.*, *42*, RG1005, doi:10.1029/2003RG000,128.

Henry, L. G., J. F. McManus, W. B. Curry, N. L. Roberts, A. M. Piotrowski, and L. D. Keigwin (2016), North Atlantic ocean circulation and abrupt climate change during the last glaciation, *Nature*, *353*, 470–474.

Hoff, U., T. L. Rasmussen, R. Stein, M. M. Ezat, and K. Fahl (2016), Sea ice and millennial-scale climate variability in the Nordic seas 90 kyr ago to present, *Nature Communications*, *7*, doi:doi:10.1038/ncomms12247.

Huang, R. (1999), Mixing and energetics of the oceanic thermohaline circulation, *J. Phys. Oceanogr.*, *29*(4), 727–746.

Huber, C., M. Leuenberger, R. Spahni, J. Flückiger, J. Schwander, T. F. Stocker, S. Johnsen, A. Landais, and J. Jouzel (2006), Isotope calibrated Greenland temperature record over marine isotope stage 3 and its relation to CH4, *Earth and Planetary Science Letters*, *243*, 504–519.

Jakobsson, M., J. Nilsson, L. Anderson, J. Backman, G. Björk, T. M. Cronin, N. Kirchner, A. Koshurnikov, L. Mayer, R. Noormets, et al. (2016), Evidence for an ice shelf covering the central Arctic Ocean during the penultimate glaciation, *Nature communications*, *7*.

Jayne, S. R., and J. Marotzke (1999), A Destabilizing Thermohaline Circulation-Atmosphere-Sea Ice Feedback, *J. Clim*, *12*, 642–651.

Johnsen, S. J., W. Dansgaard, H. B. Clausen, and C. C. L. Jun (1972), Oxygen Isotope Profiles through the Antarctic and Greenland Ice Sheets, *Nature*, *235*, 429–434, doi: doi:10.1038/235429a0.

Johnsen, S. J., H. B. Clausen, W. Dansgaard, K. Fuhrer, N. Gundestrup, C. U. Hammer, P. Iversen, J. Jouzel, B. Stauffer, and J. P. Steffensen (1992), Irregular glacial interstadials recorded in a new Greenland ice core, *Nature*, *359*, 311–313.

Jouzel, J., V. Masson-Delmotte, M. Stiévenard, A. Landais, F. Vimeux, S. J. Johnsen, A. E. Sveinbjörnsdottir, and J. W. White (2005), Rapid deuterium-excess changes in Greenland ice cores: A link between the ocean and the atmosphere, *C. R. Geoscience*, *337*, 957–969.

Kindler, P., M. Guillevic, M. Baumgartner, J. Schwander, A. Landais, and M. Leuenberger (2014), Temperature reconstruction from 10 to 120 kyr b2k from the NGRIP ice core, *Climate of the Past*, *10*, 887–902, doi:10.5194/cp-10-887-2014.

Kissel, C., C. Laj, L. Labeyrie, T. Dokken, A. Voelker, and D. Blamart (1999), Rapid climatic variations during marine isotope stage 3: magnetic analysis of sediments from Nordic Seas and North Atlantic, *Earth and Planetary Science Letters*, *171*, 489–502.

Kissel, C., C. Laj, A. M. Piotrowski, S. L. Goldstein, and S. R. Hemming (2008), Millennial-scale propagation of Atlantic deep waters to the glacial Southern Ocean, *Paleoceanography*, *23*(2), n/a–n/a, doi:10.1029/2008PA001624, pA2102.

Kvingedal, B. (2013), *Sea-Ice Extent and Variability in the Nordic Seas, 1967—2002*pp.39–49, American Geophysical Union, doi:10.1029/158GM04.

Kwok, R., and D. A. Rothrock (2009), Decline in Arctic sea ice thickness from submarine and ICESat records: 1958–2008, *Geophysical Research Letters*, *36*(15), doi: 10.1029/2009GL039035, l15501.

Labeyrie, L., L. Vidal, E. Cortijo, M. Paterne, M. Arnold, J. C. Duplessy, M. Vautravers, M. Labracherie, J. Duprat, J. L. Turon, F. Grousset, and T. V. Weering (1995), Surface and Deep Hydrology of the Northern Atlantic Ocean during the past 150 000 Years, *Philosophical Transactions of the Royal Society of London B: Biological Sciences*, *348*(1324), 255–264, doi:10.1098/rstb.1995.0067.

Labeyrie, L., H. Leclaire, C. Waelbroeck, E. Cortijo, J.-C. Duplessy, L. Vidal, M. Elliot, and B. L. Coat (1999), Geophysical Monograph Series.

Landais, A., J. M. Barnola, V. Masson-Delmotte, J. Jouzel, J. Chappellaz, N. Caillon, C. Huber, M. Leuenberger, and S. J. Johnsen (2004), A continuous record of temperature evolution over a sequence of Dansgaard-Oeschger events during Marine Isotopic Stage 4 (76 to 62 kyr BP), *Geophysical Research Letters*, *31*(22), doi: 10.1029/2004GL021193, l22211.

Li, C., D. S. Battisti, D. P. Schrag, and E. Tziperman (2005), Abrupt climate shifts in Greenland due to displacements of the sea ice edge, *Geophys. Res. Lett.*, *32*, L19,702, doi:10.1029/2005GL023,492.

Li, C., D. S. Battisti, and C. M. Bitz (2010), Can North Atlantic sea ice anomalies account for Dansgaard-Oeschger climate signals?, *J. Clim*, *23*, 5457–5475.

Longworth, H., J. Marotzke, and T. F. Stocker (2005), Ocean Gyres and Abrupt Climate Change in the Thermohaline Circulation: A Conceptual Analysis, *J. Clim*, *18*, 2403–2416.

Lozier, M. S. (2012), Overturning in the North Atlantic, *Annual Review of Marine Science*, *4*(1), 291–315, doi:10.1146/annurev-marine-120710-100740, pMID: 22457977.

Lyle, M. (1997), Could early Cenozoic thermohaline circulation have warmed the poles?, *Paleoceanography*, *12*, 161–167.

Manabe, S., and R. J. Stouffer (1988), Two stable equilibria of a coupled ocean-atmosphere model, *Journal of Climate*, *1*(9), 841–866, doi:10.1175/1520-0442(1988)001<0841:TSEOAC>2.0.CO;2.

Manabe, S., and R. J. Stouffer (1995), Simulation of abrupt climate change induced by freshwater input to the North Atlantic Ocean, *Nature*, *378*, 165–167.

Marchitto, T. M., W. B. Curry, and D. W. Oppo (1998), Millennial-scale changes in North Atlantic circulation since the last glaciation, *Nature*, *393*(6685), 557–561.

Marotzke, J. (2000), Abrupt climate change and the thermohaline circulation: mechanisms and predictability, *P. Natl. Acad. Sci. U.S.A.*, *97*, 1347–1350.

Masson-Delmotte, V., J. Jouzel, A. Landais, M. Stievenard, S. J. Johnsen, J. W. C. White, M. Werner, A. Sveinbjornsdottir, and K. Fuhrer (2005), GRIP deuterium excess reveals rapid and orbital-scale changes in Greenland moisture origin,, *Science*, *309*, 118–121.

Mauritzen, C. (1996), Production of dense overflow water feeding the North Atlantic across the Greenland–Scotland Ridge. part 1: Evidence for a revised circulation scheme, *Deep Sea Res. Part 1*, *43*, 769–806.

Mayewski, P. A., L. D. Meeker, S. Whitlow, M. S. Twickler, M. C. Morrison, P. Bloomfield, G. C. Bond, R. B. Alley, A. J. Gow, P. M. Grootes, D. A. Meese, M. Ram, K. C. Taylor, and W. Wumkes (1994), Changes in atmospheric circulation and ocean ice cover over the North Atlantic during the last 41,000 years, *Science*, *263*, 1747–1751.

Mayewski, P. A., L. D. Meeker, M. S. Twickler, S. I. Whitlow, Q. Yang, W. B. Lyons, and M. Prentice (1997), Major features and forcing of high latitude northern hemisphere atmospheric circulation over the last 110,000 years, *J. Geophys. Res.*, *102*, 26,345–26,366.

Maykut, G. A., and N. Untersteiner (1971), Some results from a time-dependent thermodynamic model of sea ice, *Journal of Geophysical Research*, *76*(6).

Nilsson, J., and G. Walin (2001), Freshwater forcing as a booster of thermohaline circulation, *Tellus*, *53A*, 629–641.

Nilsson, J., and G. Walin (2010), Salinity-dominated thermohaline circulation in sill basins: can two stable equilibria exist?, *Tellus*, *62A*, 123–133.

Ninnemann, U. S., C. D. Charles, and D. A. Hodell (2013), *Origin of Global Millennial Scale Climate Events: Constraints from the Southern Ocean Deep Sea Sedimentary Record*pp.99–112, American Geophysical Union, doi:10.1029/GM112p0099.

North Greenland Ice Core Project members (2004), High-resolution record of Northern Hemisphere climate extending into the last interglacial period, *Nature*, *431*, 147–151.

Nøst, O. A., and P. E. Isachsen (2003), The large-scale time-mean ocean circulation in the Nordic Seas and Arctic Ocean estimated from simplified dynamics, *Journal of Marine Research*, *61*(2), 175–210.

Nummelin, A., C. Li, and L. H. Smedsrud (2015), Response of Arctic Ocean stratification to changing river runoff in a column model, *Journal of Geophysical Research: Oceans*, *120*(4), 2655–2675, doi:10.1002/2014JC010571.

Nurser, A., and S. Bacon (2014), The Rossby radius in the Arctic Ocean, *Ocean Science*, *10*(6), 967–975.

Orvik, K. A., and P. Niiler (2002), Major pathways of Atlantic water in the northern North Atlantic and Nordic Seas toward Arctic, *Geophys. Res. Lett.*, *29*, doi:10.1029/2002GL015002.

Pausata, F., D. Battisti, K. Nisancioglu, , and C. Bitz (2011), Chinese stalagmites: Proxies for the Indian monsoon response to an archetypal Heinrich event, *Nature Geoscience*, *4*, 474–480, doi:doi:10.1038/ngeo1169.

Peltier, W. R., and G. Vettoretti (2014), Dansgaard-Oeschger oscillations predicted in a comprehensive model of glacial climate: A "kicked" salt oscillator in the Atlantic, *Geophysical Research Letters*, *41*(20), 7306–7313, doi:10.1002/2014GL061413, 2014GL061413.

Pemberton, P., and J. Nilsson (2015), The response of the central Arctic Ocean stratification to freshwater perturbations, *92*.

Petersen, S. V., D. P. Schrag, and P. U. Clark (2013), A new mechanism for Dansgaard-Oeschger cycles, *Paleoceanography*, *28*, 24–30.

Peterson, A. K., I. Fer, M. G. McPhee, and A. Randelhoff (2017), Turbulent heat and momentum fluxes in the upper ocean under Arctic sea ice, *Journal of Geophysical Research: Oceans*, *122*(2), 1439–1456, doi:10.1002/2016JC012283.

Polyakov, I. V., A. V. Pnyushkov, and L. A. Timokhov (2012a), Warming of the Intermediate Atlantic Water of the Arctic Ocean in the 2000s, *Journal of Climate*, *25*(23), 8362–8370, doi:10.1175/JCLI-D-12-00266.1.

Polyakov, I. V., J. E. Walsh, and R. Kwok (2012b), Recent Changes of Arctic Multiyear Sea Ice Coverage and the Likely Causes, *Bulletin of the American Meteorological Society*, *93*(2), 145–151, doi:10.1175/BAMS-D-11-00070.1.

Polyakov, I. V., A. V. Pnyushkov, M. B. Alkire, I. M. Ashik, T. M. Baumann, E. C. Carmack, I. Goszczko, J. Guthrie, V. V. Ivanov, T. Kanzow, R. Krishfield, R. Kwok, A. Sundfjord, J. Morison, R. Rember, and A. Yulin (2017), Greater role for Atlantic inflows on sea-ice loss in the Eurasian Basin of the Arctic Ocean, *Science*, *356*(6335), 285–291, doi:10.1126/science.aai8204.

Rasmussen, S. O., M. Bigler, S. P. Blockley, T. Blunier, S. L. Buchardt, H. B. Clausen, I. Cvijanovic, D. Dahl-Jensen, S. J. Johnsen, H. Fischer, et al. (2014a), A stratigraphic framework for abrupt climatic changes during the Last Glacial period based on three synchronized Greenland ice-core records: refining and extending the INTIMATE event stratigraphy, *Quaternary Science Reviews*, *106*, 14–28.

Rasmussen, T. L., and E. Thomsen (2004), The role of the North Atlantic Drift in the millennial timescale glacial climate fluctuations, *Palaeogeogr. Palaeoclimatol. Palaeoecol.*, *210*, 101–116.

Rasmussen, T. L., E. Thomsen, L. Labeyrie, and T. C. E. van Weering (1996), Circulation changes in the Faeroe-Shetland Channel correlating with cold events during the last glacial period (58-10 ka), *Geology*, *24*(937).

Rasmussen, T. L., E. Thomsen, and T. Nielsen (2014b), Water mass exchange between the Nordic seas and the Arctic Ocean on millennial timescale during MIS 4–MIS 2, *Geochemistry, Geophysics, Geosystems*, *15*(3), 530–544, doi: 10.1002/2013GC005020.

Rasmussen, T. L., E. Thomsen, and M. Moros (2016), North Atlantic warming during Dansgaard-Oeschger events synchronous with Antarctic warming and out-of-phase with Greenland climate, *Sci. Rep.*, *6*.

Rudels, B., E. Jones, L. Anderson, and G. Kattner (1994), On the intermediate depth waters of the Arctic Ocean, *The polar oceans and their role in shaping the global environment*pp.33–46.

Rudels, B., L. G. Anderson, and E. P. Jones (1996), Formation and evolution of the surface mixed layer and halocline of the Arctic Ocean, *Journal of Geophysical Research: Oceans*, *101*(C4), 8807–8821, doi:10.1029/96JC00143.

Rudels, B., R. Meyer, E. Fahrbach, V. Ivanov, S. Østerhus, D. Quadfasel, U. Schauer, V. Tverberg, and R. Woodgate (2000), Water mass distribution in Fram Strait and over the Yermak Plateau in summer 1997, *Ann. Geophys.*, *18*, 687–705, doi: 10.1007/s00585-000-0687-5.

Ruth, U., D. Wagenbach, J. P. Steffensen, and M. Bigler (2003), Continuous record of microparticle concentration and size distribution in the central Greenland NGRIP ice core during the last glacial period, *Journal of Geophysical Research: Atmospheres*, *108*(D3), doi:10.1029/2002JD002376, 4098.

Sachs, J. P., and S. J. Lehman (1999), Subtropical North Atlantic Temperatures 60,000 to 30,000 Years Ago, *Science*, *286*(5440), 756–759, doi: 10.1126/science.286.5440.756.

Seager, R. (2006), The source of Europe's mild climate, *American Scientist*, *94*, 334–341.

Segtnan, O. H., T. Furevik, and A. D. Jenkins (2011), Heat and freshwater budgets of the Nordic seas computed from atmospheric reanalysis and ocean observations, *Journal of Geophysical Research: Oceans*, *116*(C11), doi:10.1029/2011JC006939, c11003.

Seidov, D., O. K. Baranova, M. Biddle, T. P. Boyer, D. R. Johnson, A. V. Mishonov, C. Paver, and M. Zweng (2013), Greenland-Iceland-Norwegian Seas Regional Climatology (NODC Accession 0112824). Version 3.5. National Oceanographic Data Center, NOAA. Dataset, doi:doi:10.7289/V5GT5K30, (2013) Dataset.

Seidov, D., J. Antonov, K. Arzayus, O. Baranova, M. Biddle, T. Boyer, D. Johnson, A. Mishonov, C. Paver, and M. Zweng (2015), Oceanography north of 60N from World Ocean Database, *Progress in Oceanography*, *132*, 153 – 173, doi: https://doi.org/10.1016/j.pocean.2014.02.003, oceanography of the Arctic and North Atlantic Basins.

Serreze, M. C., and J. Stroeve (2015), Arctic sea ice trends, variability and implications for seasonal ice forecasting, *Philosophical Transactions of the Royal Society of London A: Mathematical, Physical and Engineering Sciences*, *373*(2045), doi: 10.1098/rsta.2014.0159.

Sevellec, F., and A. V. Fedorov (2015), Unstable AMOC during glacial intervals and millennial variability: The role of mean sea ice extent, *Earth and Planetary Science Letters*, *429*, 60–68, doi:10.1016/j.epsl.2015.07.022.

Siddall, M., E. J. Rohling, W. G. Thompson, and C. Waelbroeck (2008), Marine isotope stage 3 sea level fluctuations: Data synthesis and new outlook, *Reviews of Geophysics*, *46*(4), doi:10.1029/2007RG000226.

Singh, H. A., D. S. Battisti, and C. M. Bitz (2014), A Heuristic Model of Dansgaard–Oeschger Cycles. Part I: Description, Results, and Sensitivity Studies, *Journal of Climate*, *27*(12), 4337–4358, doi:10.1175/JCLI-D-12-00672.1.

Skagseth, Ø., T. Furevik, R. Ingvaldsen, H. Loeng, K. A. Mork, K. A. Orvik, and V. Ozhigin (2008), *Volume and Heat Transports to the Arctic Ocean Via the Norwegian and Barents Sea*pp.45–64, Springer Netherlands, Dordrecht.

Skjelvan, I., A. Olsen, L. G. Anderson, R. G. J. Bellerby, E. Falck, Y. Kasajima, C. Kivimäe, A. Omar, F. Rey, K. A. Olsson, T. Johannessen, and C. Heinze (2013), *A Review of the Inorganic Carbon Cycle of the Nordic Seas and Barents Sea*pp.157–175, American Geophysical Union, doi:10.1029/158GM11.

Smedsrud, L. H., M. H. Halvorsen, J. C. Stroeve, R. Zhang, and K. Kloster (2017), Fram Strait sea ice export variability and September Arctic sea ice extent over the last 80 years, *The Cryosphere*, *11*, 65–79, doi:10.5194/tc-11-65-2017.

Spall, M. A. (2004), Boundary Current and Water Transformation in Marginal Seas, *Journal of Physical Oceanography*, *34*, 1197–1213.

Spall, M. A. (2011), On the Role of Eddies and Surface Forcing in the Heat Transport and Overturning Circulation in Marginal Seas, *Journal of Climate*, *24*, 4844–4858.

Spall, M. A. (2012), Influences of Precipitation on Water Mass Transformation and Deep Convection, *Journal of Physical Oceanography*, *42*, 1684–1699.

Spall, M. A. (2013), On the Circulation of Atlantic Water in the Arctic Ocean, *Journal of Physical Oceanography*, *43*, 2352–2371.

Stauffer, B., T. Blunier, A. Dällenbach, A. Indermühle, J. Schwander, T. F. Stocker, J. Tschumi, J. Chappellaz, D. Raynaud, C. U. Hammer, and H. B. Clausen (1998), Atmospheric CO2 concentration and millennial-scale climate change during the last glacial period, *Nature*, *392*, 59–62.

Steele, M., and T. Boyd (1998), Retreat of the cold halocline layer in the Arctic Ocean, *Journal of Geophysical Research: Oceans*, *103*(C5), 10,419–10,435, doi: 10.1029/98JC00580.

Stigebrandt, A. (1981), A model for the thickness and salinity of the upper layer in the Arctic Ocean and the relationship between the ice thickness and some external parameters, *J. Phys. Oceanogr.*, *11*, 1407–1422.

Stocker, T. F., and S. J. Johnsen (2003), A minimum thermodynamic model for the bipolar seesaw, *Paleoceanography*, *18*(4), doi:10.1029/2003PA000920, 1087.

Stockhecke, M., A. Timmermann, R. Kipfer, G. H. Haug, O. Kwiecien, T. Friedrich, L. Menviel, T. Litt, N. Pickarski, and F. S. Anselmetti (2016), Millennial to orbital-scale variations of drought intensity in the eastern mediterranean, *Quaternary Science Reviews*, *133*, 77 – 95, doi:https://doi.org/10.1016/j.quascirev.2015.12.016.

Stommel, H. M. (1961), Thermohaline convection with two stable regimes of flow, *Tellus*, *13*, 224–230.

Stouffer, R. J., J. Yin, J. M. Gregory, K. W. Dixon, M. J. Spelman, W. Hurlin, A. J. Weaver, M. Eby, G. M. Flato, H. Hasumi, A. Hu, J. H. Jungclaus, I. V. Kamenkovich, A. Levermann, M. Montoya, S. Murakami, S. Nawrath, A. Oka, W. R. Peltier, D. Y. Robitaille, A. Sokolov, G. Vettoretti, and S. L. Weber (2006), Investigating the causes of the response of the thermohaline circulation to past and future climate changes, *J. Clim*, *19*(8), 1365–1387.

Svendsen, J. I., V. I. Astakhov, D. Y. Bolshiyanov, I. Demidov, J. A. Dowdeswell, V. Gataullin, C. Hjort, H. W. Hubberten, E. Larsen, J. Mangerud, M. Melles, P. Möller, M. Saarnisto, and M. J. Siegert (1999), Maximum extent of the Eurasian ice sheets in the Barents and Kara Sea region during the Weichselian, *Boreas*, *28*(1), 234–242, doi:10.1111/j.1502-3885.1999.tb00217.x.

Timmermann, A., H. Gildor, M. Schulz, and E. Tziperman (2003), Coherent resonant millennial-scale climate oscillations triggered by massive meltwater pulses, *J. Clim*, *16*, 2569–2585.

Tziperman, E. (1997), Inherently unstable climate behaviour due to weak thermohaline ocean circulation, *Nature*, *386*, 592–595.

Vellinga, M., R. A. Wood, and J. M. Gregory (2002), Processes Governing the Recovery of a Perturbed Thermohaline Circulation in HadCM3, *Journal of Climate*, *15*(7), 764–780, doi:10.1175/1520-0442(2002)015<0764:PGTROA>2.0.CO;2.

Vettoretti, G., and W. R. Peltier (2016), Thermohaline instability and the formation of glacial North Atlantic super polynyas at the onset of Dansgaard-Oeschger warming events, *Geophysical Research Letters*, *43*(10), 5336–5344, doi: 10.1002/2016GL068891, 2016GL068891.

Voelker, A. H. (2002), Global distribution of centennial-scale records for Marine Isotope Stage (MIS) 3: a database, *Quaternary Science Reviews*, *21*, 1185–1212.

Voelker, A. H. L., and L. de Abreu (2013), *A Review of Abrupt Climate Change Events in the Northeastern Atlantic Ocean (Iberian Margin): Latitudinal, Longitudinal, and Vertical Gradients*pp.15–37, American Geophysical Union, doi: 10.1029/2010GM001021.

Waelbroeck, C., J.-C. Duplessy, E. Michel, L. Labeyrie, D. Paillard, and J. Duprat (2001), The timing of the last deglaciation in North Atlantic climate records, *Nature*, *412*, 724–727.

Waelbroeck, C., L. Labeyrie, E. Michel, J. Duplessy, J. McManus, K. Lambeck, E. Balbon, and M. Labracherie (2002), Sea-level and deep water temperature changes derived from benthic foraminifera isotopic records, *Quaternary Science Reviews*, *21*(1), 295 – 305, doi:http://dx.doi.org/10.1016/S0277-3791(01)00101-9.

WAIS Divide Project Members (2015), Precise interpolar phasing of abrupt climate change during the last ice age, *Nature*, *520*, 661–665.

Wary, M., F. Eynaud, M. Sabine, S. Zaragosi, L. Rossignol, B. Malaizé, E. Palis, J. Zumaque, C. Caulle, A. Penaud, E. Michel, and K. Charlier (2015), Stratification of surface waters during the last glacial millennial climatic events: a key factor in subsurface and deep-water mass dynamics, *Climate of the Past*, *11*(11), 1507–1525.

Wary, M., F. Eynaud, L. Rossignol, J. Lapuyade, M.-C. Gasparotto, L. Londeix, B. Malaizé, M.-H. Castéra, and K. Charlier (2016), Norwegian Sea warm pulses during Dansgaard-Oeschger stadials: Zooming in on these anomalies over the 35-41 ka cal BP interval and their impacts on proximal European ice-sheet dynamics, *Quaternary Science Reviews*, *151*, 255 – 272, doi: https://doi.org/10.1016/j.quascirev.2016.09.011.

Wolff, E., J. Chappellaz, T. Blunier, S. Rasmussen, and A. Svensson (2010), Millennial-scale variability during the last glacial: The ice core record, *Quaternary Science Reviews*, *29*(21), 2828 – 2838, doi:http://dx.doi.org/10.1016/j.quascirev.2009.10.013, vegetation Response to Millennial-scale Variability during the Last Glacial.

Wu, P., R. Wood, and P. Stott (2004), Does the recent freshening trend in the North Atlantic indicate a weakening thermohaline circulation?, *Geophysical Research Letters*, *31*(2).

Wunsch, C. (2005), The Total Meridional Heat Flux and Its Oceanic and Atmospheric Partition, *Journal of Climate*, *18*(21), 4374–4380, doi:10.1175/JCLI3539.1.

Yang, J., and J. D. Neelin (1993), Sea-ice interaction with the thermohaline circulation, *Geophys. Res. Lett.*, *20*, 217–220.

Yang, J., and J. D. Neelin (1997), Sea-ice interaction and the stability of the thermohaline circulation, *Atmos.-Ocean*, *35:4*, 433–469.

Yu, E. F., F. Francois, and M. Bacon (1996), Similar rates of modern and last-glacial ocean thermohaline circulation inferred from radiochemical data, *Nature*, *379*, 689–694.

Zhang, J., R. W. Schmitt, and R. X. Huang (1999), The relative influence of diapycnal mixing and hydrological forcing on the stability of thermohaline circulation, *J. Phys. Oceanogr.*, *29*, 1096–1108.

Zhang, R., and T. L. Delworth (2005), Simulated Tropical Response to a Substantial Weakening of the Atlantic Thermohaline Circulation, *Journal of Climate*, *18*(12), 1853–1860, doi:10.1175/JCLI3460.1.